



OPTICAL SPECTRA AND TRANSPORT BEHAVIOUR OF MOLTEN SALT SYSTEMS

**THESIS SUBMITTED FOR THE DEGREE OF
DOCTOR OF PHILOSOPHY
IN
CHEMISTRY**

**BY
ANWAR ALI**

**Department of Chemistry
ALIGARH MUSLIM UNIVERSITY
ALIGARH**

July, 1978

Department of Chemistry,
Aligarh Muslim University,
Aligarh.

This is to certify that the thesis entitled
"Optical Spectra and Transport Behaviour of Molten Salt
Systems" is the original work carried out by Mr. Anwar
Ali under my supervision and is suitable for submission
for the award of Ph.D. degree in Chemistry.



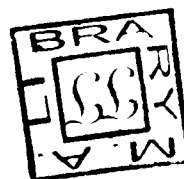
(NURUL ISLAM)
Ph.D. (New York)
Reader.



SEP 1980



T1974



SD
CHECKED-2002

A C K N O W L E D G E M E N T

I wish to express my sincere gratitude to Dr. Nurul Islam for his help, proper guidance, encouragement and unstinted devotion during the progress of this work and to Prof. W. Rahman, Head, Department of Chemistry for being kind enough to provide necessary research facilities. I am also thankful to C.S.I.R. (New Delhi) for the financial assistance.

At last, but not the least, I wish to acknowledge all kinds of cooperation shown by my research colleagues.


ANWAR ALI

C O N T E N T S

CHAPTER		<u>Page No.</u>
	Abstract	
I.	A. General Introduction	1
	B. Experimental Techniques	6
	Determination of Water Content	
	in the Hydrated Salts	7
	Temperature Control	7
	Preparation of Samples	8
	Spectral Measurement	9
	Density Measurement	9
	Viscosity Measurement	10
	Conductance Measurement	14
II.	Optical Spectra of Molten	
	Ca(NO ₃) ₂ ·3.96H ₂ O-Ni(NO ₃) ₂ ·6.03H ₂ O Systems	16
	Introduction	17
	Results and Discussion	17
III.	Temperature Dependence of Transport	
	Behaviour of Molten Salt Systems -	
	The Application of VTF Equation	21
	Introduction	22
	Results and Discussion	32

CHAPTER**Page No.**

IV.	Temperature Dependence of Transport Behaviour of Molten Salt Systems - The Application of Configurational Entropy Model	92
	Introduction	93
	Results and Discussion	96
V.	Concentration Dependence of Transport Behaviour of Molten Salt Systems	127
	Introduction	128
	Results and Discussion	132
	Appendix	160
	Bibliography	168

A B S T R A C T

Optical spectra of concentrated solutions of molten $\text{Ca}(\text{NO}_3)_2 \cdot 3.96\text{H}_2\text{O}$ - $\text{Ni}(\text{NO}_3)_2 \cdot 6.03\text{H}_2\text{O}$ systems have been recorded. Density and viscosity measurements of molten $\text{Ca}(\text{NO}_3)_2 \cdot 3.96\text{H}_2\text{O}$ - $\text{Ni}(\text{NO}_3)_2 \cdot 6.03\text{H}_2\text{O}$ systems and those of $\text{Cd}(\text{NO}_3)_2 \cdot 4.03\text{H}_2\text{O}$ - $\text{MnCl}_2 \cdot 4.00\text{H}_2\text{O}$, $\text{Ca}(\text{NO}_3)_2 \cdot 4.23\text{H}_2\text{O}$ - NH_4CNS , and $\text{Ca}(\text{NO}_3)_2 \cdot 4.1\text{H}_2\text{O}$ - NaCNS systems including the conductance measurements in the latter three cases were made as functions of temperature and concentration. Density data have been found to be described by a linear equation $\rho = a - bT$ ($^\circ\text{K}$) where a and b are the empirical constants. The viscosities and conductances of the systems were found to show non-Arrhenius behaviour and, therefore, they were least-squares fitted to the equations

$$Y (= \phi \text{ or } \Lambda) = A_Y T^{-1/2} \exp \left[- k_Y / (T - T_0) \right] \quad \text{and}$$

$$Y = A_Y' \exp \left[- k_Y' / (V - V_0) \right] \quad \text{based essentially on the free volume concept and to}$$

$$Y = A_Y'' \exp \left[- k_Y'' / T \ln (T/T_0) \right] \quad \text{based on the configurational entropy model. } A_Y, k_Y, T_0, A_Y', k_Y', V_0, A_Y'', \text{ and } k_Y'' \text{ are the empirical parameters. The concentration dependences of these parameters have been discussed and the thermodynamic nature of } T_0 \text{ and } V_0 \text{ has been emphasized. The terms } k_Y, k_Y', \text{ and } k_Y'' \text{ have been found to be concentration indepen-}$$

dent and their constancy has been examined while the parameters A_Y , A'_Y , A''_Y , T_o , and V_o were found to vary linearly with concentration. On the basis of linear concentration dependence of A''_Y and T_o terms, the concentration dependence of transport properties has been explained in the light of an apparently isentropic equation based on the configurational entropy model which is of the form

$$Y = (A''_{oY} \pm Q'_{1Y}N) \exp \left[- k_Y / (T_{o(o)} \pm Q_{2Y}N) c \ln c \right].$$

A''_{oY} and $T_{o(o)}$ are the values of A''_Y and T_o for the pure solvent while Q'_{1Y} is the slope of the plot of A''_Y versus concentration, N being in mol %, Q_{2Y} is another slope of the plot of T_o versus N and c stands for the constant T/T_o values. Due to the lack of experimental support to the above equation an alternative isoenergetic equation based on the Vogel-Tammann-Fulcher (VTF) equation has been employed to explain the concentration dependence of transport properties of the systems under investigation. The isoenergetic equation is of the form

$$Y = (A_{oY} \pm Q_{1Y}N) c^{-1/2} (T_{o(o)} \pm Q_{2Y}N)^{-1/2} \exp \left[- k_Y / (T_{o(o)} \pm Q_{2Y}N) (c - 1) \right]$$

The parameters A_{oY} , Q_{1Y} , $T_{o(o)}$, Q_{2Y} , and k_Y have their

usual significances. The values of the glass transition temperature, T_0 computed from the VTF and configurational entropy equations have been found to be in good agreement. The energies of activation, E_ϕ and E_Λ obtained from the two models are also comparable.

Even though similar relaxing species are expected to participate in the mechanisms of viscosities and conductances, the difference in the two activation energies may presumably be due to different availabilities of the relaxing entities in the two flows.

Finally, it is interesting to note that the potentially most important relations of the present investigations for the linear dependences of the preexponential terms A_Y (VTF) and A_Y' (Doolittle) equations on the values of T_0 and those of V_0 , respectively, have been proposed. In addition to these relations, a linear interdependence of the two thermodynamic quantities, T_0 and V_0 , has also been found.

C H A P T E R - I

A. G E N E R A L I N T R O D U C T I O N

It is well known that some liquids can be held at temperatures well below their freezing points over very long periods without crystallization, liquids in such a state are said to be supercooled. Every liquid can be visualized to supercool depending on its crystallization kinetic constants and the rate of cooling.¹ The important crystallization constants which mainly determine the ability of a liquid to supercool are the energy barriers to nucleation in the absence of a foreign nucleus and to the growth of finite crystal. All such supercooled liquids probably pass through the rather peculiar "transition" to a "glassy" or "vitreous" state when cooled sufficiently. The material in this state is called a "glass", and the temperature of the change or transition is called the glass-transition temperature, T_g , which is usually well below the melting temperature and provides a meaningful corresponding temperature scale for use in the comparison of fused salt properties, in particular, transport properties. Moreover, at the glass transition the values of the derivative properties, the specific heat and expansion coefficient change discontinuously and are much closer to those of the crystalline form of the substance than to those of the parent liquid. Apparently, the glassy state is a form of matter which maintains the structure, energy, and volume of a liquid, but for which the changes in

energy and volume with temperature are similar in magnitude to those of a crystalline solid. That is, a glass is a liquid in which certain degrees of freedom characteristic of liquids are "frozen in" and can no longer contribute to the specific heat and thermal expansion.

It may, however, be emphasized that in the temperature region where these changes occur, the viscosity increases rapidly to the order of 10^{13} poise and also the conductance has almost zero value. Furthermore, hydrated melts have emerged as an interesting and better media for carrying out investigations of molten salt properties due to their extremely low stable or metastable melting temperatures. Consequently, viscosity and conductance measurements of supercooled liquids including melts as a function of temperature helped in understanding the theories behind viscous and conductance flows. Such studies of molten salt systems have also been found to provide an idea regarding the value of the ideal glass transition temperature, T_0 , known as secondary glass transition temperature. The values of the experimentally determined glass transition temperature, T_g , have generally been found to be about 10 to 20° higher than the ideal glass transition temperature, T_0 . This is due to the fact that the glass transition is a relaxation phenomenon and is a consequence of a deficiency in the experimental procedure; it results

from changing the external forces acting on a system and then making measurements before the system has had time to reestablish complete thermodynamic equilibria with its changed surrounding leading to a lower value of T_0 than T_g .

In view of the interest shown above, viscosity and conductance measurements of molten salts where at least one of the components is a hydrated salt have been made as functions of temperature and concentration. The systems studied here include the pure solvents, i.e., molten tetrahydrate of cadmium and calcium nitrates, the molten mixtures of manganese (II) chloride tetrahydrate with cadmium nitrate tetrahydrate and those of ammonium thiocyanate, sodium thiocyanate, and nickel (II) nitrate hexahydrate with calcium nitrate tetrahydrate. As tetrahydrates of cadmium and calcium nitrates exhibit easily supercooling tendency, their molten mixtures with solutes given above allow exploration of molten salt properties at correspondingly lower temperatures as compared to those attainable in most anhydrous melts. A direct consequence of these low liquidus temperatures is that the temperature dependence of transport properties of the molten mixtures cited above are non-Arrhenius. Hence the Vogel-Tammann-Fulcher equation and that based on the configurational entropy concept have been employed in explaining the non-Arrhenius temperature

dependence of viscosities and conductances. In addition, these equations have also been taken as the basis for explaining the concentration dependence of these behaviours.

B. EXPERIMENTAL TECHNIQUES

Determination of Water Content in the Hydrated Salts

The exact waters of crystallization of the hydrated salts were determined before using them for the preparation of samples. The exact waters of crystallization in the cases of hydrated salts of cadmium and calcium nitrates have been estimated by comparing the measured densities of these hydrated salts with those reported^{2,3} for several concentrations. The ratios of $H_2O/Metal$ ion thus determined were 4.03 for H_2O/Cd^{2+} and 4.23, 4.10, and 3.96, respectively, for H_2O/Ca^{2+} for the three samples of hydrated calcium nitrate taken from separate bottles. The water contents in the cases of hydrated salts of manganese (II) chloride and nickel (II) nitrate, on the other hand, were estimated volumetrically⁴ using standard solution of EDTA as titrant. The values of the ratios H_2O/Mn^{2+} and H_2O/Ni^{2+} were found to be 4.00 and 6.03, respectively. The accuracy of such a volumetric analysis was checked by taking hydrated cadmium nitrate of known H_2O/Cd^{2+} ratio and was found to be within ± 0.01 .

Temperature Control

The preparation of the samples and the measurements of density, viscosity, and conductance were made in a thermostated paraffin bath in order to maintain a uniform temperature. The bath consists of stirrer, an immersion

heater (250 W), and a check and contact thermometers [TGL 4850 NAV = 0.03 Un = 250 V (GDR)], all immersed in a large corning glass container of paraffin. A relay [Jumo-type NT 15.0, 220V \approx 15A (Germany)] was used to control the variations in temperature. The overall temperature stability was within $\pm 0.1^\circ$.

Preparation of Samples

Commercial cadmium nitrate tetrahydrate [REACHIM (USSR); m.p. 59.4°] and calcium nitrate tetrahydrate (BDH; m.p. 42.7°) from three different bottles were used as solvents in their molten state. Manganese (II) chloride tetrahydrate (BDH; m.p. 58°), ammonium thiocyanate (BDH; m.p. 149.6°), sodium thiocyanate (BDH; m.p. 287° , recrystallized twice from double distilled water), and nickel (II) nitrate hexahydrate (BDH; m.p. 56.7°) were used as solutes.

Samples were prepared in the thermostated paraffin bath at about 60°C . During sample preparation, the chemicals were handled with extra care in an atmosphere of pure and dry nitrogen owing to their hygroscopic nature. Weighed amounts of cadmium nitrate tetrahydrate were taken in several tightly capped tubes and amounts of manganese (II) chloride tetrahydrate were then accurately weighed and added to the molten cadmium nitrate tetrahydrate. The mixtures were heated for several hours until clear solutions

were obtained. Several samples of different concentrations were prepared in this manner. Manganese (II) chloride tetrahydrate was found to dissolve upto ~ 12 mol % in molten cadmium nitrate tetrahydrate. Similarly, different samples of varying concentrations of calcium nitrate tetrahydrate with those of ammonium thiocyanate, of sodium thiocyanate, and of nickel (II) nitrate hexahydrate were prepared. Calcium nitrate tetrahydrate was found to dissolve ~ 60 mol % of ammonium thiocyanate, ~ 24 mol % of sodium thiocyanate, and ~ 60 mol % of nickel (II) nitrate hexahydrate. The prepared samples were stored in a vacuum desiccator.

Spectral Measurements

Absorption spectra of thin films of the samples were recorded on Beckman model DK-2A spectrophotometer using quartz optical cells.

Density Measurements

Density measurements were made using a dilatometer of approximately 6.0 ml capacity with graduated stem of 0.01 ml divisions. The graduated stem of the dilatometer was calibrated by making use of pure quinoline (Riedel) whose densities are reported as a function of temperature. Quinoline was purified before use by drying

and then distilling over anhydrous calcium chloride (pure quinoline has b.p. 218°C). The total volume of dilatometer as well as the exact volume between the two successive divisions of the graduated stem were thus determined. The melted sample was transferred to the calibrated and exactly weighed dilatometer with the help of a vacuum pump. The weight of the dilatometer containing molten salt sample was again determined and the difference in the two weights gives the exact amount of the melt taken in the dilatometer. The dilatometer was then immersed in the thermostated bath and the volumes of the melt were recorded at several temperatures. Thus, the densities, molar volumes, and the coefficients of thermal expansion for the samples were computed at the required temperatures.

Viscosity Measurements

The viscosities of the melts were determined with the help of a Cannon-Ubbelohde⁵ type viscometer. The viscometer consists of three parallel tubes, i.e., receiving, measuring, and auxiliary tubes which form the suspended level arrangement in a triangular fashion (Fig.1a). The receiving and measuring tubes form a 'U' through a bulb D. Bulb A and another fiducial bulb B slightly below the former were sealed to the measuring tube. Two fiducial marks, a and b on the bulbs A and B, respectively, were used for

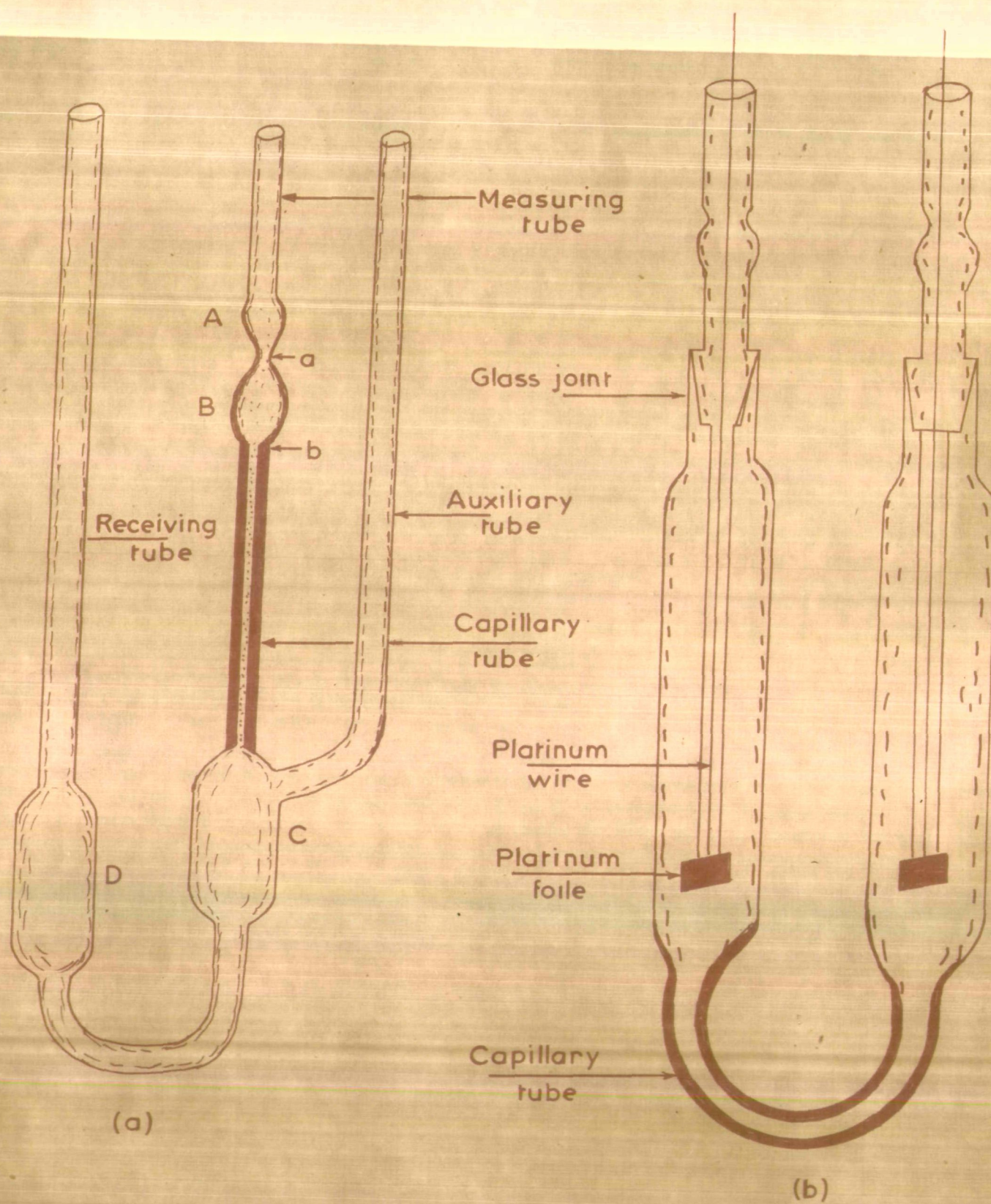


Fig. 1. (a) CANNON-UBBELOHDE TYPE VISCOMETER
(b) CAPILLARY-TYPE CONDUCTIVITY CELL

recording the efflux time. The auxiliary tube was sealed to the measuring tube through a bulb C. There lies a capillary of appropriate length and diameter between the bulbs B and C. The effect of acceleration due to gravity was minimized by aligning the centres of gravity of all the three bulbs A, B, and C in vertical position. In order to minimize the experimental error in the measurement of viscosity the dimensions of the viscometer were fixed in such a manner so as to maintain the resulting efflux time for water as more than 80 secs. The viscometer constant of such a viscometer was found to be 6.26 cSt/sec and the special feature of such a suspended level viscometer is that the transport of momentum was carried out freely under the weight of the total volume of the test liquid. Moreover, the capillary effects of the two liquid surfaces were neutralized by each other so that the surface tension correction for the apparatus was also negligible.

The viscometer was clamped in a vertical position in the thermostated bath in order to measure viscosities and then filled with a required amount of the test liquid. The volume taken of the test liquid in the viscometer should be *adequate to avoid any* air bubble

introduced in the capillary tube during the course of transfer of the liquid to the fiducial bulb B. To avoid the absorption of atmospheric moisture by the sample, the

open ends of the viscometer were connected through the rubber tubes to dry calcium chloride tubes. The viscometer containing the sample was allowed to stand in the thermostated bath for about 30-45 minutes in order to attain the thermal homogeneity. The heater was connected to the relay through a dimmerstat which helps in controlling the heating rate by adjusting its output voltage and this device further helps in minimizing the thermal fluctuations. Next the sample was sucked into the bulb A with the help of a vacuum pump and allowed to stand there for about 40 minutes by closing the calcium chloride tubes with rubber corks. The rubber stoppers were then removed from the tubes and the time of fall of the melt from the upper fiducial mark 'a' to the lower mark 'b' was noted for three to four times with the help of a stop watch. The mean of these measurements were recorded at a set temperature.

The times of fall of the reference liquid, pure ~~and~~ dry quinoline, were also recorded at the corresponding temperatures. The viscosity of the melt was then calculated using the expression given in the Appendix A. Overall accuracy of the viscosity measurements by suspended level principle was estimated to be better than ± 2.5 %.

Conductance Measurements

The cells used for the conductance measurements were of capillary-type^{6,7} with high cell constant values and the conductance bridge of Philips Model PR 9500 type. The cell was constructed by sealing two platinum foils each having an area of $\sim 0.25 \text{ cm}^2$ to the ends of two platinum wires which were in turn sealed to the ends of two corning glass tubes. Electrical contacts were made through the sealed platinum wires. The two independent electrodes thus constructed can be properly fixed into the two limbs of 'U' shaped corning glass tube having a capillary at its lower part. The cell constants of the two capillary-type cells used were found to be 542 cm^{-1} and 730 cm^{-1} at 25°C , respectively (Fig. 1b).

The melt was transferred into the 'U' tube by removing the electrodes from its two limbs. Then the electrodes were replaced into the limbs of the capillary cell in such a way that the platinum foils dip into the molten sample. Care was taken to remove any air bubble sticking to the surface of the electrodes or in the capillary. The absorption of moisture by the sample during the measurement was avoided by keeping the platinum electrodes fixed airtightly into the limbs through glass joints. Now the cell containing electrodes was suspended in the thermostated bath and the electrical connections between the con-

ductivity bridge and the cell were made using copper wires. The electrical resistances of the samples were recorded at 1 kHz several temperatures after the attainment of thermal equilibria and the equivalent conductances were calculated as given in Appendix B.

All the measurements were made in a descending order of temperature.

C H A P T E R - I I

Optical Spectra of Molten $\text{Ca}(\text{NO}_3)_2 \cdot 3.96\text{H}_2\text{O}$ -
 $\text{Ni}(\text{NO}_3)_2 \cdot 6.03\text{H}_2\text{O}$ Systems

Introduction

Extensive studies have been made on the absorption spectra of dilute solutions of transition metal halides in molten halides.⁸ These studies provide information regarding the geometry of the transition metal complex ions. The divalent 3d ions in aqueous solutions are generally believed to occur as the well-known hexahydrate ions $M(H_2O)_6^{2+}$.

Out of the four samples of molten salts chosen for the study of their transport properties only two of them contained the transition metal ions, i.e., nickel (II)- and manganese (II)-ions. The absorption spectra of the sample containing manganese (II) ion could not be recorded because of its extremely weak spin-forbidden bands. The ligand-field spectra of $Ni(NO_3)_2 \cdot 6.03H_2O$ in molten $Ca(NO_3)_2 \cdot 3.96H_2O$ being quite intense have been recorded here in order to ascertain the geometry of the metal ion. The solvent in the molten state helps in recording the absorption spectra of the solute.

Results and Discussion

The ligand-field (LF) spectrum (Fig. 2) of $Ni(NO_3)_2 \cdot 6.03H_2O$ in molten $Ca(NO_3)_2 \cdot 3.96H_2O$ consists of three bands. A relatively intense band at $\sim 25,640 \text{ cm}^{-1}$ and two weak bands with components at $\sim 14,280$ and $15,150$;

C H A P T E R - I I I

Temperature Dependence of Transport Behaviour of Molten
Salt Systems - The Application of VTF Equation

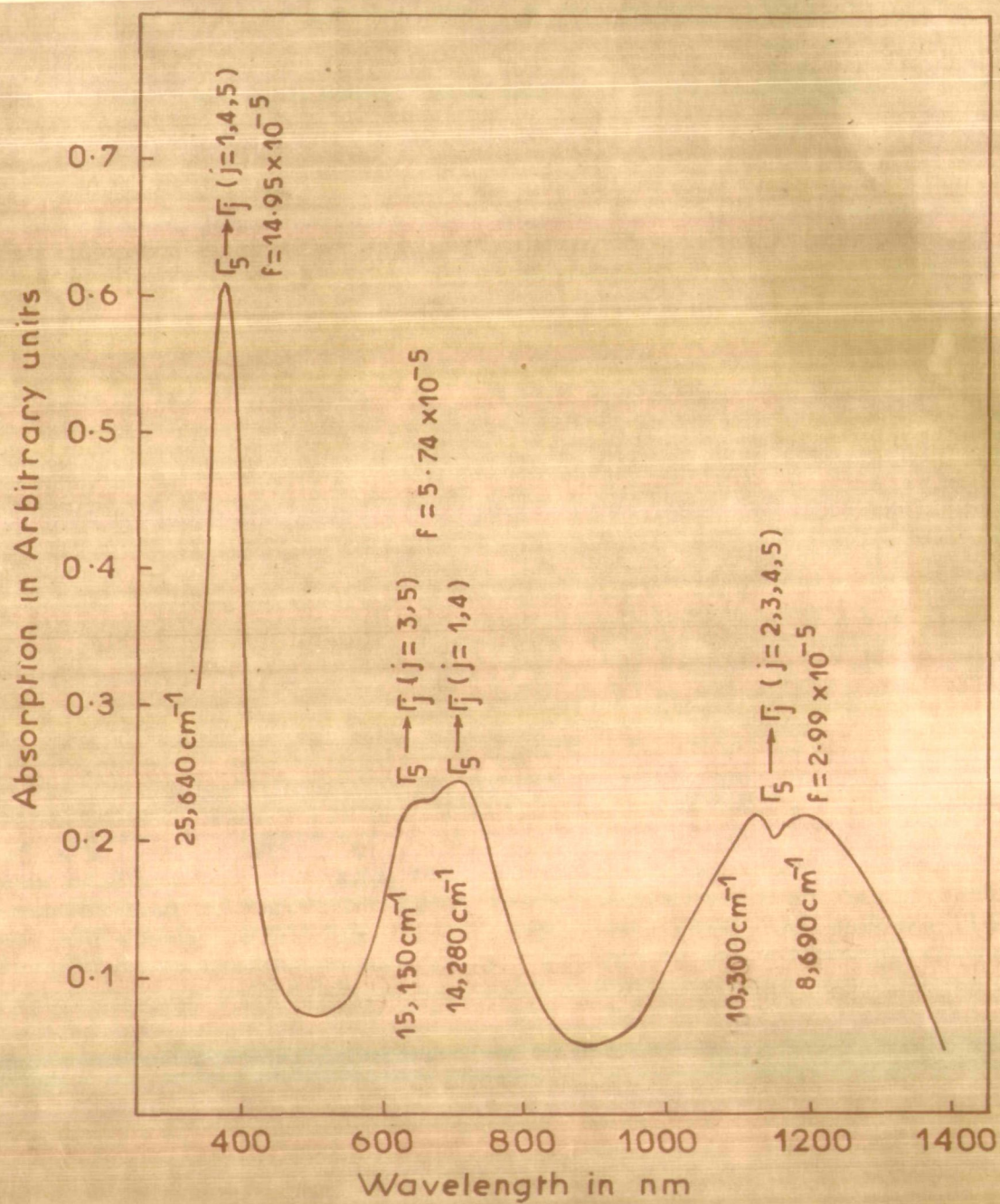


Fig. 2. Ligand-field spectrum of $\text{Ni}(\text{NO}_3)_2 \cdot 6.03\text{H}_2\text{O}$ in molten $\text{Ca}(\text{NO}_3)_2 \cdot 3.96\text{H}_2\text{O}$ (f is the oscillator or strength).

and at ~ 8690 and $\sim 10300 \text{ cm}^{-1}$, respectively, have been recorded. The identification of the absorbing species is based on the comparison of the recorded spectra with those reported earlier.⁸⁻¹⁰ The expected species may be identified as $\text{Ni}(\text{H}_2\text{O})_6^{2+}$ in which $\text{Ni}(\text{II})$ ion is surrounded by six water molecules in a regular octahedral arrangement. This observation is in agreement with the usual assignment of the intense band at $\sim 26,000 \text{ cm}^{-1}$ as was observed in the cases of crystalline $\text{NiSO}_4 \cdot 6\text{H}_2\text{O}$ and $\text{Ni}(\text{NO}_3)_2 \cdot 6\text{H}_2\text{O}$.⁸

The assignment of the bands is made by constructing the energy level diagram (Fig. 3) on the basis of four ligand-field parameter model using Liehr-Ballhausen matrices. The predicted spectrum of $\text{Ni}(\text{H}_2\text{O})_6^{2+}$ with $D_q = -907$, $\lambda = -275$, $B = 810$, and $C/B = 3.889 \text{ cm}^{-1}$ has been found to agree with that observed. Accordingly, the above three bands may be assigned as due to $\Gamma_5 \rightarrow \Gamma_j$ ($j = 1, 4, 5$), $\Gamma_5 \rightarrow \Gamma_j$ ($j = 1, 4$), $\Gamma_5 \rightarrow \Gamma_j$ ($j = 3, 5$), and $\Gamma_5 \rightarrow \Gamma_j$ ($j = 2, 3, 4, 5$) transitions, respectively.

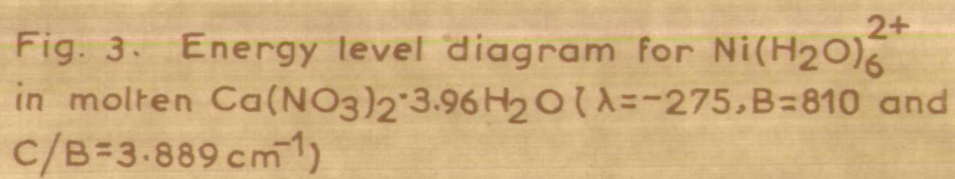


Fig. 3. Energy level diagram for $\text{Ni}(\text{H}_2\text{O})_6^{2+}$ in molten $\text{Ca}(\text{NO}_3)_2 \cdot 3.96\text{H}_2\text{O}$ ($\lambda = -275$, $B = 810$ and $C/B = 3.889 \text{ cm}^{-1}$)

C H A P T E R - I I I

Temperature Dependence of Transport Behaviour of Molten
Salt Systems - The Application of VTF Equation

Introduction

Many investigators have studied the temperature dependence of transport properties and various relations between temperature and transport behaviour have been proposed. One of the most widely quoted is the Arrhenius or Andrade equation which in the integrated form may be written as

$$\ln Y = \ln A_Y - E_Y/RT \quad (1)$$

where Y corresponds to fluidity, ϕ or equivalent conductance, \wedge , A_Y is a constant, R is the gas constant, T is the absolute temperature, and E_Y is the activation energy for the transport process and is independent of temperature. On the other hand, in the case of supercooled liquids, the temperature dependence of relaxation processes show departure from simple Arrhenius behaviour with a temperature dependent activation energy and the deviation becomes quite marked as the glass-transition temperature is approached. The Arrhenius equation also fails to account for the temperature dependence of transport properties under conditions of constant volume.¹¹ Batchinski¹² was the first to note that the proper independent variable to which the viscosity of a liquid should be related is not the temperature but the specific volume (v). Batchinski relation is of the form

$$\eta = B/(v - b)$$

where B and b are constants, the latter bearing some analogy to the co-volume of the Van der Waals equation. The constant b turns out to lie between the specific Volume of the solid and the liquid at the freezing point. It may be interpreted as the minimum specific volume at which flow can occur and (v - b) may be regarded as the free volume. This generalization appears to hold at relatively high specific volumes for simple Van der Waals type of liquids.¹³ In fact, Batchinski tested his equation for about eighty liquids and found that except for "associated" liquids it represents experimental data very well over a temperature range of about 100° . The important role of the free volume in the molecular transport was also stressed in the "hole" theories of Frenkel¹⁴ and Eyring and his associates.¹⁵ Frenkel explains the sharp increase in fluidity on fusion in broad outline by assuming that the fluidity of a body implies the possibility of the individual displacement of its molecules which in turn, require a certain amount of free volume within the liquid. The sudden increase in volume on fusion is sufficient to provide room for individual displacements of molecules from one equilibrium position to another, the two equilibrium positions being separated by a potential energy barrier. Frenkel considered holes in the liquid as any gap between the

spheres of influence of the constituent molecules, the hole having no definite size and shape. Eyring assumed a liquid to be quasi-crystalline to which a large number of equilibrium positions or holes have been added. Viscous flow, according to Eyring is assumed to take place by the activated jumping of an aggregate composed of one or more molecules from an initial normal configuration to a second normal position, the two being separated by an intermediate activated state. This is equivalent to passages of the system over a potential energy barrier. The height of the barrier is independent of the temperature, but is influenced by external forces acting on the liquid. However, Fox and Flory¹⁶ ascribed the glass transition to the falling of the free volume below some critical value. They introduced the concept that the molecular mobility at low temperature depends mainly upon the free volume. The probability of molecular jump is then governed by the probability that sufficient free volume is available in the region surrounding the molecule thereby producing a space into which the molecule can move - rather than by the rate at which a molecule can overcome an energy barrier.

Hildebrand¹⁷ recently showed that the fluidity of a simple liquid at atmospheric pressure and at any temperature is proportional to the fractional excess of its molar volume, V over the molal volume, V_0 , at which the

molecules are so closely crowded as to prevent viscous flow while still retaining rotational freedom. Hildebrand had applied this concept to modify the Batchinski equation to an equation of the form

$$\phi = B'(V - V_0)/V_0 \quad (2)$$

where B' is the constant of proportionality.

The above expressions, however, were found to be incapable of explaining the variation of viscosity with temperature in the cases of associated or highly supercooled liquids. Another approach to liquid viscosity is based upon the concept of free volume and Doolittle¹⁸ developed an empirical free volume equation

$$\phi = A' \exp \left[- B'' v_0 / v_f \right] \quad (3)$$

which accurately represents many viscosity data in the non-Arrhenius region. Here A' and B'' are constants, the latter is of the order of unity, v_f is the free volume defined as

$$v_f = v - v_0$$

where v is the specific volume mentioned above and v_0 is the limiting specific volume of the liquid at 0°K . Doolittle considered v_f/v_0 as relative free space which is defined as

the space arising from the total thermal expansion of the liquid without change of phase. At fixed pressure, v_f/v_0 is a function of temperature only. It is evident that Doolittle's equation predicts an abrupt decrease in fluidity in narrow temperature range where v_f becomes very small. Equation (3) may be modified to

$$Y = A'_Y \exp \left[- k'_Y / (V - V_0) \right] \quad (4)$$

where A'_Y and k'_Y are empirical constants. V_0 is defined as the molal volume at the glass-transition temperature, T_0 , and V is the molal volume at any temperature. Williams, Landel, and Ferry (WLF)¹⁹ were able to show that the dependence of fluidity on temperature in the glass transition region is satisfactorily described by Doolittle equation. They showed that the relaxation times for a large number of glass-forming substances are described by equation (3) in the glass transition range. They took the free volume to be

$$v_f = v_g \left[0.025 + \alpha (T - T_g) \right] \quad (5)$$

where v_g is the volume at the glass transition temperature, T_g and α is the difference between the thermal expansion coefficients of the liquid and that of the glass.

A further widely used empirical equation has

the form

$$\ln \eta = A'' + B''/T^n \quad (6)$$

Litovitz²⁰ has found that with $n = 3$ this equation represents the viscosity of associated liquids over a temperature range of some 100° above and below the melting point. Barlow and Lamb²¹ have also used this equation with $n = 4$ to describe the viscosity of lubricating oil over a 40° range of temperature. This form of equation is convenient for immediate analysis of experimental results since it involves no prior knowledge of the variation of free volume with temperature.

Cohen and Turnbull²² laid a theoretical foundation to the empirical equation of Doolittle based on the free volume concept. They considered that molecular transport occurs by the movement of molecules into voids, with a size greater than some critical value, formed by redistribution of the free volume. This is generally known as the "Free Volume Model" theory. In this model molecules are considered as hard spheres and they move with the gas kinetic velocity u but most of the time are confined to a cage bounded by their immediate neighbours. Occasionally there is a fluctuation in density which opens up a hole within a cage large enough to permit a considerable displacement of the molecule contained by it. Such a displacement gives

rise to diffusive motion only if another molecule jumps into the hole before the first can return to its original position. They defined the free volume v_f of a given molecule to be the volume within its cage less the volume of the molecule and it can be redistributed among the cage without change in overall energy. The probability of occurrence of a critical void adjacent to a given particle was shown to be an exponential function of the ratio of the critical void volume to the total free-volume; and the resulting expression obtained for diffusion coefficient was

$$D = ga^*u \exp \left[- \gamma v^*/v_f \right] \quad (7)$$

where g is a geometric factor equal to $1/6$, ' a^* ' is the jump distance or approximately the particle diameter for molecular liquids, u is the gas-kinetic velocity of the particle equal to $(3kT/m)^{1/2}$, γ is the factor to correct for the overlap of free-volume, v^* is the critical void volume and v_f is the total free volume. This equation was found to be identical to the Doolittle empirical relationship¹⁸ for viscosity. Assuming that v_f is approximately equal to the total thermal expansion of the liquid above T_0 , at which free volume begins to appear, then

$$v_f = \alpha v_m (T - T_0) \quad (8)$$

Here, α is the mean expansion coefficient in the range T to T_0 , and \bar{v}_m is the mean molecular volume derived from the molar volume. From equations (7) and (8), we get

$$D = ga^*(3kT/m)^{1/2} \exp \left[- \gamma v^* / \bar{v}_m (T - T_0) \right]$$

or

$$D = A''' T^{1/2} \exp \left[- k_Y / (T - T_0) \right] \quad (9)$$

where A''' and k_Y are constants. Now if $T_0 = 0^\circ\text{K}$ or $T \gg T_0$, equation (9) may formally become equivalent to the expression of the rate theory. On the other hand, if $T_0 > 0^\circ\text{K}$, it follows that the probability of molecular motion decreases rapidly as T_0 is approached from above, and the liquid will become rigid, i.e., will transform to a glass in the vicinity of T_0 if crystallization does not occur.

Making use of the Stokes-Einstein and Nernst-Einstein relations,²³ Angell expressed the above expression in the form

$$Y = A_Y T^{-1/2} \exp \left[- k_Y / (T - T_0) \right] \quad (10)$$

A_Y and k_Y are constants characteristic of the transport process and the chemical system. T_0 is another constant independent of the transport process and depends on the chemical system alone provided the external pressure is kept constant. The T_0 has been called the "ideal glass

transition" or "zero mobility" temperature at the specified concentration and interpreted as the temperature below which no further changes in internal energy by means of rearrangement of particles into configurations of lower potential energy are possible. In most cases T_0 is expected to be somewhat lower than the experimental glass transition temperature, T_g , because of the long relaxation times encountered in the measurement of T_g . This is due to the fact that the glass transition itself is a time-dependent phenomenon. The temperature of the transition, T_g is lower the more slowly the experiment used to determine it is performed. The molecular relaxation time at the transition temperature may be deduced from a simple Maxwell model of a viscoelastic liquid which shows that

$$\eta = TG_{\infty} \quad (11)$$

where G_{∞} is the limiting rigidity modulus of the liquid. G_{∞} is typically 10^9 to 10^{11} dynes/cm², and Litovitz²⁴ showed that it varies much less rapidly with temperature than does the viscosity. Equation (11) shows that at the T_g temperature, the relaxation time for molecular motion exceeds 10^3 seconds which is comparable with the duration of a normal experiment. At temperature below T_g but above T_0 the relaxation times are so long that, in an experiment of normal duration, the properties of the liquid are essen-

tially those which appear to have been frozen in at T_g . Equation (11) also shows that an experiment of infinite duration would be required to provide a glass in equilibrium at T_0 , at which temperature the viscosity is infinite and the free volume zero.

Moreover, in equation (10) the contribution of the preexponential temperature term to the temperature dependence of transport properties has been found to be negligible in most cases and the exponential part predominantly accounts for the non-Arrhenius transport behaviour. Therefore, sometimes in literature equation (10) has also been employed without the preexponential temperature term. Equation (10) is also known as the Vogel-Tammann-Fulcher (VTF) equation. Several authors successfully employed this equation before the establishment of free volume model to describe the non-Arrhenius transport behaviours in glass forming melts.

The transport properties of glass-forming molten mixtures of manganese (II) chloride tetrahydrate with cadmium nitrate tetrahydrate, and those of ammonium thiocyanate, sodium thiocyanate, and nickel (II) nitrate hexahydrate with calcium nitrate tetrahydrate have been studied here as function of temperature. The data have been analysed and interpreted in terms of the VTF equation and are presented in this chapter.

Results and Discussion

The measured density of molten cadmium nitrate tetrahydrate at 25°C is found to be 0.43 per cent higher than that reported by Ewing and Hertey.² In the cases of the three separate samples of molten calcium nitrate tetrahydrate taken from three different bottles the measured densities in the respective cases are found to be 0.98 and 0.57 per cents lower and 0.17 per cent higher than those reported by Ewing and Mikovsky.³ Such a comparison of measured densities gave the actual H_2O/M^{2+} ($M^{2+} = Cd^{2+}$ or Ca^{2+}) ratios as 4.03, 4.23, 4.1, and 3.96 in the respective hydrated melts. However, due to the lack of precise density versus concentration data in literature for manganese (II) chloride tetrahydrate and nickel (II) nitrate hexahydrate, the density comparison method could not be employed to determine the exact water of crystallization in these melts. Therefore, the correct H_2O/Mn^{2+} and H_2O/Ni^{2+} mol ratios have been estimated by the EDTA titration⁴ method as described in the experimental section and were found to be equal to 4.00 and 6.03, respectively. The densities of pure solvents as well as of their mixtures in the molten state have been found to vary linearly with temperature and, hence, least-squares fitted to a linear function of the form $\rho = a - bT(^{\circ}K)$ where ρ denotes the density, while a and b are empirical constants. The

computed values of these constants along with the molar volume, V_m are given in Table 1. The values of thermal expansivities are listed in Table 2.

The measured viscosity and conductance data of $\text{Cd}(\text{NO}_3)_2 \cdot 4.03\text{H}_2\text{O}$ at 40°C were found to differ by ~ 20 and ~ 0.44 per cents, respectively, when compared with those reported for $\text{Cd}(\text{NO}_3)_2 \cdot 4.07\text{H}_2\text{O}$.²⁵ A difference of ~ 30 and ~ 36 per cents for $\text{Ca}(\text{NO}_3)_2 \cdot 4.23\text{H}_2\text{O}$ and ~ 9 and ~ 17 per cents for $\text{Ca}(\text{NO}_3)_2 \cdot 4.1\text{H}_2\text{O}$ at 50°C were observed from those reported earlier.²⁶ Also a difference of ~ 6 per cent in the viscosity for $\text{Ca}(\text{NO}_3)_2 \cdot 3.96\text{H}_2\text{O}$ may be noted. However, this value is somewhat low. Such a discrepancy in viscosities and conductances observed here may be accorded to the difference in water contents of the corresponding melts studied. It may, however, be noted that a difference of ~ 2 per cent in viscosities and conductances for every 0.01 change in the $\text{H}_2\text{O}/\text{M}^{2+}$ ($\text{M}^{2+} = \text{Cd}^{2+}$ or Ca^{2+}) ratio are in good agreement with those suggested by Moynihan et al.²⁵

Both conductance and fluidity data (Tables 3-6) exhibit a non-Arrhenius temperature dependence for the systems studied and are, therefore, least-squares fitted to equation (10). The corresponding parameters along with the standard deviations in $\ln \Lambda$ and $\ln \phi$ are listed in Tables 7-10. The linearity of the plots (Figs. 4-7) of $\ln Y$ ($= \phi$ or Λ) $T^{1/2}$ versus $1/(T - T_0)$ reinforce such an attempt to explain

TABLE 1 : Parameters for Density Equation* and Molar
Volumes for Molten Mixtures

Melt	Mol %	a	b x 10 ⁻³	V _m at 55°C (cm ³ /mol)
Cd(NO ₃) ₂ ·4.03H ₂ O + MnCl ₂ ·4.00H ₂ O	Mn ²⁺			
	0.00	2.6445	1.1534	136.32
	2.27	2.6067	1.0640	135.72
	4.14	2.6216	1.1243	135.09
	6.63	2.5763	1.0630	134.65
	9.07	2.5708	1.0503	134.24
	12.31	2.5583	1.0480	133.34
Ca(NO ₃) ₂ ·4.23H ₂ O + NH ₄ CNS	NH ₄ ⁺			
	0.00	1.9635	0.7752	140.52
	10.11	1.9520	0.7841	131.93
	20.02	1.9185	0.7639	124.31
	30.35	1.8783	0.7451	116.53
	40.48	1.8424	0.7526	108.94
	51.30	1.7823	0.7054	100.60
	63.42	1.7035	0.6642	91.63

(Continued)

TABLE 1 : (Continued)

Melt	Mol %	a	b x 10 ⁻³	V _m at 55°C (cm ³ /mol)
Ca(NO ₃) ₂ ·4.1H ₂ O	Na ⁺			
+ NaCNS	0.00	1.9813	0.7941	138.23
	5.58	1.9745	0.7884	133.53
	10.28	1.9782	0.8009	129.27
	16.02	1.9738	0.8014	124.35
	20.13	1.9704	0.7926	120.62
	24.84	1.9702	0.8002	117.03
Ca(NO ₃) ₂ ·3.96H ₂ O	Ni ²⁺			
+ Ni(NO ₃) ₂ ·6.03H ₂ O	0.00	2.0009	0.8317	136.33
	10.19	2.0068	0.8069	138.50
	19.80	2.0085	0.8040	141.37
	29.10	2.0072	0.7670	143.46
	39.83	2.0377	0.8203	145.79
	49.65	2.0339	0.7826	148.18
	60.83	2.0539	0.7990	150.46

* The Density Equation is ρ (gm/cm³) = a - bT(°K)

TABLE 2 : Expansivities at 55°C for Molten Salt Systems

Mol % Mn ²⁺	10 ⁴ α (deg ⁻¹)	Mol % NH ₄ ⁺	10 ⁴ α (deg ⁻¹)	Mol % Na ⁺	10 ⁴ α (deg ⁻¹)	Mol % Ni ²⁺	10 ⁴ α (deg ⁻¹)
0.00	5.0898	0.00	4.5351	0.00	4.6147	0.00	4.8131
2.27	4.7129	10.11	4.6266	5.58	4.5952	10.19	4.6320
4.14	4.9905	20.02	4.5799	10.28	4.6688	19.80	4.6082
6.63	4.6683	30.35	4.5603	16.02	4.6840	29.10	4.3689
9.07	4.7178	40.48	4.7169	20.13	4.6344	39.83	4.6385
12.31	4.7321	51.30	4.5482	24.84	4.6860	49.65	4.4038
		63.42	4.4708			60.83	4.4596

TABLE 3 : Equivalent Conductance ($\text{cm}^2 \text{equiv}^{-1} \text{ohm}^{-1}$) and Fluidity (P^{-1}) Data as
a Function of Temperature for $\text{Cd}(\text{NO}_3)_2 \cdot 4.03\text{H}_2\text{O}-\text{MnCl}_2 \cdot 4.00\text{H}_2\text{O}$ Melts*

T, °K	Mol % Mn ²⁺					
	0.00	2.27	4.14	6.63	9.07	12.31
308.0	1.2963 (2.0960)	1.1741 (1.7977)	0.9964 (1.5477)	1.1175 (1.8025)	1.0328 (1.6401)	- -
313.0	1.5930 (2.5858)	1.4341 (2.2397)	1.2549 (1.9454)	1.3550 (2.2348)	1.2804 (2.0527)	- -
318.0	1.9041 (3.1975)	1.7484 (2.7932)	1.5332 (2.4372)	1.6393 (2.7787)	1.5582 (2.5596)	- -
323.0	2.2978 (3.8420)	2.0766 (3.3919)	1.8561 (2.9951)	1.9718 (3.3795)	1.8588 (3.1125)	1.7655 (2.9994)
328.0	2.6468 (4.5084)	2.4769 (4.0938)	2.1916 (3.6328)	2.3418 (4.0732)	2.2072 (3.7608)	2.1068 (3.6288)
333.0	3.0234 (5.4576)	2.8374 (4.8626)	2.5749 (4.3344)	2.7067 (4.8340)	2.5716 (4.4701)	2.4638 (4.3238)
338.0	3.4023 (6.3939)	3.2531 (5.7316)	2.9675 (5.1140)	3.1032 (5.6792)	2.9305 (5.2670)	2.8429 (5.1015)

(Continued)

TABLE 3 : (Continued)

T, °K	Mol % Mn ²⁺					
	0.00	2.27	4.14	6.63	9.07	12.31
343.0	3.9796 (7.4101)	3.6955 (6.6450)	3.4264 (5.9457)	3.5550 (6.5501)	3.3572 (6.1501)	3.2678 (5.9270)
348.0	4.4885 (8.4538)	4.1675 (7.6121)	3.8912 (6.8148)	4.0561 (7.4349)	3.8346 (7.0422)	3.7506 (6.7413)
353.0	5.1430 (9.5202)	4.7292 (8.5940)	4.4583 (7.7997)	4.5881 (8.4696)	4.4273 (8.0399)	4.2093 (7.7346)

* Fluidity data are within parentheses.

TABLE 4 : Equivalent Conductance ($\text{cm}^2 \text{equiv}^{-1} \text{ohm}^{-1}$) and Fluidity (P^{-1}) Data
as a Function of Temperature for $\text{Ca}(\text{NO}_3)_2 \cdot 4.23\text{H}_2\text{O} \cdot \text{NH}_4\text{CNS}$ Melts*

T, °K	Mol % NH_4^+					
	0.00	10.11	20.02	30.35	40.48	51.30
313.0	1.2494 (1.2458)	1.1815 (1.1096)	1.0847 (1.2012)	1.4226 (1.3377)	1.7057 (1.4126)	2.0583 (1.8137)
318.0	1.6165 (1.6000)	1.4361 (1.3941)	1.3475 (1.5868)	1.6477 (1.7242)	2.0876 (1.7894)	2.4908 (2.3295)
323.0	1.8826 (2.0045)	1.7493 (1.7614)	1.6554 (1.9755)	1.9450 (2.1638)	2.4955 (2.2004)	2.9306 (2.8407)
328.0	2.2456 (2.4539)	2.0965 (2.2001)	1.9691 (2.4844)	2.3394 (2.6988)	3.0275 (2.9496)	3.3124 (3.4084)
333.0	2.6267 (2.9736)	2.4820 (2.5994)	2.3174 (3.0301)	2.7055 (3.1537)	3.5970 (3.4151)	3.8190 (4.1315)
338.0	3.1323 (3.5695)	2.9223 (3.1544)	2.6669 (3.6342)	3.1197 (3.7769)	4.1480 (3.9261)	4.2747 (4.8137)

(Continued)

TABLE 4 : (Continued)

T, °K	Mol % NH ₄ ⁺						
	0.00	10.11	20.02	30.35	40.48	51.30	63.42
343.0	3.5845 (4.3700)	3.3552 (3.7661)	3.1379 (4.2731)	3.5690 (4.4663)	4.7783 (5.0043)	4.9292 (5.6596)	5.7862 (7.0180)
348.0	4.0510 (4.9065)	3.8535 (4.3879)	3.5460 (4.9771)	4.1665 (5.1549)	5.4595 (5.8668)	5.3557 (6.4160)	6.4691 (7.8846)
353.0	4.5440 (5.6644)	4.4143 (5.1214)	4.0281 (5.7409)	4.6100 (5.9485)	6.1404 (6.7003)	5.9944 (7.3335)	7.1727 (8.8715)

* Fluidity data are within parentheses.

TABLE 5 : Equivalent Conductance ($\text{cm}^2 \text{equiv}^{-1} \text{ohm}^{-1}$) and Fluidity (P^{-1}) Data
as a Function of Temperature for $\text{Ca}(\text{NO}_3)_2 \cdot 4.1\text{H}_2\text{O}$ -NaCNS Melts*

T, °K	Mol % Na^+					
	0.00	5.58	10.28	16.02	20.13	24.84
313.0	0.9824 (1.0170)	0.8854 (0.9906)	0.5635 (0.9248)	0.5105 (0.9028)	0.5037 (0.8107)	-
318.0	1.2191 (1.3332)	1.0861 (1.2989)	0.7533 (1.2185)	0.6529 (1.1799)	0.6441 (1.0816)	-
323.0	1.4606 (1.6752)	1.3437 (1.6499)	0.9376 (1.5552)	0.8068 (1.5117)	0.7959 (1.3992)	0.7233 (1.3370)
328.0	1.7467 (2.0782)	1.6391 (2.0515)	1.0905 (1.9436)	0.9949 (1.8938)	0.9815 (1.7660)	0.8876 (1.7321)
333.0	2.1388 (2.5453)	2.0354 (2.5218)	1.3042 (2.4073)	1.1914 (2.3410)	1.1753 (2.1866)	1.0753 (2.1591)
338.0	2.1870 (3.0801)	2.4001 (3.0529)	1.6097 (2.9234)	1.4178 (2.8659)	1.3986 (2.6792)	1.2814 (2.6530)
343.0	2.5690 (3.6589)	2.7674 (3.6410)	1.8096 (3.4874)	1.6142 (3.4211)	1.5922 (3.2220)	1.5013 (3.1899)

(Continued)

TABLE 5 : (Continued)

T, °K	Mol % Na ⁺					
	0.00	5.58	10.28	16.02	20.13	24.84
348.0	2.9449 (4.2858)	3.2079 (4.2677)	2.0124 (4.0957)	1.8719 (4.0354)	1.8466 (3.7832)	1.7469 (3.7696)
353.0	3.3750 (4.9975)	3.6611 (4.9697)	2.3874 (4.7719)	2.1853 (4.7015)	2.1043 (4.4362)	2.0142 (4.4175)

* Fluidity data are within parentheses.

TABLE 6 : Fluidity (P^{-1}) Data as a Function of Temperature for $\text{Ca}(\text{NO}_3)_2 \cdot 3.96\text{H}_2\text{O}-$
 $\text{Ni}(\text{NO}_3)_2 \cdot 6.03\text{H}_2\text{O}$ Melts

T, °K	Mol % Ni^{2+}					
	0.00	10.19	19.80	29.10	39.83	49.65
308.0	0.6482	0.6820	0.8280	0.8880	0.9415	1.0402
313.0	0.8622	0.9052	1.0778	1.1466	1.1975	1.3160
318.0	1.1365	1.1762	1.3919	1.4728	1.5294	1.6645
323.0	1.4589	1.4986	1.7493	1.8446	1.9053	2.0767
328.0	1.8320	1.8778	2.1659	2.2563	2.3048	2.5273
333.0	2.2649	2.3137	2.6410	2.7504	2.8234	3.0429
338.0	2.7683	2.8155	3.1756	3.2877	3.3771	3.6054

(continued)

TABLE 6 : (continued)

T, °K	Mol % Ni ²⁺					
	0.00	10.19	19.80	29.10	39.83	49.65
343.0	3.3271	3.3648	3.7690	3.8818	3.9769	4.2382
348.0	3.9427	3.9626	4.4101	4.5151	4.6085	4.8890
353.0	4.5890	4.6007	5.0852	5.1843	5.2798	5.5841
358.0	5.3118	5.3282	5.8568	5.9598	6.0680	6.3637
						6.4338

TABLE 7 : Computed Parameters for Equation(10)for the Fluidity and Equivalent

Conductance of $\text{Cd}(\text{NO}_3)_2 \cdot 4.03\text{H}_2\text{O}-\text{MnCl}_2 \cdot 4.00\text{H}_2\text{O}$ Melts

Mol % Mn^{2+}	A_ϕ	k_ϕ	$T_{o,\phi}$	Std. dev. in $\ln \phi$	A_Λ	k_Λ	$T_{o,\Lambda}$	Std. dev. in $\ln \Lambda$
0.00	11163.0	664.10	192.22	0.012	3610.0	585.00	192.56	0.016
2.27	10973.0	673.21	193.20	0.006	3532.7	587.39	193.85	0.006
4.14	10760.0	672.50	194.10	0.008	3460.0	589.00	194.80	0.025
6.63	10520.0	663.00	195.35	0.018	3369.8	575.75	196.49	0.009
9.07	10320.0	664.50	196.50	0.017	3290.2	580.50	197.80	0.013
12.31	10002.0	664.00	198.10	0.015	3180.0	576.00	199.50	0.004

TABLE 8 : Computed Parameters for Equation(10)for the Fluidity and Equivalent

Conductance of $\text{Ca}(\text{NO}_3)_2 \cdot 4.23\text{H}_2\text{O} \cdot \text{NH}_4\text{CNS}$ Melts

Mol % NH_4^+	A_ϕ	k_ϕ	$T_{O,\phi}$	Std. dev. in $\ln \phi$	A_λ	k_λ	$T_{O,\lambda}$	Std. dev. in $\ln \lambda$
0.00	9140.5	672.00	201.70	0.013	3620.0	567.00	201.31	0.015
10.11	9260.4	672.10	200.40	0.014	3695.4	570.00	199.90	0.024
20.02	9382.3	672.13	199.17	0.030	3775.4	563.00	198.75	0.031
30.35	9500.9	671.00	198.00	0.016	3861.0	568.50	197.40	0.020
40.48	9620.0	671.50	196.80	0.059	3935.0	570.00	196.50	0.035
51.30	9773.0	672.00	195.33	0.008	4021.5	563.00	194.50	0.030
63.42	9920.0	670.00	193.72	0.024	4110.0	562.80	192.70	0.024

TABLE 9 : Computed Parameters for Equation(10) for the Fluidity and Equivalent Conductance of $\text{Ca}(\text{NO}_3)_2 \cdot 4.1\text{H}_2\text{O-NaCNS}$ Melts

Mol % Na^+	A_ϕ	k_ϕ	$T_{O,\phi}$	Std. dev. in $\ln \phi$	A_λ	k_λ	$T_{O,\lambda}$	Std. dev. in $\ln \lambda$
0.00	8357.0	670.00	203.90	0.004	3300.0	580.00	203.60	0.063
5.58	8461.2	670.00	205.08	0.004	3370.0	590.00	204.50	0.019
10.28	8555.2	670.02	206.00	0.003	3460.0	593.20	205.80	0.029
16.02	8668.1	671.00	207.15	0.009	3550.0	592.00	207.00	0.014
20.13	8740.6	671.10	207.99	0.004	3620.0	586.20	208.00	0.019
24.84	8841.0	670.00	209.00	0.013	3700.6	586.40	208.90	0.007

TABLE 10 : Computed Parameters for Equation(10)for the
Fluidity of $\text{Ca}(\text{NO}_3)_2 \cdot 3.96\text{H}_2\text{O}-\text{Ni}(\text{NO}_3)_2 \cdot 6.03\text{H}_2\text{O}$
Melts

Mol % Ni^{2+}	A_ϕ	k_ϕ	$T_{o,\phi}$	Std. Dev. in $\ln \phi$
0.00	8443.8	671.00	206.60	0.006
10.19	8325.3	677.05	204.75	0.006
19.80	8175.0	671.00	202.00	0.006
29.10	8025.0	672.00	200.50	0.004
39.83	7875.0	671.20	199.41	0.009
49.65	7725.0	671.50	197.00	0.008
60.83	7600.0	668.70	196.55	0.006

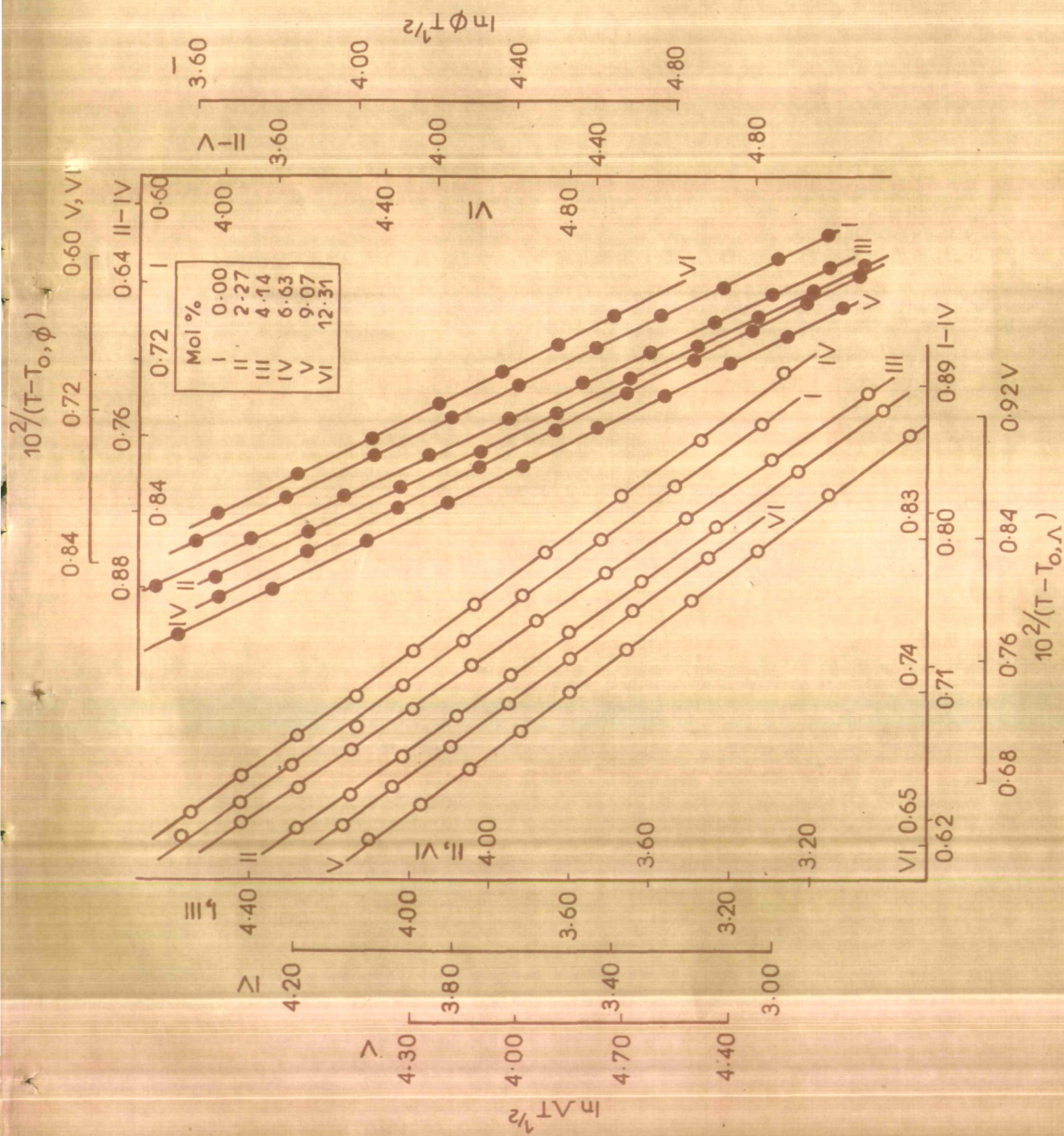


Fig. 4. Plots of $\ln \gamma (= \phi \text{ or } \Lambda) T^{1/2}$ vs. $1/(T-T_0)$ for molten $\text{Cd}(\text{NO}_3)_2 \cdot 4.03\text{H}_2\text{O} - \text{MnCl}_2 \cdot 4.00 \text{H}_2\text{O}$ systems.

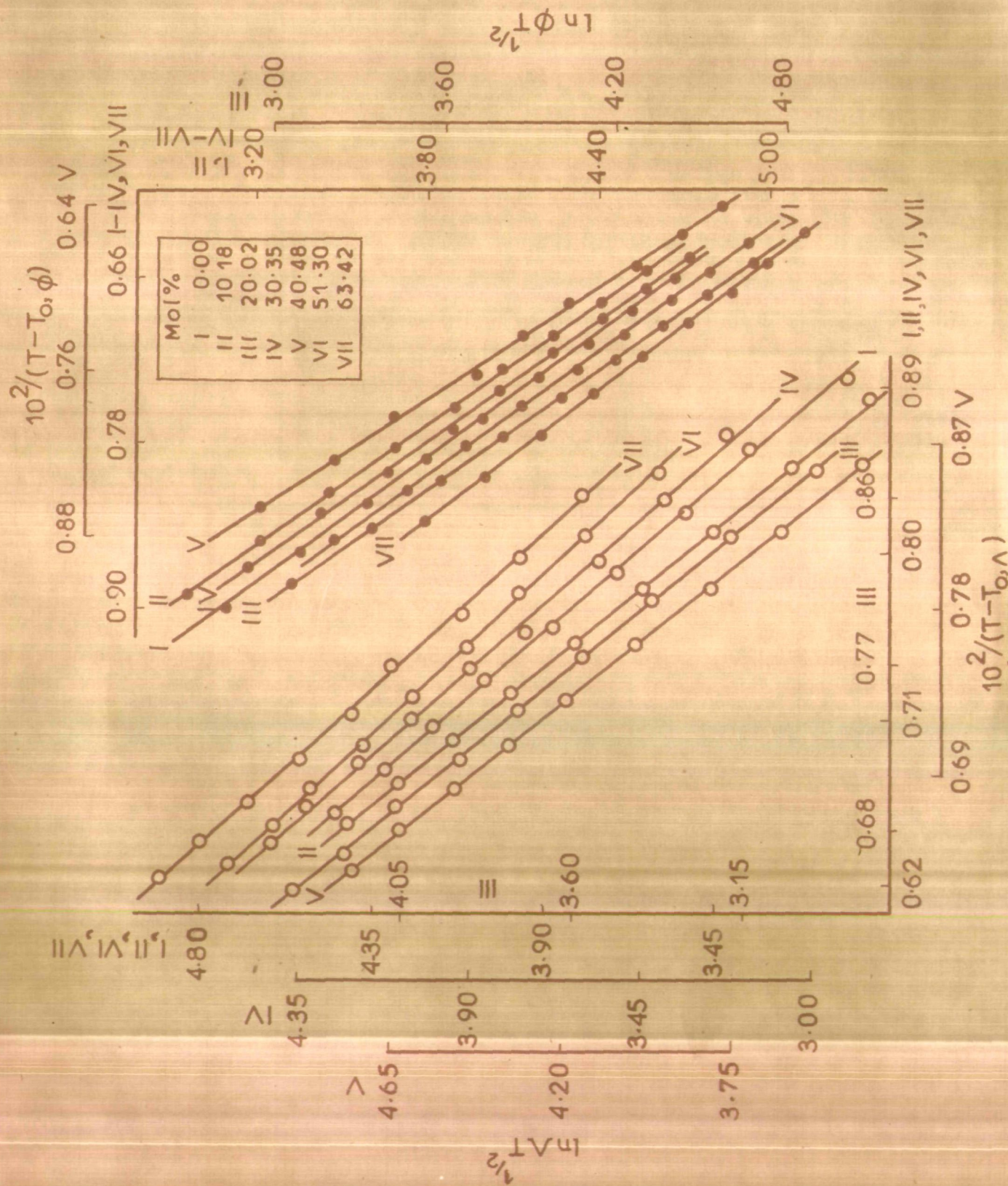


Fig. 5. Plots of $\ln \gamma (= \phi \text{ or } \Lambda)$ vs. $1/(T-T_0)$ for molten $\text{Ca}(\text{NO}_3)_2 \cdot 4.23\text{H}_2\text{O} - \text{NH}_4\text{CNS}$ systems.

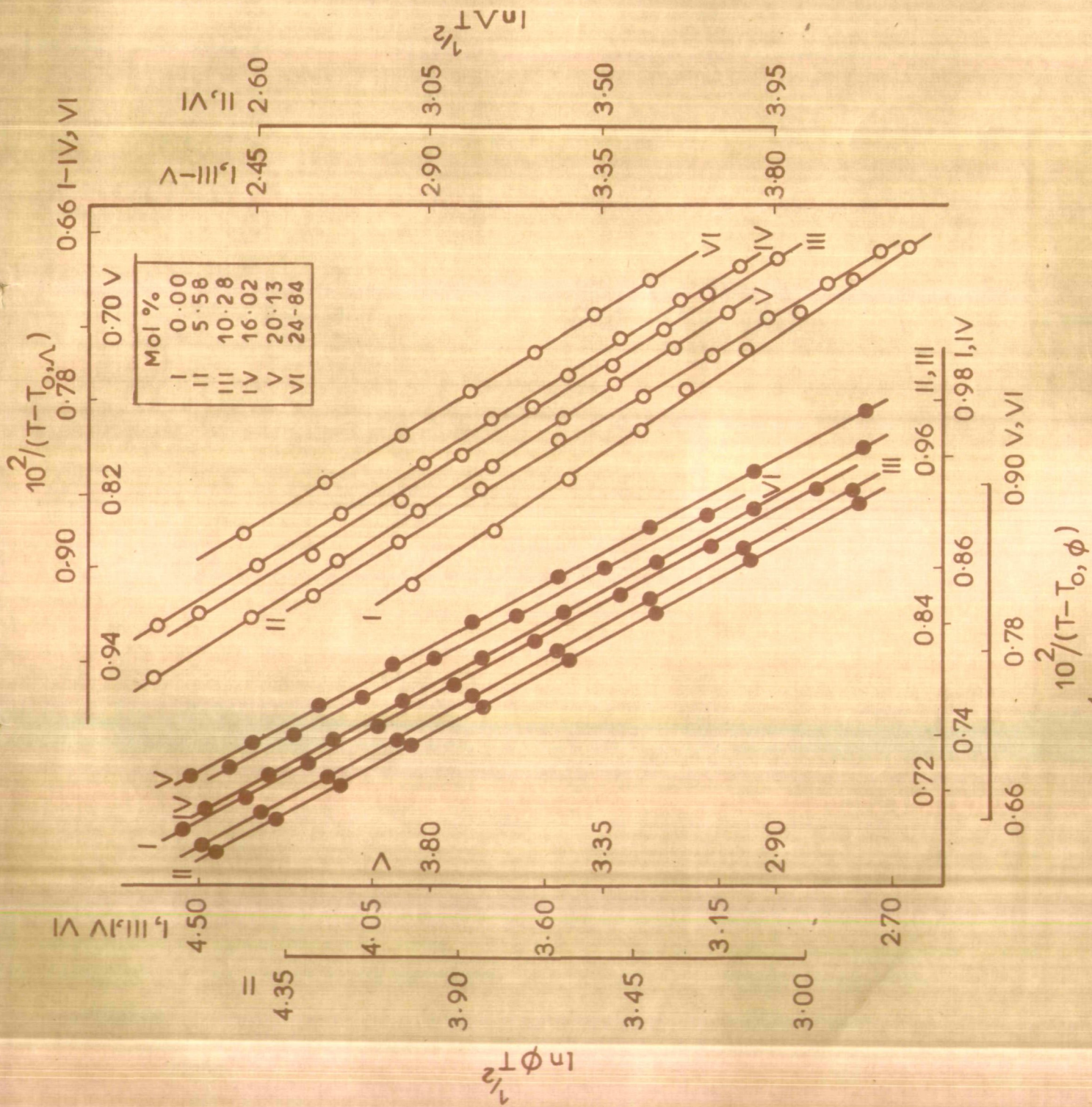


Fig. 6. Plots of $\ln \gamma$ ($= \phi$ or Λ) $T^{1/2}$ vs. $1/(T-T_0, \phi)$ for molten $\text{Ca}(\text{NO}_3)_2 \cdot 4\text{H}_2\text{O}$ - NaCNS systems.

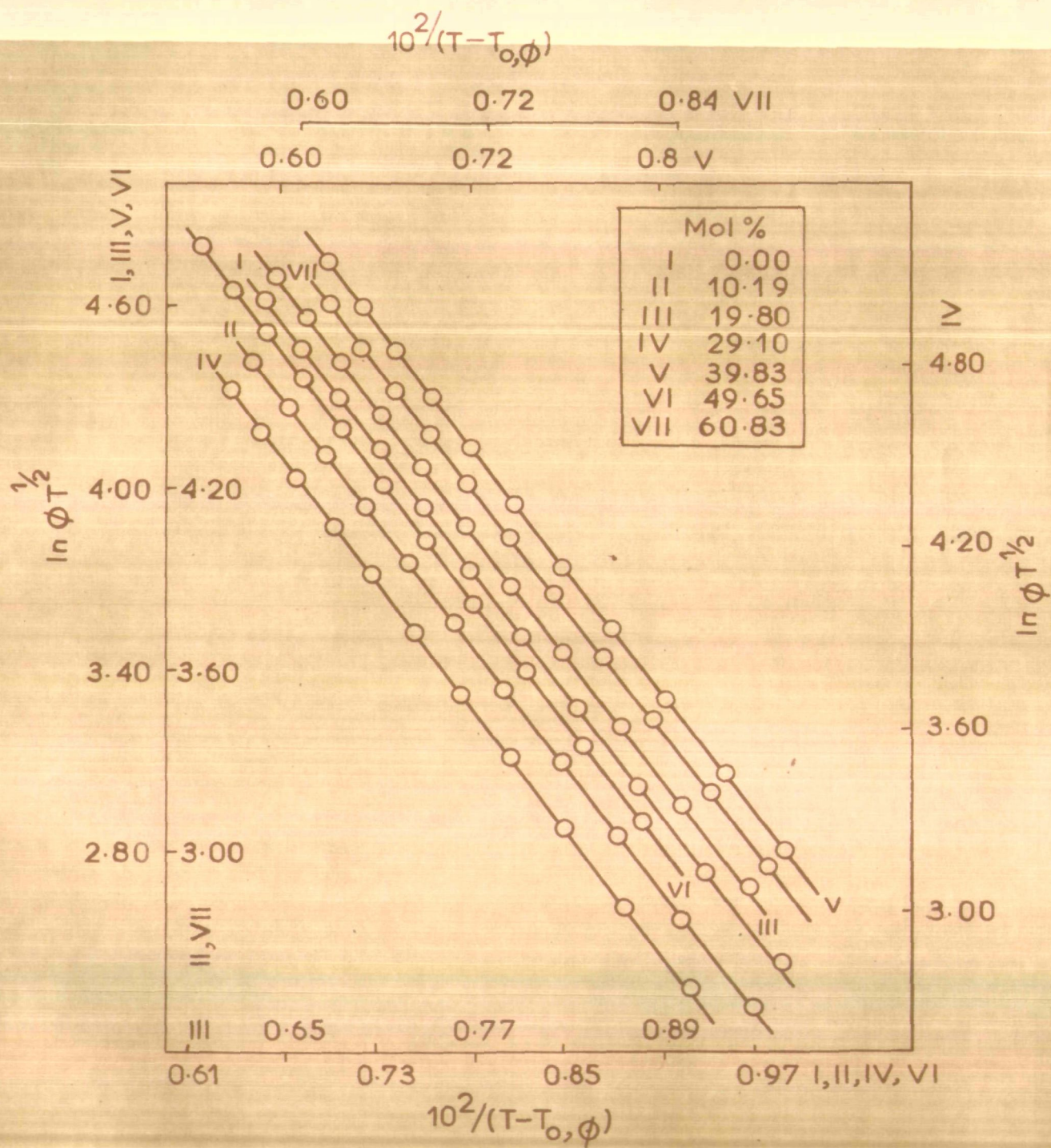


Fig. 7. Plots of $\ln \phi$ vs. $1/(T - T_o, \phi)$ for molten $\text{Ca}(\text{NO}_3)_2 \cdot 3.96\text{H}_2\text{O} - \text{Ni}(\text{NO}_3)_2 \cdot 6.03\text{H}_2\text{O}$ systems.

the transport behaviour of all the systems under investigation. The Hildebrand equation (2), on the other hand, was found to be incapable of explaining the transport behaviour in the present systems. However, the linear plots (Figs 8-11) of $\ln Y$ ($= \phi$ or Λ) versus $1/(V - V_0)$ signify the feasibility of equation (4) in such an analysis. The molar intrinsic volumes employed in these plots and other computed parameters of equation (4) are given in Tables 11-14.

The conventional activation energies, E_Λ and E_ϕ , were computed from the corresponding derivatives (Appendix C) and their corrected values are given in Tables 15-18.

Several sets of computed values of A_Y , k_Y , and T_0 were obtained with reasonable standard deviations which may explain the data well. Nevertheless, in order to obtain meaningful parameters the dependence of A_Y and k_Y on the value of T_0 should be examined. The values of T_0 for the system under study do not seem to depend largely on concentration, hence, one does not expect meaningful trends in the concentration dependences of the A_Y and k_Y terms.

Angell and Brassel²⁷ pointed out that k_Y varies linearly with T_0 in aqueous melts of calcium nitrate tetrahydrate and substituted DT_0 for k_Y in equation (10) where D is taken as independent of concentration. Currently

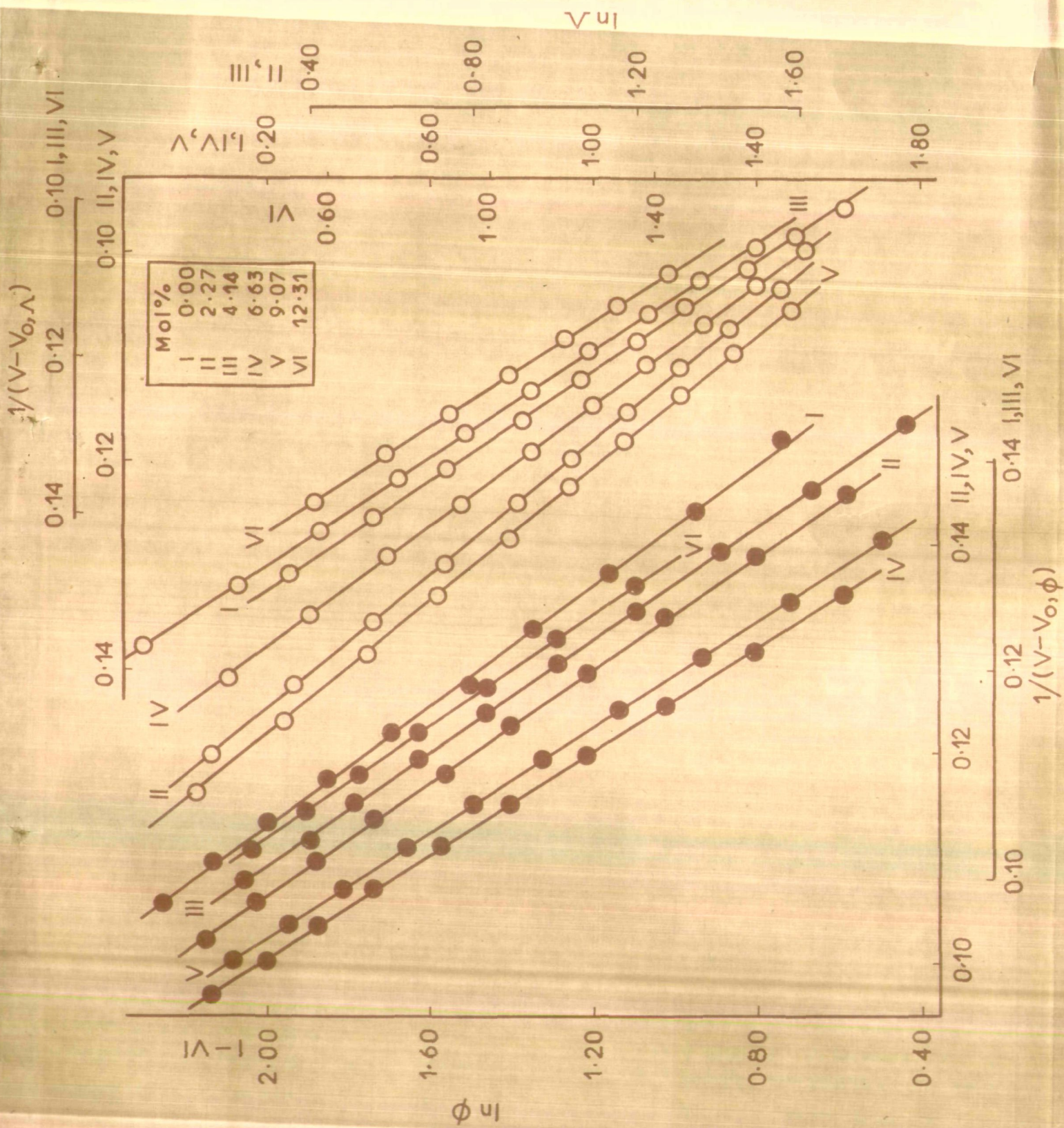


Fig. 8. Plots of $\ln \gamma (= \phi \text{ or } \Lambda)$ vs. $1/(V - V_0)$ for molten $\text{Cd}(\text{NO}_3)_2 \cdot 4.03\text{H}_2\text{O} - \text{MnCl}_2 \cdot 4.00\text{H}_2\text{O}$ systems.

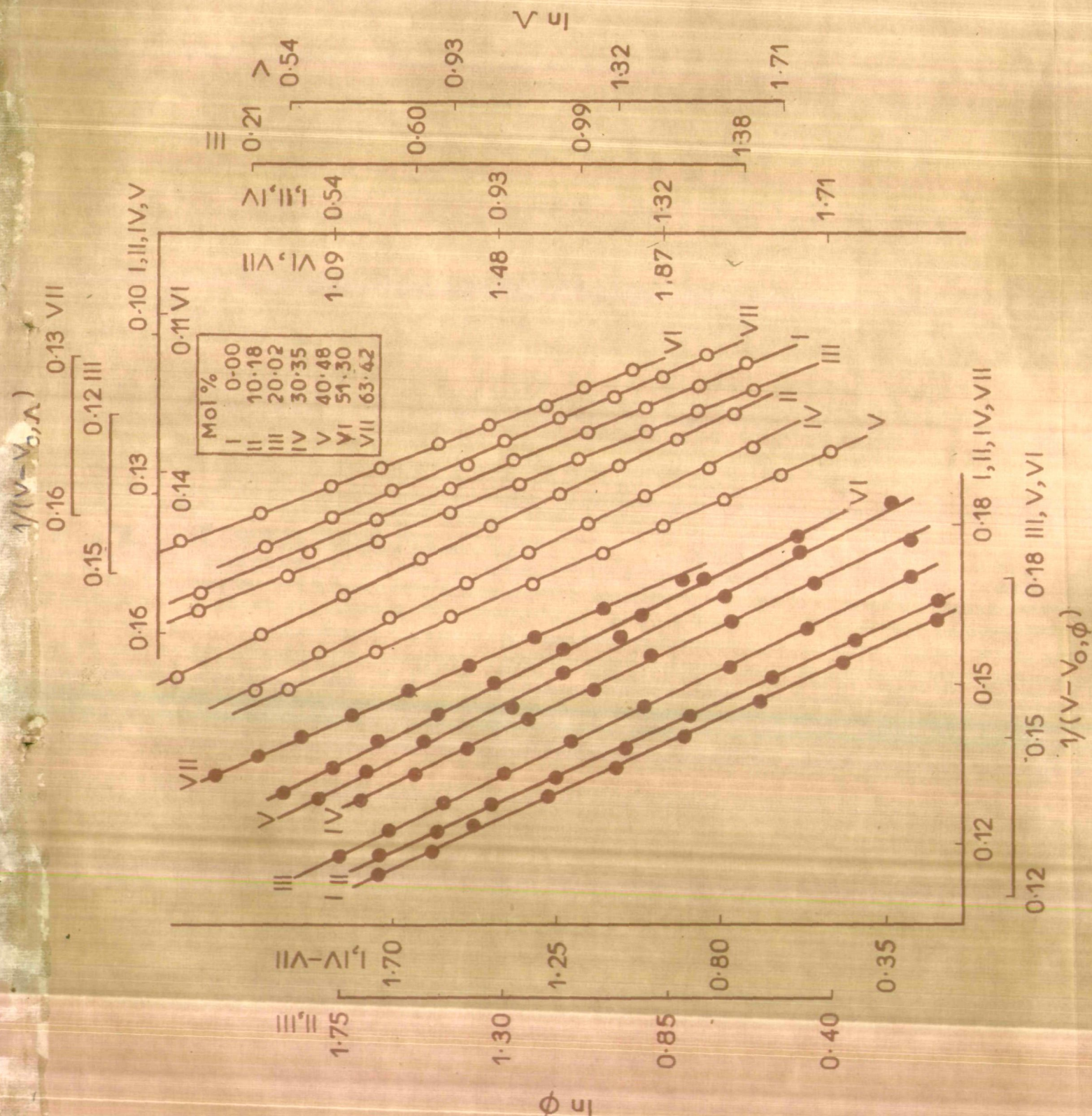


Fig. 9. Plots of $\ln \gamma (= \phi \text{ or } \Lambda)$ vs. $1/(V-V_0)$ for molten $\text{Ca}(\text{NO}_3)_2 \cdot 4.23\text{H}_2\text{O} - \text{NH}_4\text{CNS}$ systems.

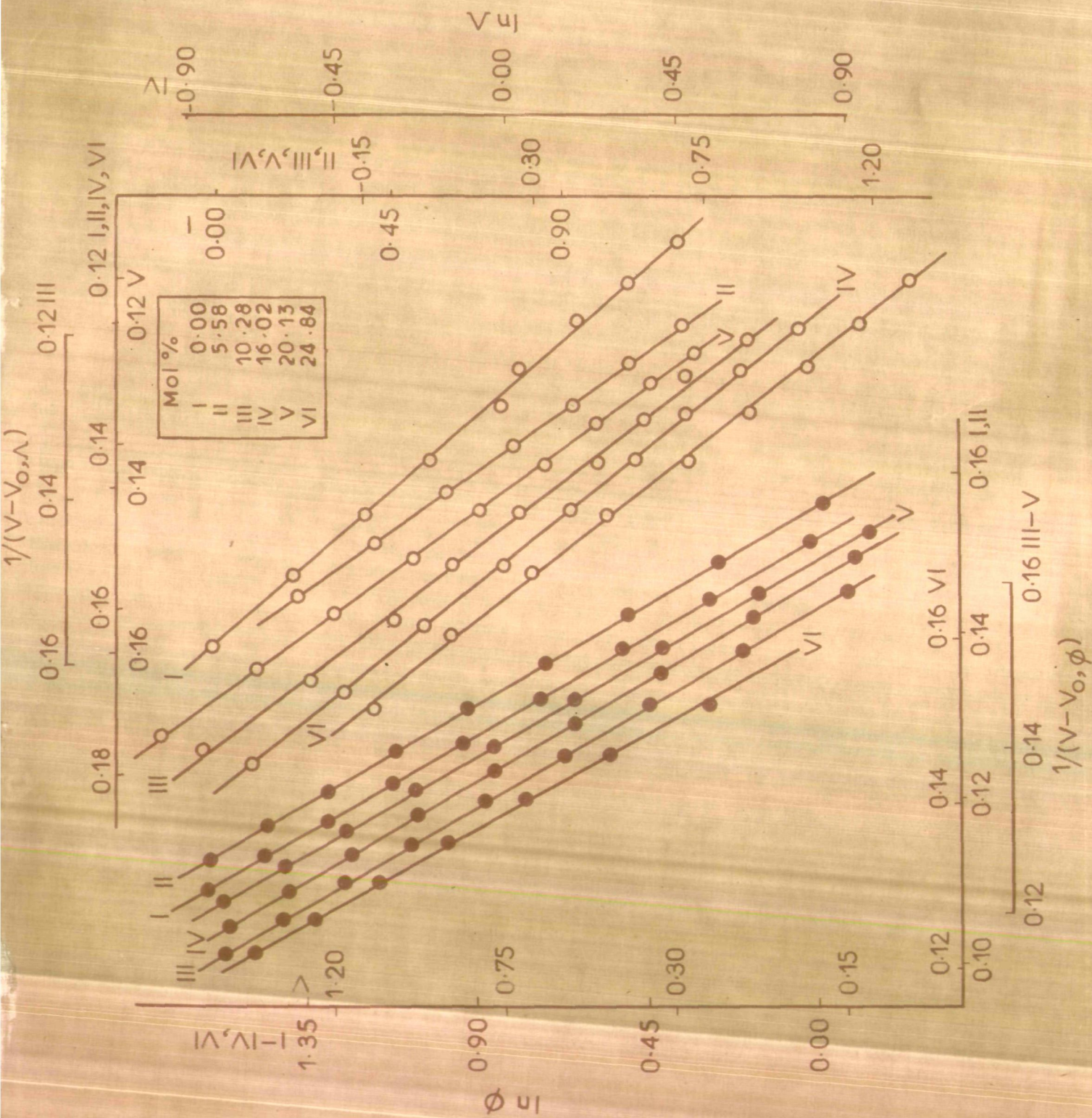


Fig.10. Plots of $\ln \gamma (= \phi \text{ or } \Lambda)$ vs. $1/(V-V_0)$ for molten $\text{Ca}(\text{NO}_3)_2 \cdot 4\text{H}_2\text{O}$ -NaCNS systems.

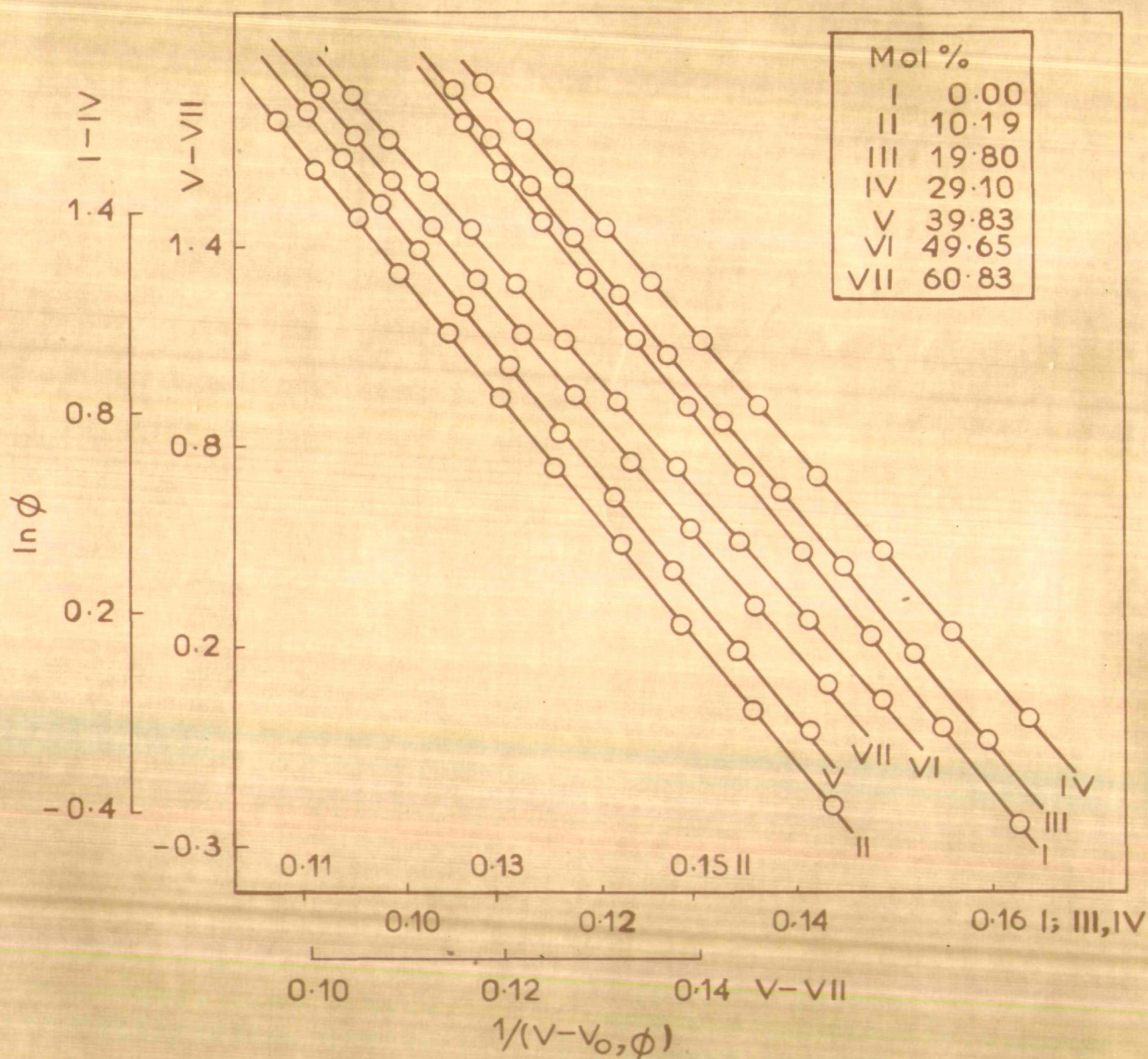


Fig. 11. Plots of $\ln \phi$ vs. $1/(V-V_0, \phi)$ for molten $\text{Ca}(\text{NO}_3)_2 \cdot 3.96\text{H}_2\text{O} - \text{Ni}(\text{NO}_3)_2 \cdot 6.03\text{H}_2\text{O}$ systems.

TABLE 11 : Computed Parameters for Equation (4) for the Fluidity and Equivalent Conductance of $\text{Cd}(\text{NO}_3)_2 \cdot 4.03\text{H}_2\text{O}-\text{MnCl}_2 \cdot 4.00\text{H}_2\text{O}$ Melts

Mol % Mn^{2+}	A'_ϕ	k'_ϕ	$V_{o,\phi}$	Std. dev. in $\ln \phi$	A'_λ	k'_λ	$V_{o,\lambda}$	Std. dev. in $\ln \lambda$
0.00	296.16	35.39	127.90	0.013	129.00	30.00	128.20	0.024
2.27	286.50	36.70	127.57	0.005	121.00	31.40	127.70	0.006
4.14	280.00	37.00	126.80	0.005	115.20	31.20	127.40	0.034
6.63	271.00	39.50	126.50	0.018	105.00	32.00	127.00	0.035
9.07	258.20	39.00	125.87	0.010	97.30	31.10	126.40	0.010
12.31	248.80	36.00	125.20	0.016	85.60	30.00	125.80	0.003

TABLE 12 : Computed Parameters for Equation (4) for the Fluidity and Equivalent

Conductance of $\text{Ca}(\text{NO}_3)_2 \cdot 4.23\text{H}_2\text{O} \cdot \text{NH}_4\text{CNS}$ Melts

Mol % NH_4^+	A'_ϕ	k'_ϕ	$V_{O,\phi}$	Std. dev. in $\ln \phi$	A'_Λ	k'_Λ	$V_{O,\Lambda}$	Std. Dev. in $\ln \Lambda$
0.00	218.00	31.43	133.40	0.017	94.30	28.00	133.00	0.033
10.11	240.00	32.70	125.00	0.017	105.12	26.64	125.10	0.024
20.02	261.80	29.73	117.91	0.008	117.00	28.00	117.10	0.049
30.35	287.43	30.17	110.10	0.012	127.34	26.50	109.90	0.019
40.48	312.00	32.00	103.00	0.077	138.00	25.00	102.30	0.060
51.30	336.50	28.00	94.60	0.017	150.00	31.00	93.20	0.026
63.42	363.00	31.00	85.13	0.047	166.00	31.00	85.00	0.022

TABLE 13 : Computed Parameters for Equation (4) for the Fluidity and Equivalent
Conductance of $\text{Ca}(\text{NO}_3)_2 \cdot 4.1\text{H}_2\text{O}-\text{NaCNS}$ Melts

Mol % Na^+	A'_ϕ	k'_ϕ	$V_{O,\phi}$	Std. dev. in $\ln \phi$	A'_Λ	k'_Λ	$V_{O,\Lambda}$	Std. dev. in $\ln \Lambda$
0.00	295.35	37.37	130.69	0.004	48.00	26.50	131.20	0.044
5.58	322.75	37.00	126.21	0.003	57.13	28.00	126.80	0.015
10.28	337.21	37.09	122.07	0.005	66.10	28.03	122.51	0.026
16.02	362.19	36.77	117.35	0.004	75.13	27.00	117.90	0.010
20.13	392.15	37.50	113.77	0.008	81.50	29.00	113.90	0.026
24.84	414.00	36.00	109.60	0.034	90.20	29.97	109.91	0.017

TABLE 14 : Computed Parameters for Equation (4) for the
Fluidity of $\text{Ca}(\text{NO}_3)_2 \cdot 3.96\text{H}_2\text{O}$ - $\text{Ni}(\text{NO}_3)_2 \cdot 6.03\text{H}_2\text{O}$
Melts

Mol % Ni^{2+}	A'_ϕ	k'_ϕ	$V_{o,\phi}$	Std. dev. in $\ln \phi$
0.00	271.20	37.114	128.90	0.006
10.19	260.00	36.221	131.15	0.005
19.80	250.00	35.866	133.81	0.005
29.10	240.30	34.224	136.11	0.005
39.83	230.10	36.463	137.84	0.009
49.65	210.00	33.514	140.58	0.007
60.83	200.00	34.140	142.59	0.008

TABLE 15 : Corrected Activation Energy (Kcal/mol) for Conductance and Fluidity*
as a Function of Temperature for $\text{Cd}(\text{NO}_3)_2 \cdot 4.03\text{H}_2\text{O} - \text{MnCl}_2 \cdot 4.00\text{H}_2\text{O}$ Melts

T, °K	Mol % Mn^{2+}				
	0.00	2.27	4.14	6.63	9.07
308.0	8.274 (9.338)	8.497 (9.628)	8.664 (9.771)	8.727 (9.848)	9.010 (10.070)
313.0	7.850 (8.861)	8.054 (9.131)	8.206 (9.260)	8.256 (9.324)	8.514 (9.530)
318.0	7.470 (8.434)	7.657 (8.685)	7.797 (8.802)	7.835 (8.855)	8.073 (9.044)
323.0	7.127 (8.049)	7.300 (8.283)	7.429 (8.390)	7.457 (8.434)	7.677 (8.608)
328.0	6.817 (7.700)	6.977 (7.919)	7.096 (8.018)	7.116 (8.054)	7.320 (8.214)
333.0	6.535 (7.383)	6.684 (7.589)	6.794 (7.680)	6.807 (7.709)	6.997 (7.858)

(continued)

TABLE 15 : (continued)

T, °K	Mol % Mn ²⁺				
	0.00	2.27	4.14	6.63	9.07
338.0	6.277 (7.093)	6.416 (7.288)	6.520 (7.372)	6.526 (7.396)	6.704 (7.533)
343.0	6.042 (6.828)	6.172 (7.013)	6.269 (7.090)	6.270 (7.109)	6.436 (7.237)
348.0	5.826 (6.585)	5.948 (6.760)	6.038 (6.832)	6.035 (6.846)	6.191 (6.966)
353.0	5.627 (6.360)	5.741 (6.527)	5.827 (6.594)	5.819 (6.604)	5.967 (6.717)
					6.816 (7.701)
					6.538 (7.392)
					6.285 (7.110)
					6.052 (6.851)

* Corrected activation energy for fluidity are within parentheses.

TABLE 16 : Corrected Activation Energy (Kcal/mol) for Conductance and Fluidity*
as a Function of Temperature for $\text{Ca}(\text{NO}_3)_2 \cdot 4.23\text{H}_2\text{O} \cdot \text{NH}_4\text{CNS}$ Melts

T, °K	Mol % NH_4^+							
	0.00	10.11	20.02	30.35	40.48	51.30	63.42	
313.0	8.847 (10.560)	8.674 (10.310)	8.396 (10.090)	8.281 (9.876)	8.175 (9.680)	7.804 (9.447)	7.570 (9.166)	
318.0	8.366 (9.983)	8.211 (9.764)	7.955 (9.564)	7.853 (9.362)	7.758 (9.185)	7.416 (8.973)	7.202 (8.716)	
323.0	7.937 (9.467)	7.797 (9.269)	7.559 (9.086)	7.470 (8.902)	7.384 (8.740)	7.068 (8.546)	6.871 (8.310)	
328.0	7.551 (9.005)	7.425 (8.824)	7.204 (8.656)	7.125 (8.487)	7.046 (8.339)	6.752 (8.161)	6.572 (7.943)	
333.0	7.203 (8.588)	7.089 (8.422)	6.882 (8.268)	6.812 (8.112)	6.740 (7.975)	6.466 (7.812)	6.299 (7.609)	
338.0	6.888 (8.211)	6.784 (8.058)	6.590 (7.916)	6.528 (7.771)	6.462 (7.645)	6.206 (7.494)	6.051 (7.306)	

(continued)

TABLE 16 : (continued)

		Mol % NH_4^+					
T, °K	0.00	10.11	20.02	30.35	40.48	51.30	63.42
343.0	6.602 (7.868)	6.507 (7.726)	6.325 (7.595)	6.268 (7.460)	6.208 (7.344)	5.968 (7.203)	5.824 (7.028)
348.0	6.340 (7.555)	6.253 (7.423)	6.081 (7.301)	6.031 (7.176)	5.975 (7.068)	5.749 (6.937)	5.615 (6.773)
353.0	6.101 (7.268)	6.021 (7.146)	5.858 (7.032)	5.813 (6.915)	5.762 (6.814)	5.548 (6.692)	5.422 (6.538)

* Corrected activation energy for fluidity are within parentheses.

TABLE 17 : Corrected Activation Energy (Kcal/mol) for Fluidity* and Conductance
as a Function of Temperature for $\text{Ca}(\text{NO}_3)_2 \cdot 4.1\text{H}_2\text{O}$ -NaCNS Melts

T, °K	Mol % Na^+					
	0.00	5.58	10.28	16.02	20.13	24.84
313.0	9.434 (10.957)	9.756 (11.198)	10.048 (11.392)	10.256 (11.658)	10.350 (11.847)	-
318.0	8.905 (10.340)	9.203 (10.558)	9.468 (10.732)	9.654 (10.972)	9.734 (11.142)	-
323.0	8.434 (9.792)	8.710 (9.988)	8.953 (10.146)	9.120 (10.364)	9.189 (10.517)	9.337 (10.687)
328.0	8.012 (9.299)	8.269 (9.479)	8.492 (9.623)	8.644 (9.821)	8.702 (9.961)	8.837 (10.114)
333.0	7.632 (8.857)	7.873 (9.022)	8.078 (9.153)	8.216 (9.335)	8.266 (9.462)	8.389 (9.601)

(continued)

TABLE 17 : (continued)

T, °K	Mol % Na ⁺					
	0.00	5.58	10.28	16.02	20.13	24.84
338.0	7.289 (8.457)	7.515 (8.608)	7.705 (8.729)	7.831 (8.896)	7.874 (9.013)	7.987 (9.139)
343.0	6.977 (8.095)	7.190 (8.234)	7.367 (8.345)	7.482 (8.499)	7.519 (8.607)	7.623 (8.723)
348.0	6.693 (7.764)	6.894 (7.893)	7.059 (7.996)	7.165 (8.139)	7.197 (8.238)	7.293 (8.344)
353.0	6.434 (7.462)	6.624 (7.582)	6.778 (7.677)	6.876 (7.810)	6.903 (7.902)	6.992 (8.000)

* Corrected activation energy for fluidity are within parentheses.

TABLE 18 : Corrected Activation Energy (Kcal/mol) for Fluidity as a Function of
Temperature for $\text{Ca}(\text{NO}_3)_2 \cdot 3.96\text{H}_2\text{O}-\text{Ni}(\text{NO}_3)_2 \cdot 6.03\text{H}_2\text{O}$ Melts

T, °K	Mol % Ni^{2+}					
	0.00	10.19	19.80	29.10	39.83	49.65
308.0	12.300	11.970	11.250	10.960	10.720	10.270
313.0	11.530	11.240	10.600	10.330	10.120	9.714
318.0	10.860	10.600	10.010	9.780	9.589	9.215
323.0	10.260	10.030	9.500	9.283	9.109	8.768
328.0	9.732	9.527	9.034	8.836	8.677	8.364
333.0	9.253	9.069	8.615	8.433	8.286	7.999
338.0	8.821	8.656	8.235	8.068	7.932	7.667

(continued)

TABLE 18 : (continued)

T, °K	Mol % Ni ²⁺					
	0.00	10.19	19.80	29.10	39.83	49.65
343.0	8.431	8.280	7.889	7.736	7.610	7.364
348.0	8.075	7.939	7.574	7.432	7.315	7.086
353.0	7.751	7.627	7.286	7.154	7.044	6.831
358.0	7.454	7.341	7.021	6.898	6.796	6.597
						6.533

available data show the variation of k_Y with concentration for the ZnCl_2 -KCl and a number of silicate systems.²⁸ Such a concentration dependence of k_Y has not been observed in any of the present systems. In fact, one finds often that the values of k_Y are nearly same for the systems which do not differ markedly. An empirical relation²⁹⁻³³ has been noted in which the term k_Y remains concentration independent. This is true for the systems in which concentration variations do not change the melt structure in too radical a fashion. This was indeed the case found in a large variety of fused nitrates, chlorides, and concentrated aqueous solutions.

The above view has been employed in selecting the parameters A_Y , k_Y , and T_0 . Therefore, instead of choosing the best fit values of these parameters they were selected to give almost similar values of k_Y unlike the method of keeping k_Y as fixed as adopted by others.^{25,34} Such a selection of the computed parameters provides $T_{0,\phi} \approx T_{0,\lambda}$ for each concentration studied here. It has been found that A_Y increases with concentration for $\text{Ca}(\text{NO}_3)_2 \cdot 4.23\text{H}_2\text{O}-\text{NH}_4\text{CNS}$ and $\text{Ca}(\text{NO}_3)_2 \cdot 4.1\text{H}_2\text{O}-\text{NaCNS}$ while a decrease in A_Y is observed in the cases of $\text{Cd}(\text{NO}_3)_2 \cdot 4.03\text{H}_2\text{O}-\text{MnCl}_2 \cdot 4.004\text{H}_2\text{O}$ and $\text{Ca}(\text{NO}_3)_2 \cdot 3.96\text{H}_2\text{O}-\text{Ni}(\text{NO}_3)_2 \cdot 6.03\text{H}_2\text{O}$ melts. Similarly, we note an increase in T_0 with increase in concentration for $\text{Cd}(\text{NO}_3)_2 \cdot 4.03\text{H}_2\text{O}-\text{MnCl}_2 \cdot 4.004\text{H}_2\text{O}$ and

$\text{Ca}(\text{NO}_3)_2 \cdot 4.1\text{H}_2\text{O}$ -NaCNS melts while an opposite trend has been noticed in $\text{Ca}(\text{NO}_3)_2 \cdot 4.23\text{H}_2\text{O}$ - NH_4CNS and $\text{Ca}(\text{NO}_3)_2 \cdot 3.96\text{H}_2\text{O}$ - $\text{Ni}(\text{NO}_3)_2 \cdot 6.03\text{H}_2\text{O}$ systems (Figs. 12-15). It may be useful to compare the computed values of T_0 viz., $\sim 192^\circ\text{K}$, $\sim 201^\circ\text{K}$, and 203°K for the pure molten $\text{Cd}(\text{NO}_3)_2 \cdot 4.03\text{H}_2\text{O}$, $\text{Ca}(\text{NO}_3)_2 \cdot 4.23\text{H}_2\text{O}$, and $\text{Ca}(\text{NO}_3)_2 \cdot 4.1\text{H}_2\text{O}$ systems, respectively, with those reported for the corresponding hydrated melts.^{25,34} The value of $T_{0,\phi}$ for $\text{Ca}(\text{NO}_3)_2 \cdot 3.96\text{H}_2\text{O}$, viz., $\sim 206^\circ\text{K}$ is also comparable. Moreover, the T_0 values of molten mixtures studied are not much different from those of the pure solvents. This is supported by Angell and Moynihan's²⁸ view that for dilute molten salt mixtures the glass transition temperature, T_0 , are mainly determined by those of the pure solvents. The values of k_Y seems to be rather insensitive to the nature of the liquid, e.g., for a variety of ionic liquids the value $680 \pm 5\%$ seems to apply.³² The conductance and viscosity studies of the pure molten solvents $\text{Cd}(\text{NO}_3)_2 \cdot 4.03\text{H}_2\text{O}$, $\text{Ca}(\text{NO}_3)_2 \cdot 4.23\text{H}_2\text{O}$, and $\text{Ca}(\text{NO}_3)_2 \cdot 4.1\text{H}_2\text{O}$ and their mixtures with $\text{MnCl}_2 \cdot 4.00\text{H}_2\text{O}$, NH_4CNS , and NaCNS have yielded the values of $k_\phi \approx 670$ and those of $k_A \approx 580^\circ\text{K}$, respectively. Also an almost identical value of $k_\phi \approx 670^\circ\text{K}$ for molten $\text{Ca}(\text{NO}_3)_2 \cdot 3.96\text{H}_2\text{O}$ and its mixtures with $\text{Ni}(\text{NO}_3)_2 \cdot 6.03\text{H}_2\text{O}$ is observed. The values of k_Y agree with those reported by Moynihan et al.²⁵

Since the preexponential factor A_Y varies linearly

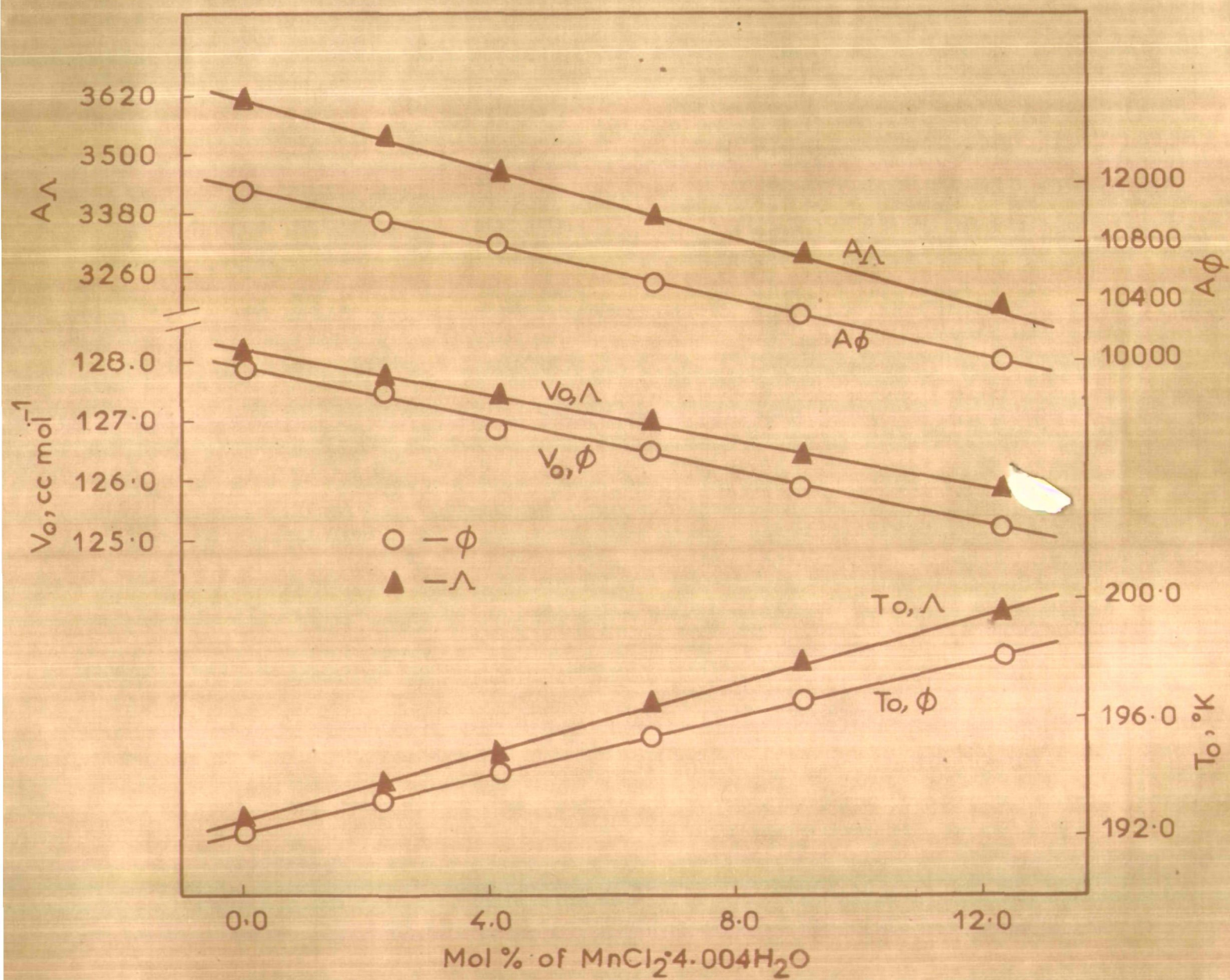


Fig.12. Variation of A_{Λ} , V_0 , and T_0 with mol % of molten $\text{Cd}(\text{NO}_3)_2 \cdot 4.03\text{H}_2\text{O} - \text{MnCl}_2 \cdot 4.00\text{H}_2\text{O}$ systems.

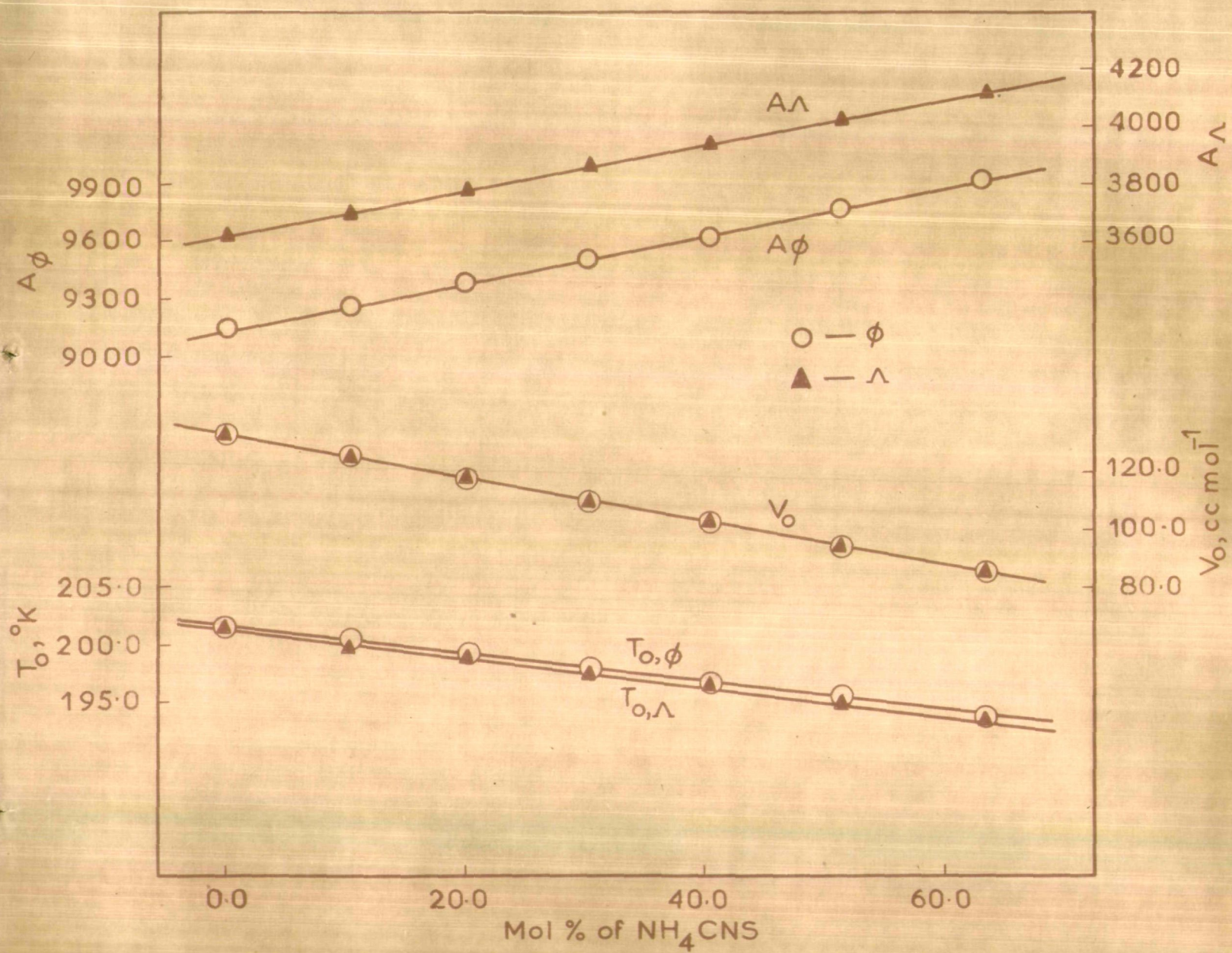


Fig. 13. Variation of A_γ , V_0 , and T_0 with mol % of molten $\text{Ca}(\text{NO}_3)_2 \cdot 4.23\text{H}_2\text{O} - \text{NH}_4\text{CNS}$ systems.

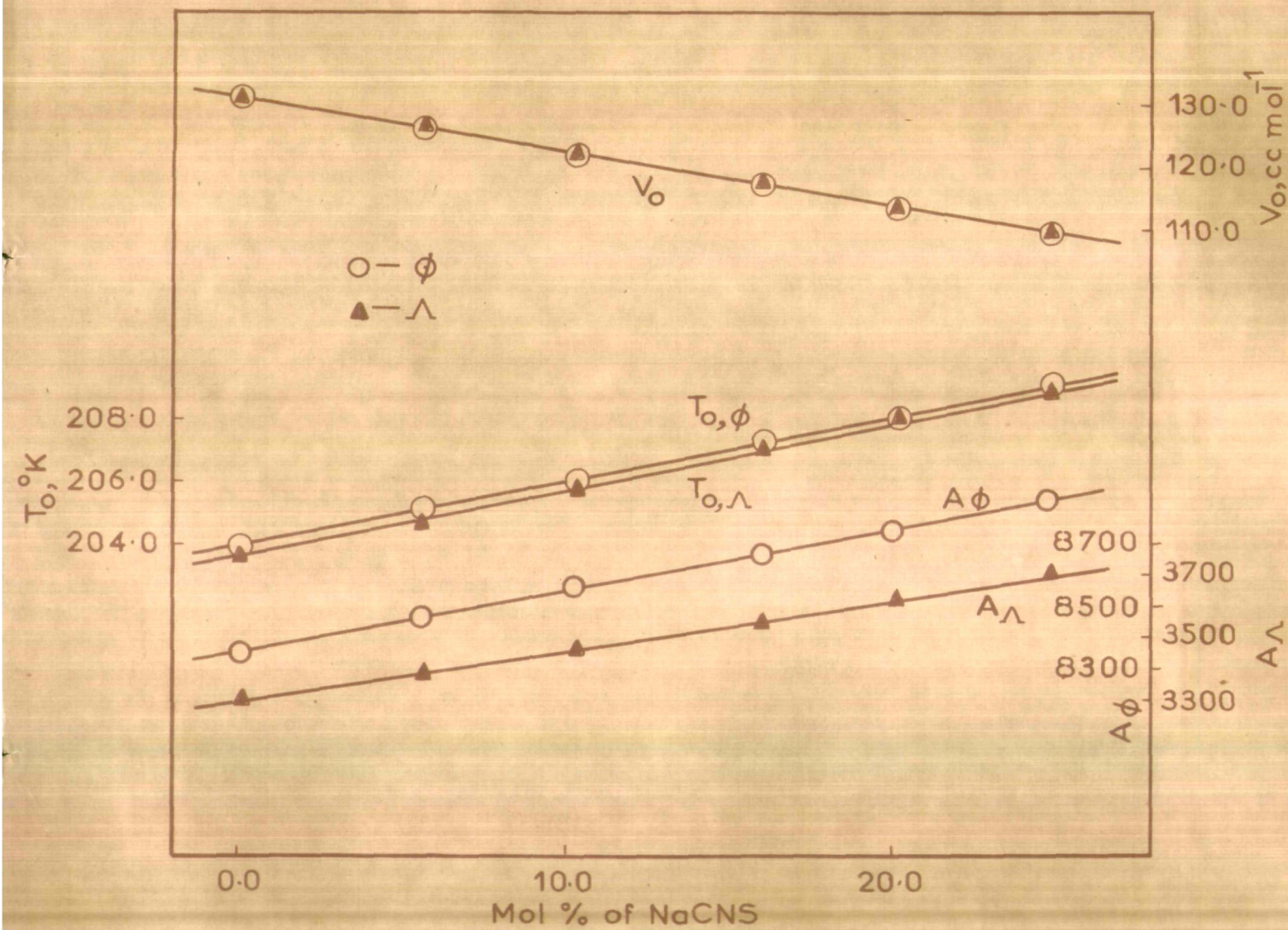


Fig.14 Variation of A_γ , V_o , and T_o with mol % of molten $\text{Ca}(\text{NO}_3)_2 \cdot 4.1\text{H}_2\text{O} - \text{NaCNS}$ systems.

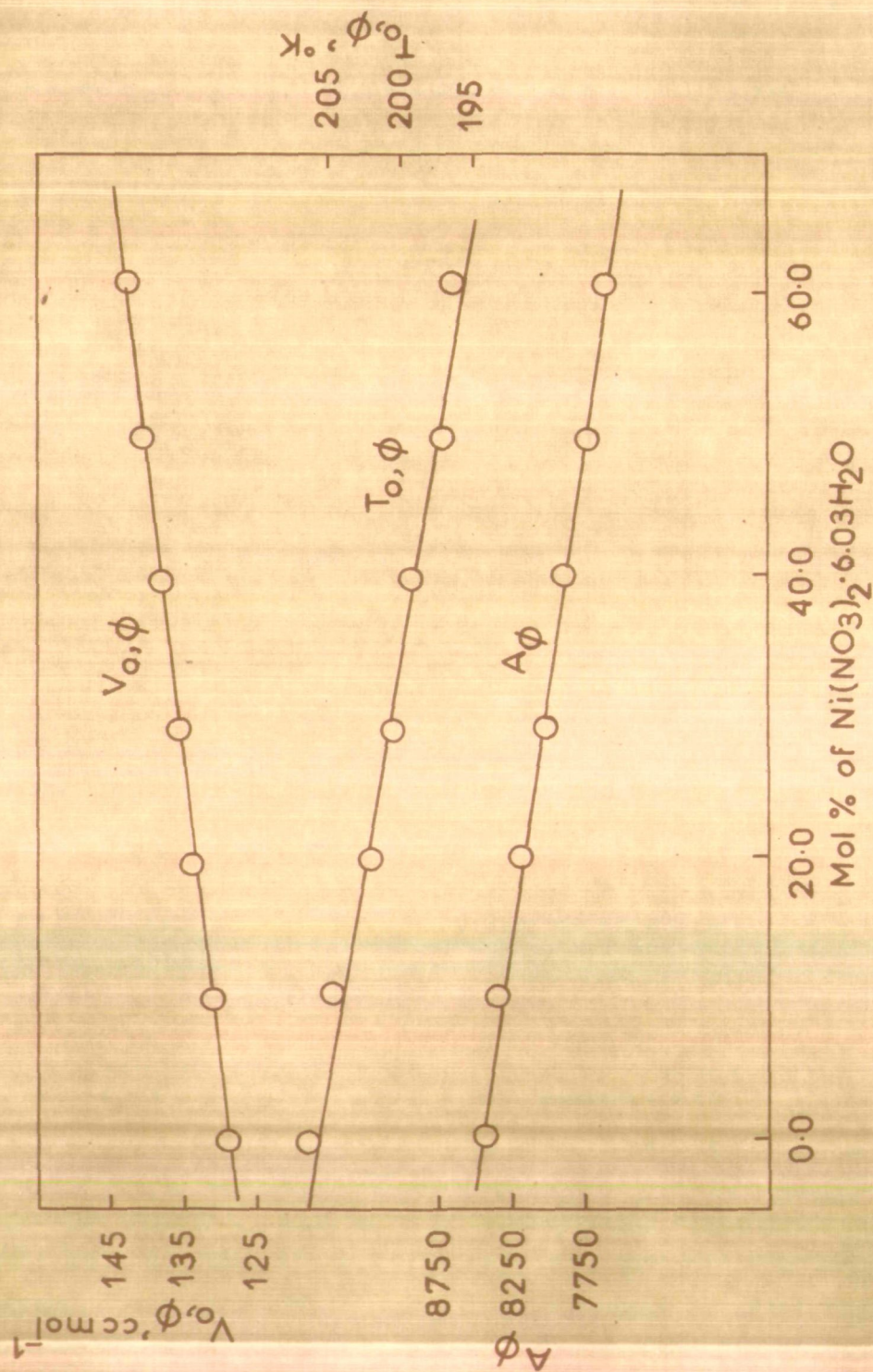
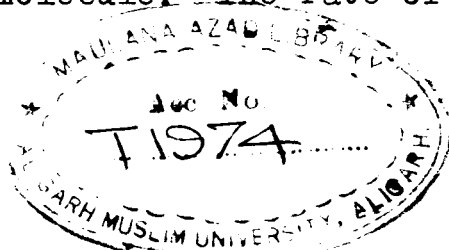


Fig.15. Variation of A_ϕ , V_ϕ , and T_ϕ with mol % of molten $\text{Ca}(\text{NO}_3)_2 \cdot 3.96\text{H}_2\text{O} - \text{Ni}(\text{NO}_3)_2 \cdot 6.03\text{H}_2\text{O}$ systems.

with a slight variation in T_0 , therefore, its estimation to match adequately the computed data of k_Y and T_0 is not so easy. On the theoretical ground the preexponential term A_Y varies linearly with $m^{-1/2}$ where m is the average mass of the component particles of the system. In the cases of the systems $\text{Ca}(\text{NO}_3)_2 \cdot 4.23\text{H}_2\text{O} - \text{NH}_4\text{CNS}$ and $\text{Ca}(\text{NO}_3)_2 \cdot 4.1\text{H}_2\text{O} - \text{NaCNS}$, the mean molecular mass have been found to decrease on adding the corresponding solute to the solvent. Hence, one can expect an increase in the A_Y term with increase in the solute concentration. This has indeed been found in the above systems as has also been reported earlier.^{35,36} In the case of $\text{Ca}(\text{NO}_3)_2 \cdot 3.96\text{H}_2\text{O} - \text{Ni}(\text{NO}_3)_2 \cdot 6.03\text{H}_2\text{O}$, too, the $m^{-1/2}$ dependence of A_Y seems to be feasible since the mean molecular mass, m , increases with increase in solute concentration which leads to a decrease in the A_Y term. However, in the case of $\text{Cd}(\text{NO}_3)_2 \cdot 4.03\text{H}_2\text{O} - \text{MnCl}_2 \cdot 4.00\text{H}_2\text{O}$ the term A_Y decreases with decrease in the mean molecular mass of Mn^{2+} in the reverse direction of that expected. Such a discrepancy in A_Y with concentration has also been suggested in other systems.^{35,36} Alternatively, this reverse effect may be related to the differences in the lability of water or nitrate ions in the coordination shells of the respective cations of the molten system as was given by Moynihan et al.²⁵ Hence, in order to visualize the concentration dependence of transport properties

those of A_Y and T_0 terms may be examined. For the systems at temperatures corresponding to low T/T_0 ratios the concentration dependence of transport properties are mainly guided by the concentration dependence of T_0 . However, at high temperatures the preexponential terms may become dominant in determining the concentration dependence of transport properties.

The exponent term k_Y of equation (10) based on the VTF model is nearly independent of concentration in the systems under investigation. The constancy of the k_Y term may be emphasized as suggested earlier.^{34,36} According to "hard-sphere" model²² of Cohen and Turnbull this term is given as $k_Y = \gamma v^* / \alpha \bar{v}_m$, where γ is a geometric factor to correct for the overlap of free volume in the calculation of the probability of occurrence of a critical void and α is the mean value of the coefficient of expansion from T_0 to T . The volume v^* of the critical void governs the rate of diffusion and, in turn, is determined by the size of the larger molecule of the system. On the basis of this model if the solute molecule is equal or somewhat smaller than that of the solvent molecule it will diffuse at the same rate as that of the solvent since the diffusive transport is completed only by the jumping of a neighbour solvent molecule into the void left by the transfer of solute molecule. The rate of diffusion, no doubt,



will be changed by the addition of solute molecule due to the decrease in the average free volume, the critical size of the void necessary for diffusion will not change with concentration. For the melts studied here the hydrated solvent cations of the type $\text{Cd}(\text{H}_2\text{O})_4^{2+}$ and $\text{Ca}(\text{H}_2\text{O})_4^{2+}$ may act as the cations of larger size in the case of conductance and presumably this plays an important role in determining the value of v^* . Furthermore, the variation of α over the whole concentration range studied is found to be insignificant. Therefore, the term $\gamma v^*/\alpha \bar{v}_m$ or k_γ itself seems to be independent of concentration. In the case of fluidity and conductance the constant term $\gamma v^*/\bar{v}_m$ has the values of about 0.33 and 0.29 for the pure $\text{Cd}(\text{NO}_3)_2 \cdot 4.03\text{H}_2\text{O}$ and its mixtures with $\text{MnCl}_2 \cdot 4.00\text{H}_2\text{O}$, respectively. Similarly these values are 0.33 and 0.25 for the pure $\text{Ca}(\text{NO}_3)_2 \cdot 4.23\text{H}_2\text{O}$ and its mixtures with NH_4CNS , respectively. These values are comparable with those reported for $\text{Ca}(\text{NO}_3)_2 \cdot 3.99\text{H}_2\text{O} - \text{KCNS}$ ³⁴ and $\text{Ca}(\text{NO}_3)_2 \cdot 4.1\text{H}_2\text{O} - \text{Cu}(\text{NO}_3)_2 \cdot 2.92\text{H}_2\text{O}$ ³⁶ melts.

It may be noted that the values of k_ϕ are always greater than those of k_λ for all the molten systems investigated here. This is the manifestation of the differences in activation energies, E_ϕ and E_λ , for fluidity and conductance generally found for molten salts.^{38,39} Also it is apparent from the plots (Figs. 12-15) that the slopes for fluidity are greater than the corresponding

slopes for conductance for the same molten salt system showing further that $k_{\phi} > k_{\Lambda}$. The values k_{ϕ}/k_{Λ} lie in the range 1.13-1.18 and may be compared to those reported by others.²⁸ Thus the higher value of k_{ϕ} than k_{Λ} is a reflection of the general result for molten salts that the ratio E_{ϕ}/E_{Λ} is likewise invariably greater than one. In fact, for nitrates and other melts with complex anions the ratios E_{ϕ}/E_{Λ} are quite low (<1.5), while in the case of simple halide systems²⁸ the ratios E_{ϕ}/E_{Λ} are generally found to be in the range of 2 to 7. The ratios E_{ϕ}/E_{Λ} for $\text{Cd}(\text{NO}_3)_2 \cdot 4.03\text{H}_2\text{O}$ - $\text{MnCl}_2 \cdot 4.00\text{H}_2\text{O}$, $\text{Ca}(\text{NO}_3)_2 \cdot 4.23\text{H}_2\text{O}$ - NH_4CNS , and $\text{Ca}(\text{NO}_3)_2 \cdot 4.1\text{H}_2\text{O}$ - NaCNS melts are found to be 1.13 ± 0.01 , 1.20 ± 0.01 , and 1.15 ± 0.01 (Tables 19-21), respectively, and are almost temperature independent. These values are close to the values reported earlier^{34,40} in the cases of $\text{Ca}(\text{NO}_3)_2 \cdot 3.99\text{H}_2\text{O}$ - KCNS and MCl_2 ($\text{M} = \text{Mn}^{2+}$, Co^{2+} , Ni^{2+})- Bu_4NCl melts. For ionic melts the ratio $E_{\phi}/E_{\Lambda} > 1$ implies that conductivity is predominantly governed by the more mobile ion of the melt resulting in a lower activation energy to surmount the energy barriers for ionic conductance than those for viscous flow in which ions move in clusters or pairs and less mobile entities determine the fate of viscous flow resulting in higher activation energy. The difference of about 2 Kcal/mol between E_{ϕ} and E_{Λ} is of the order of Van der Waals forces

TABLE 19 : The Ratio E_{ϕ}/E_A as a Function of Temperature for $\text{Cd}(\text{NO}_3)_2 \cdot 4.03\text{H}_2\text{O} - \text{MnCl}_2 \cdot 4.00\text{H}_2\text{O}$ Melts

T, °K	Mol % Mn^{2+}				
	0.00	2.27	4.14	6.63	9.07
308.0	1.1335	1.1380	1.1324	1.1331	1.1222
313.0	1.1341	1.1391	1.1335	1.1344	1.1237
318.0	1.1347	1.1400	1.1343	1.1356	1.1252
323.0	1.1354	1.1408	1.1351	1.1369	1.1265
328.0	1.1360	1.1416	1.1361	1.1381	1.1278
333.0	1.1366	1.1424	1.1369	1.1394	1.1292

(continued)

TABLE 19 : (continued)

T, °K	Mol % Mn ²⁺				
	0.00	2.27	4.14	6.63	9.07
338.0	1.1371	1.1432	1.1377	1.1405	1.1302
343.0	1.1378	1.1442	1.1384	1.1415	1.1316
348.0	1.1385	1.1449	1.1393	1.1425	1.1324
353.0	1.1391	1.1456	1.1400	1.1437	1.1335
					1.1320

TABLE 20 : The Ratio E_{ϕ}/E_{λ} as a Function of Temperature for $\text{Ca}(\text{NO}_3)_2 \cdot 4.23\text{H}_2\text{O} - \text{NH}_4\text{CNS}$ Melts

T, °K	Mol % NH ₄ ⁺						
	0.00	10.11	20.02	30.35	40.48	51.30	63.42
313.0	1.1996	1.1957	1.2104	1.2001	1.1915	1.2193	1.2200
318.0	1.2007	1.1968	1.2106	1.2002	1.1917	1.2191	1.2199
323.0	1.2008	1.1969	1.2108	1.2003	1.1920	1.2191	1.2196
328.0	1.2012	1.1971	1.2112	1.2003	1.1924	1.2190	1.2195
333.0	1.2015	1.1972	1.2116	1.2005	1.1929	1.2192	1.2197
338.0	1.2019	1.1976	1.2118	1.2007	1.1931	1.2197	1.2196

(continued)

TABLE 20 : (continued)

T, °K	Mol % NH ₄ ⁺					
	0.00	10.11	20.02	30.35	40.48	51.30
343.0	1.2022	1.1977	1.2122	1.2009	1.1936	1.2196
348.0	1.2027	1.1981	1.2127	1.2014	1.1939	1.2201
353.0	1.2029	1.1984	1.2129	1.2015	1.1944	1.2201
						1.2200

TABLE 21 : The Ratio E_p/E_λ as a Function of Temperature for $\text{Ca}(\text{NO}_3)_2 \cdot 4.1\text{H}_2\text{O}$ -
NaCNS Melts

T, °K	Mol % Na^+					
	0.00	5.58	10.28	16.02	20.13	24.84
313.0	1.1839	1.1688	1.1577	1.1564	1.1645	-
318.0	1.1853	1.1692	1.1549	1.1576	1.1658	-
323.0	1.1871	1.1714	1.1568	1.1592	1.1672	1.1668
328.0	1.1886	1.1771	1.1582	1.1611	1.1694	1.1691
333.0	1.1904	1.1741	1.1599	1.1627	1.1713	1.1765

(continued)

TABLE 21 : (continued)

T, °K	Mol % Na ⁺				
	0.00	5.58	10.28	16.02	20.13
338.0	1.1920	1.1755	1.1615	1.1644	1.1730
					1.1725
343.0	1.1939	1.1771	1.1632	1.1662	1.1749
					1.1743
348.0	1.1958	1.1788	1.1650	1.1679	1.1767
					1.1760
353.0	1.1976	1.1804	1.1669	1.1653	1.1788
					1.1779

expected for the intermolecular or interentities forces responsible for determining the magnitude of viscosities of such systems. Therefore, it may be anticipated that an additional Van der Waals force appears to be involved in the viscous flow. This may be a molecule-molecule interaction whose contribution to ionic conductance appears to be insignificant.

Furthermore, the activation energies for fluidity and conductance (Table 15-18) increase with increase in concentration of solutes in $\text{Cd}(\text{NO}_3)_2 \cdot 4.03\text{H}_2\text{O}$ - $\text{MnCl}_2 \cdot 4.00\text{H}_2\text{O}$ and $\text{Ca}(\text{NO}_3)_2 \cdot 4.1\text{H}_2\text{O}$ - NaCNS melts. On the other hand, the reverse trend has been observed in molten $\text{Ca}(\text{NO}_3)_2 \cdot 4.23\text{H}_2\text{O}$ - NH_4CNS system. Similar decrease in activation energy for fluidity is observed in the case of $\text{Ca}(\text{NO}_3)_2 \cdot 3.96\text{H}_2\text{O}$ - $\text{Ni}(\text{NO}_3)_2 \cdot 6.03\text{H}_2\text{O}$ melts. This may be visualized in terms of the free volume concept. Accordingly, there is a decrease in the free volume per molecule on increasing the concentration of the solute. This causes an increase in the compactness of the system. As the concentration increases the molecules get closer resulting in higher intermolecular forces. Consequently, it causes difficulty in the flow of such clusters which need higher energy of activation as compared to that required for the system having unassociated species. It is probably also worthwhile to find increase in the activation energies with decrease in the water of hydration in $\text{Ca}(\text{NO}_3)_2 \cdot 4.23\text{H}_2\text{O}$, $\text{Ca}(\text{NO}_3)_2 \cdot 4.1\text{H}_2\text{O}$, and $\text{Ca}(\text{NO}_3)_2 \cdot 3.96\text{H}_2\text{O}$

melts. Similar explanation may also be accorded to this trend. As the temperature increases the average free volume increases due to thermal expansion of the melt resulting in a decrease in the intermolecular forces, thereby, lowering the value of the activation energies.

The glass transition temperature, T_0 which is the most important factor in determining the concentration dependence of transport properties particularly in dilute aqueous melts forming complex species is reviewed here. The T_0 values listed in Tables 7-10 show linear dependence on concentration in all the molten mixtures investigated. In the cases of $\text{Cd}(\text{NO}_3)_2 \cdot 4.03\text{H}_2\text{O}$ - $\text{MnCl}_2 \cdot 4.00\text{H}_2\text{O}$ and $\text{Ca}(\text{NO}_3)_2 \cdot 4.1\text{H}_2\text{O}$ - NaCNS melts the values of T_0 increase linearly with concentration of the solute. This observation is similar to those reported for several other systems.^{27,31,34,41} T_0 in equation (10) represents a thermodynamic rather than kinetic parameter. Hence, values of T_0 derived from different transport properties of the same liquid should be identical. The expectation of equal T_0 values from different transport properties have been tested by others^{22,26,42,43} and holds fairly well. The above prediction of equal T_0 values also holds good in the molten systems investigated here. The linear increase in T_0 with concentration may be anticipated in the light of the correlation⁴⁴ that has been suggested between T_g or T_0 and

the characteristic Debye temperature, θ_D which shows an $m^{-1/2}$ dependence on the effective masses of the component particles of the amorphous phase. Thus, an increase in T_0 for the systems $\text{Cd}(\text{NO}_3)_2 \cdot 4.03\text{H}_2\text{O}$ - $\text{MnCl}_2 \cdot 4.00\text{H}_2\text{O}$ and $\text{Ca}(\text{NO}_3)_2 \cdot 4.1\text{H}_2\text{O}$ - NaCNS may be due to a decrease in the average molecular mass by increasing the solute concentrations. The same expectation may be accorded to $\text{Ca}(\text{NO}_3)_2 \cdot 3.96\text{H}_2\text{O}$ - $\text{Ni}(\text{NO}_3)_2 \cdot 6.03\text{H}_2\text{O}$ molten mixtures where an increase in average molecular mass by the addition of $\text{Ni}(\text{NO}_3)_2 \cdot 6.03\text{H}_2\text{O}$ to $\text{Ca}(\text{NO}_3)_2 \cdot 3.96\text{H}_2\text{O}$ causes a decrease in the value of T_0 . However, such an $m^{-1/2}$ dependence does not apply to $\text{Ca}(\text{NO}_3)_2 \cdot 4.23\text{H}_2\text{O}$ - NH_4CNS melts. Such behaviours have also been reported for other systems.^{25,36}

An alternative explanation may be emphasized on the basis of cationic potential which is defined as $\sum_i N_i Z_i / r_i$, where N_i is the mol fraction, Z_i the cationic charge, and r_i is the cationic radius of cationic species i . A relationship between T_0 of a system and the cationic potential was suggested by Angell^{45,46} which states that there will be a decrease in T_0 with decrease in cationic potential of the system and vice-versa due to change in concentration. The Ca^{2+} ion has greater cationic charge and lower ionic radius as compared to NH_4^+ . So one may expect a decrease in cationic potential with an increase in $[\text{NH}_4^+]$ in molten $\text{Ca}(\text{NO}_3)_2 \cdot 4.23\text{H}_2\text{O}$, resulting in a decrease in T_0 value.

The dependence of T_0 on cationic potential is also observed in the case of $\text{Cd}(\text{NO}_3)_2 \cdot 4.03\text{H}_2\text{O}$ - $\text{MnCl}_2 \cdot 4.00\text{H}_2\text{O}$ melts. The T_0 of a particular system is interpreted as a theoretical glass transition temperature or, in other words, the extent of cooling to reach the zero free volume. Addition of solute to the molten solvent causes the decrease in the free volume of the melt and therefore, less cooling may be required to reach the zero free volume or amorphous phase at higher concentrations. Accordingly, higher values of T_0 may be expected for concentrated solutions.

The intrinsic volume, V_0 , has been found to decrease linearly with concentration in the cases of $\text{Cd}(\text{NO}_3)_2 \cdot 4.03\text{H}_2\text{O}$ - $\text{MnCl}_2 \cdot 4.00\text{H}_2\text{O}$, $\text{Ca}(\text{NO}_3)_2 \cdot 4.23\text{H}_2\text{O}$ - NH_4CNS , and $\text{Ca}(\text{NO}_3)_2 \cdot 4.1\text{H}_2\text{O}$ - NaCNS melts (Figs. 12-15), thereby showing a direct dependence on m . On the other hand, $V_{0,\phi}$ increases linearly with concentration in $\text{Ca}(\text{NO}_3)_2 \cdot 3.96\text{H}_2\text{O}$ - $\text{Ni}(\text{NO}_3)_2 \cdot 6.03\text{H}_2\text{O}$ melts and contradicts the above m dependence. It is worthy of note that for all the melts studied here V_0 's have been found to be additive in nature. This additive nature of V_0 may be attributed to the ideal behaviour of these melts with respect to the molal volume. Therefore, V_0 can be given by the relation $V_{0,x_1} = \sum_i x_1 V_{0,i}$, where V_{0,x_1} represents the molar intrinsic volume of the melt having the i th component of mol fraction x_1 . However, it is apparent from the viscosity and equivalent conductance

isotherms that these properties are not additive in nature in these melts. Such behaviours are also observed in the cases of $(\text{CdCl}_2 + \text{CdBr}_2, \text{PbCl}_2 + \text{PbBr}_2, \text{AgCl} + \text{AgBr})^{47}$, $\text{Ca}(\text{NO}_3)_2 \cdot 3.99\text{H}_2\text{O} - \text{KCNS}$,³⁴ and $\text{Zn}(\text{NO}_3)_2 \cdot 6.33\text{H}_2\text{O} - \text{Ca}(\text{NO}_3)_2 \cdot 4.1\text{H}_2\text{O}$ ³⁶ melts, $4.1\text{H}_2\text{O}$ ³⁶ melt. Now it would be useful to compare the Doolittle's model with that of Cohen and Turnbull's. The term k_Y' in the exponential term of equation (4) is related to γv^* per mol and appears to be concentration independent like that of the k_Y term of the VTF model. The constancy of k_Y' is also emphasized by the identical slopes of the linear plots (Figs. 8-11) of $\ln Y (= \phi \text{ or } \Lambda)$ versus $1/(V - V_0)$. The absence of the factor $T^{-1/2}$ in the preexponential term in Doolittle's model may be responsible for the higher standard deviations in $\ln \phi$ and $\ln \Lambda$ although it affects insignificantly even in VTF equation. The preexponential term A_Y' has been found to be concentration dependent like that of the A_Y term of the VTF equation. It is equally important to find almost identical values for $V_{0,\phi}$ and $V_{0,\Lambda}$ thereby implying the thermodynamic nature of V_0 . Thus the computed values of $V_{0,\phi,\Lambda}$ refer to the molar volumes of the corresponding melt at T_0 and not at 0°K which supports the view that the origin of the free volume is not at 0°K but rather T_0 .

Finally, it seems important to note that, even though the VTF model successfully describes the present data,

it may not explain many facts well. According to the VTF model the molecules are assumed to be hard-spheres and they require the size of molecular diameter for their jumps in the process of diffusion. However, recent studies on molecular dynamics show that at least for hard-spheres there is no characteristic jump distance in fluid diffusion⁴⁸. Secondly, the influence of intermolecular forces on transport phenomena was neglected in the VTF model. Its inadequacy in explaining the redistribution of zero energy free volume to molecularly complex systems may also be pointed out. Moreover, the VTF model failed badly during the study of the effect of pressure on viscosity and on electrical conductivity.⁴⁹⁻⁵¹ Adam and Gibbs⁵² model seems better in explaining the experimental data than that of the VTF model based on the free volume concept.

C H A P T E R - I V

Temperature Dependence of Transport Behaviour of Molten
Salt Systems - The Application of Configurational
Entropy Model

Introduction

The VTF equation based on the free volume concept appears to be ill defined operationally and its main shortcomings were pointed out in the earlier chapter. An alternative theory which cannot be criticized either on the grounds of restrictive mechanism or of inapplicability to complex systems has been proposed by Adam and Gibbs.⁵² In this theory Cohen and Turnbull's²² idea regarding glass transition and free volume disappearance at T_0 has not been lost. Rather it is replaced by the even more appealing proposition that the essential liquid state characteristic which becomes zero at the temperature T_0 is the configurational entropy of the liquid. Furthermore, where the free volume disappears at T_0 was an assumption in Cohen and Turnbull's model, in the Adam and Gibbs theory the vanishing entropy comes as a central result of a successful statistical mechanical theory at T_0 of chain polymer liquids at high particle densities, which can presumably be generalized to include nonpolymeric liquids.

Moreover, the "quasistatic" glass transition temperature, T_g has been defined as the temperature below which molecular relaxation times are too long to permit establishment of equilibrium in the duration of even the slowest experiment. Kauzmann⁵³ noted, in fact, the extra-

polated values of the plots of observed equilibrium properties such as entropy, heat content, and specific volume versus temperature for several substances to the temperatures not very far below the glass-transformation but still far above 0°K are found to be less than those of the crystalline solid. This peculiar result can only mean that somehow the above extrapolation is not permissible. Among these crises, the entropy crisis was the fundamental paradox requiring resolution.

The decrease in entropy to small values and the paradox of negative configurational entropies at lower temperatures was settled by Gibbs and DiMarzio⁵⁴ through their statistico-mechanical theory by demonstrating a second-order transition at the temperature, T_g where the configurational entropy vanishes. Below T_g , the configurational entropy remains, of course, zero, rather than going to meaningless negative values.

The above idea expressed by Gibbs and DiMarzio⁵⁴ finds quantitative statement in the theory of Adam and Gibbs.⁵² The temperature-dependent relaxation times in dynamic mechanical or dielectric experiments in liquids are determined by the probabilities of cooperative rearrangements. The cooperatively rearranging region is defined as a subsystem of the sample which, upon a suffi-

cient fluctuation in energy, can rearrange into another configuration independently of its environment. On showing that at T_g the cooperatively rearranging region must, of course, comprise the whole system since, at this temperature, there is only one available configuration for even the whole system, there resulted for the average transition probability, $\bar{w}(T)$, the expression

$$\bar{w}(T) = \bar{A} \exp(-\Delta\mu S_c^*/kTS_c) \quad (12)$$

where \bar{A} is a frequency factor, $\Delta\mu$ is the free energy barrier per mol of particles opposing the cooperative rearrangement, S_c^* is the minimum configurational entropy which a region of the liquid must possess in order to undergo cooperative rearrangement, k is the Boltzmann constant, and S_c is the configurational entropy of the macroscopic supersystem.

By making the approximation

$$S_c \cong C_p \ln T/T_0$$

where ΔC_p is the change in the heat capacity at the glass transition, we arrive at the expression

$$\bar{w}(T) = \bar{A} \exp(-\Delta\mu S_c^*/kT\Delta C_p \ln(T/T_0)) \quad (13)$$

Equation (13) can be written as

$$\bar{w}(T) = \bar{A} \exp \left[-k''/T \ln (T/T_0) \right] \quad (14)$$

where $k'' = \Delta \mu S_c^* / k \Delta C_p$

Equation (14) represents the final equation by Adam and Gibbs⁵² obtained for the relaxation processes in glass-forming melts. It is known that the transition probability, $\bar{w}(T)$ is directly related to the mass transport processes like diffusion, fluidity, and conductance. Therefore equation (14) may be transformed into the expression

$$Y = A_Y'' \exp \left[-k_Y''/T \ln (T/T_0) \right] \quad (15)$$

In this equation A_Y'' is another constant.

The temperature dependent transport data given in Chapter III have been analyzed and discussed in the light of the configurational entropy model and are presented in this Chapter.

Results and Discussion

The fluidity and conductance data of all the molten mixtures studied here were least-squares fitted to the equation (15) based on the configurational entropy model. The feasibility of the model is tested by the linear plots (Figs. 16-19) of $\ln Y (= \phi \text{ or } \Lambda)$ versus

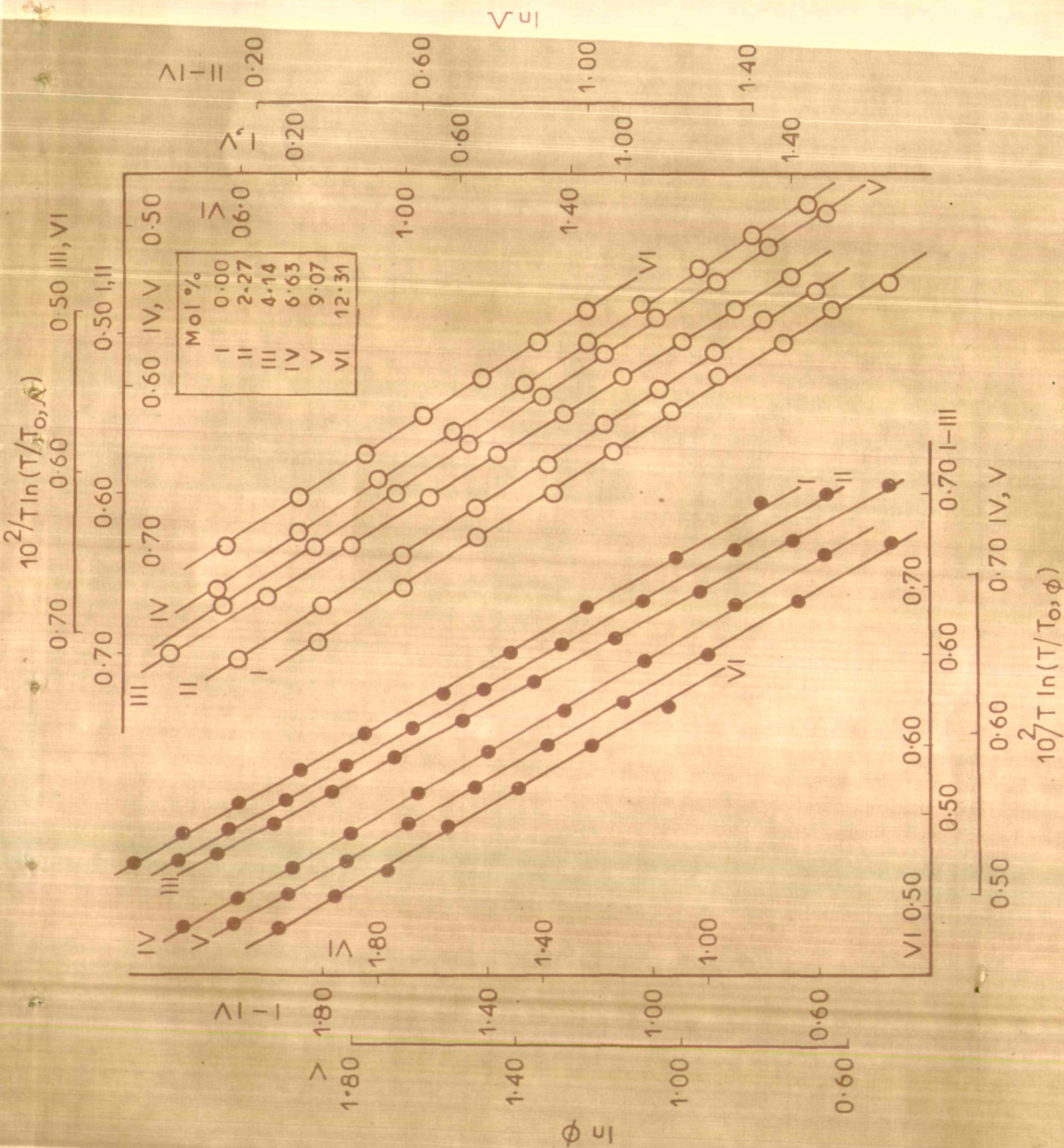


Fig. 16. Plots of $\ln Y (= \phi \text{ or } \Lambda)$ vs. $1/T \ln(T/T_0)$ for molten $\text{Cd}(\text{NO}_3)_2 \cdot 4.03\text{H}_2\text{O} - \text{MnCl}_2 \cdot 4.00 \cdot \text{H}_2\text{O}$ systems.

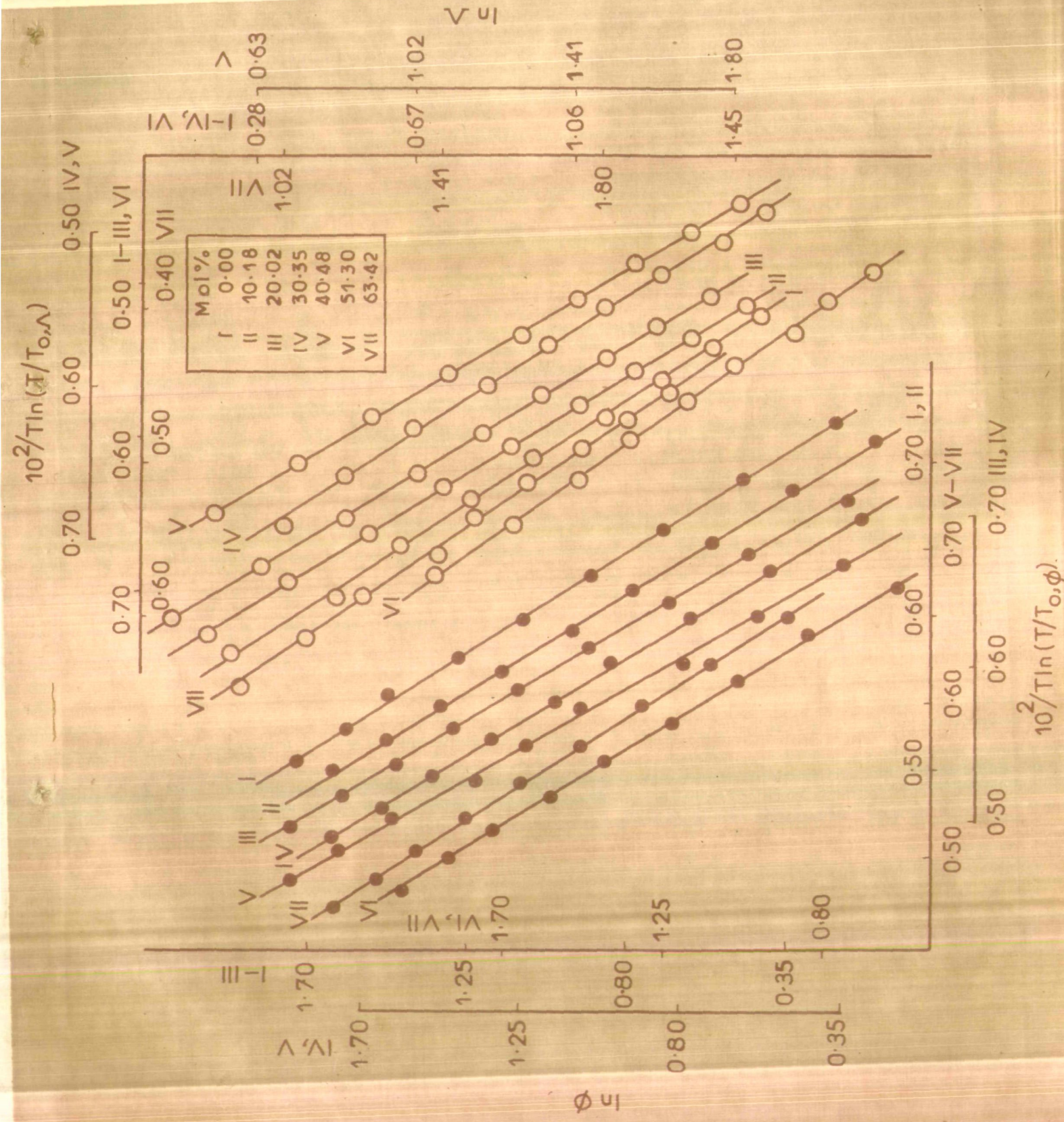


Fig. 17. Plots of $\ln \gamma (= \phi \text{ or } \Lambda)$ vs. $1/T \ln(T/T_0)$ for molten $\text{Ca}(\text{NO}_3)_2 \cdot 4.23\text{H}_2\text{O}$ - NH_4CNS systems.

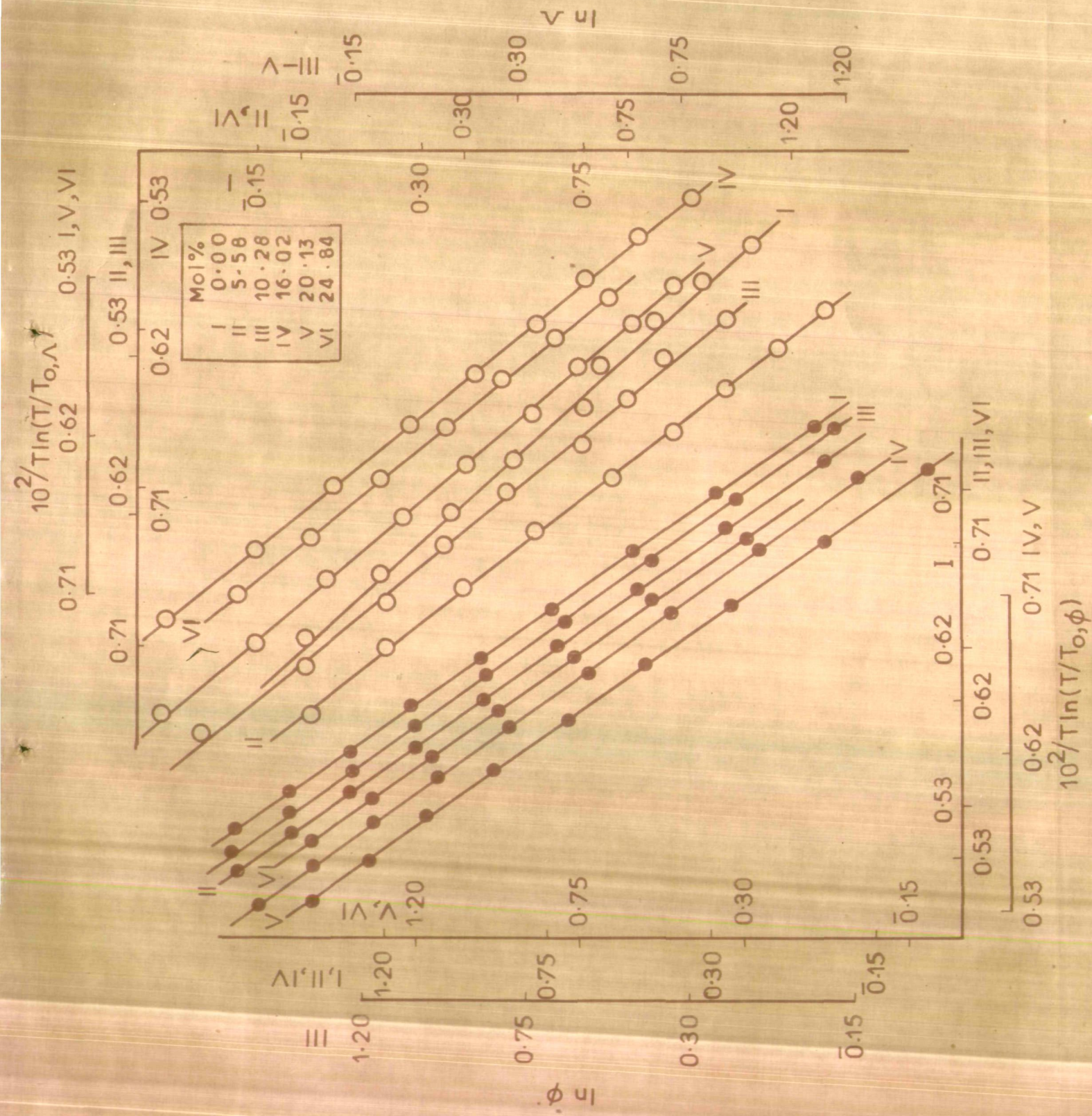


Fig.18. Plots of $\ln \gamma$ ($\equiv \phi$ or Λ) vs. $1/T \ln(T/T_0, \phi)$ for molten $\text{Ca}(\text{NO}_3)_2 \cdot 4\text{H}_2\text{O} - \text{NaCNS}$ systems.

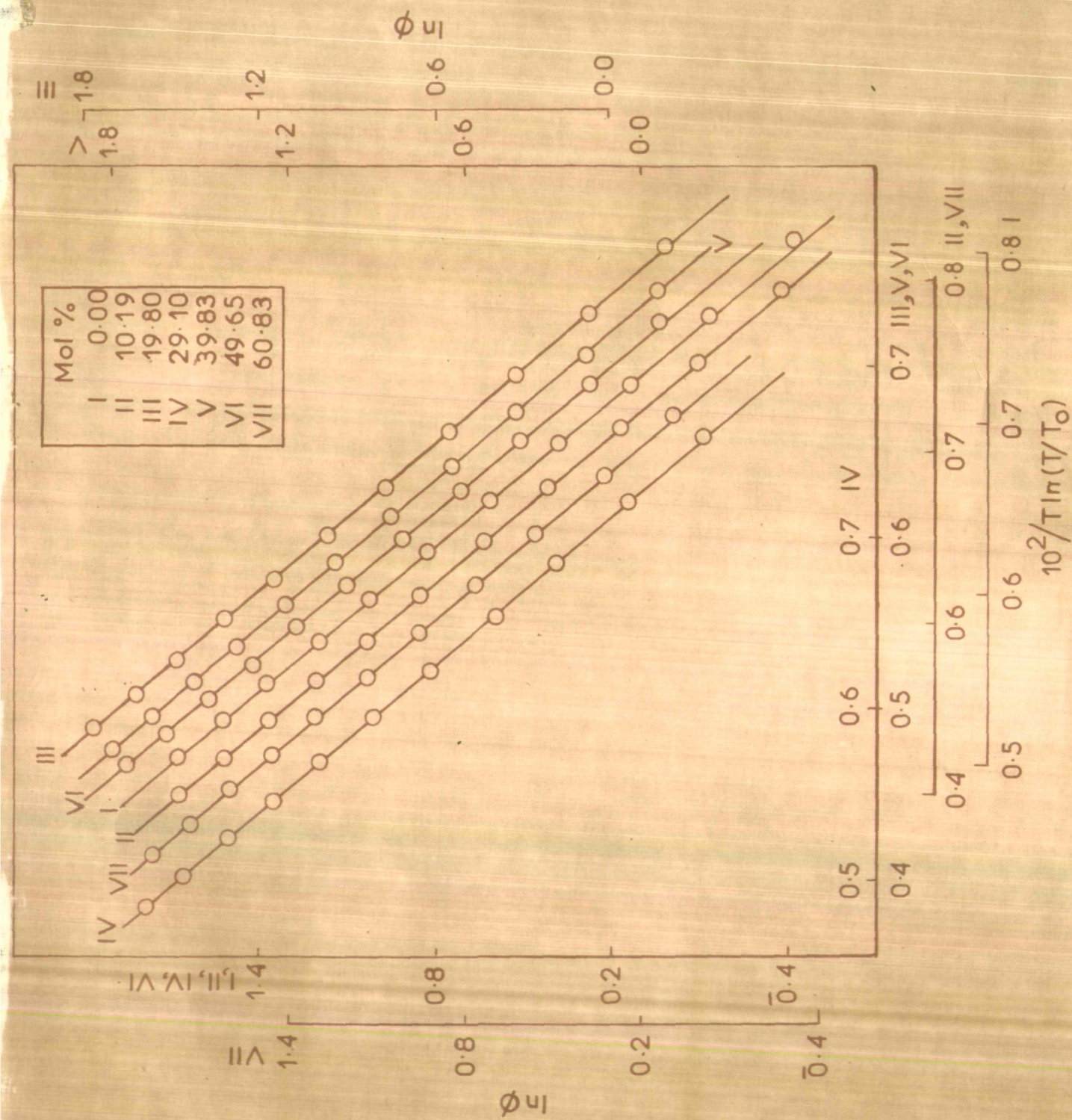


Fig.19. Plots of $\ln \gamma (= \phi \text{ or } \Lambda)$ vs. $1/T \ln(T/T_0)$ for molten $\text{Ca}(\text{NO}_3)_2 \cdot 3.96\text{H}_2\text{O}$ - $\text{Ni}(\text{NO}_3)_2 \cdot 6.03\text{H}_2\text{O}$ systems.

$1/[T \ln (T/T_0)]$. The computational analysis of the data have been done in a manner similar to that adopted in Chapter III. A number of $A_Y'' - k_Y'' - T_0$ sets have been found to fit the equation (15). Out of these various possible sets those which provide almost identical values for the exponential term k_Y'' like those of k_Y term of the VTF equation (10) were selected. These selected values of the parameters are presented in Tables 22-25 along with the standard deviations in $\ln \phi$ and $\ln \Lambda$. The activation energies (Tables 26-29) were computed using the standard procedure as given in Appendix C. The activation energies obtained from both the VTF and the configurational entropy models are in good agreement with each other.

Some striking similarities of the VTF equation (10) and of equation (15) may be visualized. The parameter T_0 of equation (10) represents the temperature below which the free volume of the system is zero, while in the case of equation (15) based on the cooperative rearrangement model, T_0 refers to the temperature below which the configurational entropy of the system is zero. Thus, apart from the preexponential factor, equations (10) and (15) are functionally related.⁵⁵ Furthermore, Angell^{32,33} applied Clapeyron equation⁵⁶ for ΔC_p to relate the Adam-Gibbs equation (15) with that of the Doolittle type equation (4). Such a substitution of ΔC_p in equation (13)

TABLE 22 : Computed Parameters for Equation (15) for the Fluidity and Equivalent

Conductance of $\text{Cd}(\text{NO}_3)_2 \cdot 4.03\text{H}_2\text{O}-\text{MnCl}_2 \cdot 4.00\text{H}_2\text{O}$ Melts

Mol % Mn^{2+}	A_ϕ''	k_ϕ''	$T_{o,\phi}$	Std. dev. in $\ln \phi$	A_Λ''	k_Λ''	$T_{o,\Lambda}$	Std. dev. in $\ln \Lambda$
0.00	239.00	686.50	193.00	0.014	83.95	600.00	192.80	0.016
2.27	227.80	694.00	193.59	0.006	82.00	597.00	194.30	0.007
4.14	220.00	690.00	194.48	0.012	80.20	600.00	195.45	0.026
6.63	212.00	682.00	195.30	0.014	77.90	587.51	197.08	0.009
9.07	200.30	685.00	196.10	0.012	75.60	590.00	198.40	0.013
12.31	186.20	684.00	197.15	0.007	73.00	595.00	200.00	0.005

TABLE 23 : Computed Parameters for Equation(15)for the Fluidity and Equivalent Conductance of $\text{Ca}(\text{NO}_3)_2 \cdot 4.23\text{H}_2\text{O}-\text{NH}_4\text{CNS}$ Melts

Mol % NH_4^+	A_ϕ''	K_ϕ''	$T_{o,\phi}$	Std. dev. in $\ln \phi$	A_Λ''	K_Λ''	$T_{o,\Lambda}$	Std. dev. in $\ln \Lambda$
0.00	160.00	693.50	201.50	0.013	50.00	586.00	201.31	0.015
10.11	171.50	690.20	200.10	0.019	60.50	593.20	200.00	0.018
20.02	180.30	691.00	199.40	0.032	71.00	580.00	198.50	0.032
30.35	189.00	695.00	197.80	0.018	80.90	590.00	197.20	0.021
40.48	200.00	691.30	197.00	0.061	92.50	596.00	196.10	0.031
51.30	210.50	690.00	195.20	0.011	102.00	585.30	194.70	0.034
	220.00	690.30	192.50	0.012	110.80	594.00	193.20	0.034

TABLE 24 : Computed Parameters for Equation(15)for the Fluidity and Equivalent Conductance of $\text{Ca}(\text{NO}_3)_2 \cdot 4.1\text{H}_2\text{O}-\text{NaCNS}$ Melts

Mol % Na^+	A_ϕ''	k_ϕ''	$T_{o,\phi}$	Std. dev. in $\ln \phi$	A_Λ''	k_Λ''	$T_{o,\Lambda}$	Std. dev. in $\ln \Lambda$
0.00	180.00	694.75	204.00	0.009	62.50	596.00	202.70	0.057
5.58	182.50	690.50	205.15	0.006	73.00	602.00	204.30	0.023
10.28	185.20	696.00	206.13	0.008	82.00	602.00	205.55	0.026
16.02	189.00	696.00	207.30	0.009	94.80	600.80	206.70	0.009
20.13	190.10	699.50	208.00	0.023	103.80	602.00	207.70	0.018
24.84	193.30	699.50	208.90	0.067	114.00	600.00	208.90	0.008

TABLE 25 : Computed Parameters for Equation(15)for the
Fluidity of $\text{Ca}(\text{NO}_3)_2 \cdot 3.96\text{H}_2\text{O}$ - $\text{Ni}(\text{NO}_3)_2 \cdot 6.03\text{H}_2\text{O}$
Melts

Mol % Ni^{2+}	A''_{ϕ}	k''_{ϕ}	$T_{o,\phi}$	Std. dev. in $\ln \phi$
0.00	179.50	696.00	206.00	0.008
10.19	175.00	697.00	204.70	0.007
19.80	170.30	689.20	202.20	0.008
29.10	166.50	689.00	201.00	0.005
39.83	160.30	687.00	199.20	0.014
49.65	157.80	683.00	197.10	0.018
60.83	154.00	680.00	196.30	0.016

**TABLE 26 : Computed Activation Energy (Kcal/mol) for Conductance and Fluidity*
as a Function of Temperature for $\text{Cd}(\text{NO}_3)_2 \cdot 4.03\text{H}_2\text{O} \cdot \text{MnCl}_2 \cdot 4.00\text{H}_2\text{O}$ Melts**

T, °K	Mol % Mn^{2+}					
	0.00	2.27	4.14	6.63	9.07	12.31
308.0	7.977 (9.162)	8.163 (9.365)	8.385 (9.468)	8.470 (9.504)	8.726 (9.692)	-
313.0	7.538 (8.656)	7.705 (8.844)	7.908 (8.935)	7.978 (8.964)	8.211 (9.136)	-
318.0	7.143 (8.202)	7.295 (8.377)	7.481 (8.458)	7.539 (8.481)	7.752 (8.639)	-
323.0	6.788 (7.793)	6.926 (7.956)	7.097 (8.029)	7.146 (8.047)	7.341 (8.193)	7.612 (8.329)
328.0	6.466 (7.422)	6.592 (7.575)	6.750 (7.641)	6.790 (7.655)	6.970 (7.790)	7.221 (7.915)

(continued)

**TABLE 27 : Computed Activation Energy (Kcal/mol) for Conductance and Fluidity*
as a Function of Temperature for $\text{Ca}(\text{NO}_3)_2 \cdot 4.23\text{H}_2\text{O} \cdot \text{NH}_4\text{CNS}$ Melts**

T, °K	Mol % NH_4^+					
	0.00	10.11	20.02	30.35	40.48	51.30 63.42
313.0	8.616 (10.233)	8.507 (9.917)	8.087 (9.799)	8.030 (9.565)	7.949 (9.375)	7.610 (9.053) 7.516 (8.626)
318.0	8.117 (9.639)	8.023 (9.351)	7.635 (9.244)	7.588 (9.034)	7.517 (8.859)	7.203 (8.566) 7.122 (8.176)
323.0	7.671 (9.109)	7.589 (8.845)	7.229 (8.748)	7.191 (8.558)	7.129 (8.396)	6.836 (8.128) 6.765 (7.771)
328.0	7.271 (8.633)	7.199 (8.390)	6.864 (8.302)	6.833 (8.129)	6.778 (7.979)	6.505 (7.732) 6.443 (7.403)
333.0	6.910 (8.203)	6.847 (7.979)	6.533 (7.898)	6.508 (7.741)	6.460 (7.601)	6.205 (7.373) 6.150 (7.069)

(continued)

TABLE 27 : (continued)

T, °K	Mol % NH ₄ ⁺					
	0.00	10.11	20.02	30.35	40.48	51.30
338.0	6.583 (7.814)	6.527 (7.606)	6.233 (7.531)	6.213 (7.388)	6.171 (7.258)	5.931 (7.046)
						5.883 (6.764)
343.0	6.285 (7.460)	6.236 (7.267)	5.959 (7.198)	5.944 (7.066)	5.906 (6.944)	5.681 (6.748)
						5.638 (6.485)
348.0	6.014 (7.137)	5.970 (6.957)	5.709 (6.893)	5.698 (6.771)	5.664 (6.657)	5.451 (6.472)
						5.414 (6.229)
353.0	5.765 (6.841)	5.726 (6.672)	5.479 (6.612)	5.471 (6.501)	5.442 (6.393)	5.239 (6.220)
						5.207 (5.992)

* Activation energy for fluidity are within parentheses.

TABLE 28 : Computed Activation Energy (Kcal/mol) for Conductance and Fluidity*
as a Function of Temperature for $\text{Ca}(\text{NO}_3)_2 \cdot 4.1\text{H}_2\text{O}$ -NaCNS Melts

T, °K	Mol % Na ⁺				
	0.00	5.58	10.28	16.02	20.13
313.0	8.999 (10.758)	9.376 (10.935)	9.609 (11.237)	9.811 (11.502)	10.029 (11.723)
318.0	8.469 (10.114)	8.813 (10.272)	9.023 (10.547)	9.204 (10.786)	9.401 (10.987)
323.0	7.997 (9.541)	8.313 (9.682)	8.502 (9.934)	8.665 (10.149)	8.844 (10.334)
328.0	7.573 (9.028)	7.864 (9.154)	8.037 (9.387)	8.184 (9.582)	8.347 (9.751)
333.0	7.191 (8.566)	7.459 (8.679)	7.618 (8.895)	7.753 (9.074)	7.902 (9.229)

(continued)

TABLE 28 : (continued)

T, °K	Mol % Na ⁺					
	0.00	5.58	10.28	16.02	20.13	24.84
338.0	6.846 (8.149)	7.095 (8.251)	7.241 (8.451)	7.364 (8.615)	7.501 (8.759)	7.626 (8.891)
343.0	6.532 (7.770)	6.764 (7.863)	6.898 (8.049)	7.011 (8.200)	7.138 (8.334)	7.253 (8.455)
348.0	6.245 (7.420)	6.462 (7.509)	6.587 (7.683)	6.691 (7.823)	6.808 (7.948)	6.913 (8.060)
353.0	5.983 (7.109)	6.186 (7.186)	6.302 (7.349)	6.398 (7.478)	6.508 (7.596)	6.604 (7.699)

* Activation energy for fluidity are within parentheses.

TABLE 29 : Computed Activation Energy (Kcal/mol) for Fluidity as a Function of Temperature for $\text{Ca}(\text{NO}_3)_2 \cdot 3.96\text{H}_2\text{O} - \text{Ni}(\text{NO}_3)_2 \cdot 6.03\text{H}_2\text{O}$ Melts

T, °K	Mol % Ni^{2+}					
	0.00	10.19	19.80	29.10	39.83	49.65
308.0	11.986	11.687	10.986	10.723	10.320	9.851
313.0	11.208	10.941	10.306	10.070	9.705	9.279
318.0	10.521	10.281	9.704	9.489	9.158	8.768
323.0	9.911	9.694	9.165	8.970	8.667	8.310
328.0	9.365	9.168	8.682	8.504	8.226	7.897
333.0	8.875	8.695	8.247	8.083	7.827	7.522

(continued)

TABLE 29 : (continued)

T, °K	Mol % Ni ²⁺					
	0.00	10.19	19.80	29.10	39.83	49.65
338.0	8.433	8.268	7.853	7.702	7.465	7.182
						7.062
343.0	8.032	7.881	7.494	7.355	7.134	6.871
						6.759
348.0	7.668	7.528	7.167	7.038	6.832	6.586
						6.480
353.0	7.335	7.206	6.868	6.747	6.556	6.325
						6.226
358.0	7.031	6.909	6.593	6.481	6.301	6.084
						5.990

leads to the expression

$$\begin{aligned} w(T) &= A \exp \left[(-c \, d \ln T_0 / dp / v \Delta \alpha (T - T_0)) \right] \\ &= A \exp \left[-b / v_f \right] \end{aligned}$$

where v and $\Delta \alpha$ are the molar volume and change in expansion coefficient, respectively. Therefore, the identical nature of equations (10) and (15) may be anticipated and the difference between the two lies only in their theoretical approaches on which these equations are based. It is apparent from the tables 22-25 that the values of k_Y'' and T_0 are in good agreement with those obtained from the VTF equation (10). The difference in the preexponential terms A_Y'' and A_Y is, on the other hand, notable. The lower values of A_Y'' than those of A_Y of the VTF equation may be due to the presence of a temperature term in the preexponential factor of the latter equation. However, the term $T^{-1/2}$ embodied in the preexponential term A_Y has a very weak effect on the temperature dependence in comparison with the exponential term.

The preexponential term A_Y'' has been found to vary linearly (Fig. 20) with concentration in a manner similar to that of the A_Y term of the VTF model. In the cases of $\text{Ca}(\text{NO}_3)_2 \cdot 4.23\text{H}_2\text{O} \cdot \text{NH}_4\text{CNS}$ and $\text{Ca}(\text{NO}_3)_2 \cdot 4.1\text{H}_2\text{O} \cdot \text{NaCNS}$ melts A_Y'' increases linearly with concentration while in the case of $\text{Cd}(\text{NO}_3)_2 \cdot 4.03\text{H}_2\text{O} \cdot \text{MnCl}_2 \cdot 4.00\text{H}_2\text{O}$ melts a linear

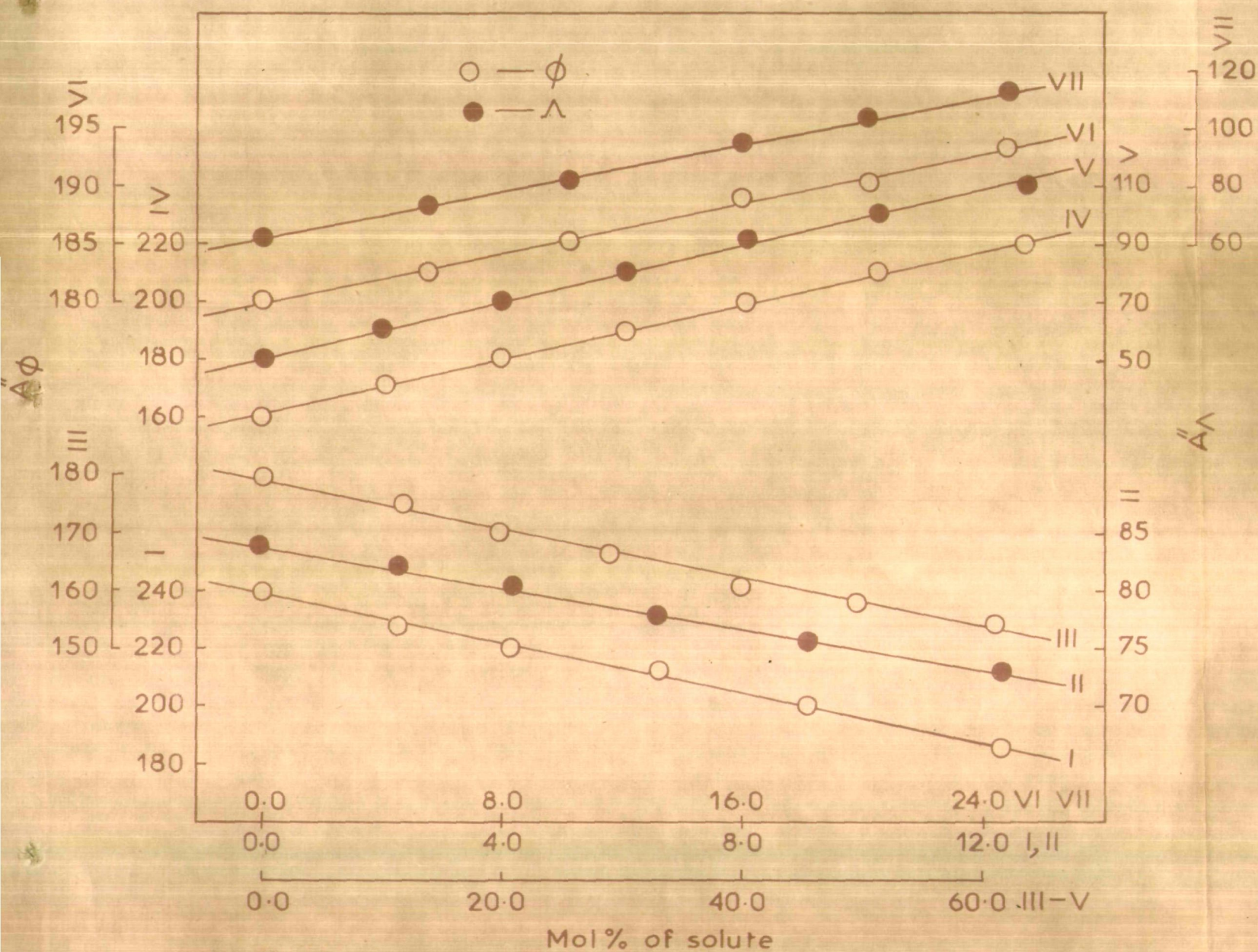


Fig.20. Variation of A''_Y with concentration of $\text{Cd}(\text{NO}_3)_2 \cdot 4.03\text{H}_2\text{O} - \text{MnCl}_2 \cdot 4.00\text{H}_2\text{O}$ (I,II), $\text{Ca}(\text{NO}_3)_2 \cdot 4.23\text{H}_2\text{O} - \text{NH}_4\text{CNS}$ (IV, V), $\text{Ca}(\text{NO}_3)_2 \cdot 4.1\text{H}_2\text{O} - \text{NaCNS}$ (VI, VII), and $\text{Ca}(\text{NO}_3)_2 \cdot 3.96\text{H}_2\text{O} - \text{Ni}(\text{NO}_3)_2 \cdot 6.03\text{H}_2\text{O}$ (III) melts.

decrease in A_Y'' has been observed. Also for $\text{Ca}(\text{NO}_3)_2 \cdot 3.96 \text{H}_2\text{O}$ - $\text{Ni}(\text{NO}_3)_2 \cdot 6.03\text{H}_2\text{O}$ system the preexponential term has been found to decrease linearly with concentration. The variation of A_Y of VTF equation (10) was explained on the basis of mean molecular masses of the component particles. However, such an $m^{-1/2}$ dependence of A_Y'' term observed here may not be emphasized. An indirect reasoning seems to be feasible to explain the variation of A_Y'' with concentration. Maxwell has suggested a relationship between the time of relaxation, τ of the flowing entities and the rigidity modulus, G of the system which is given by

$$1/\tau = GY \quad (16)$$

According to Eyring's expression the relaxation time may be given as

$$\tau = \tau_0 \exp \left[-E/RT \right] \quad (17)$$

in which τ_0 refers to the period of vibration of the flowing entities in the equilibrium position, E , the activation energy for relaxation, and R and T have their usual meaning. Combining the equations (16) and (17) one can write

$$Y = 1/G\tau_0 \exp \left[-E/RT \right] \quad (18)$$

Furthermore, the average transition probability for cooperative rearrangement of the entities, $\bar{w}(T)$ as pointed out by Adam and Gibbs is proportional to the fraction of configurations which undergo such transition and can be given as

$$\bar{w}(T) \propto n'/N \quad (19)$$

where N is the number of independent, equivalent and distinguishable subsystems or configurations of macroscopic system and n' , the number of configurations which undergo such a transition. Also it may be shown that the transition probability, $\bar{w}(T)$ is proportional to the reciprocal of the relaxation time τ . Accordingly, we find that

$$\bar{w}(T) \propto 1/\tau \quad (20)$$

On comparing the preexponential factors of equation (18) with that of equation (15), we get,

$$A_Y'' = 1/G\tau_0 \quad (21)$$

It may, therefore, be concluded that the term A_Y'' depends on the rigidity of the system. As the concentration increases the system becomes more and more rigid, the average cooperative transition probability decreases, in other words, the relaxing species will have greater

period of vibration in their equilibrium position. Therefore, a linear decrease in A_Y'' may be anticipated with increase in concentration.

The concentration independent nature of the k_Y'' term like that of k_Y term of the VTF equation may be visualized. According to the configurational entropy model the factor k_Y'' is equal to $N\Delta\mu S_C^*/R\Delta C_p$ in which the terms have their usual significance as described in the introduction. In this expression S_C^* , the minimum configurational entropy which a region of the liquid must possess in order to undergo cooperative rearrangement is taken as constant ($S_C^* = k \ln 2$, k is the Boltzmann constant). Furthermore, it has been suggested that changes in $\Delta\mu$ from one system to another may be offset by parallel changes in ΔC_p . It may, therefore, be presumed that the term k_Y'' of equation (15) is almost constant. The expectation of almost constant values of k_Y'' are actually observed here for all the molten systems studied and was found to hold fairly good in large variety of other molten salts, polymers and organic liquids at low temperatures.

Moynihan and Angell⁵⁷ during their measurements of diffusion coefficients for Ag^+ , Tl^+ , and Cd^{2+} ions in molten calcium nitrate tetrahydrate pointed out the discrepancy between the k_j (j stands for any transport pro-

property) terms (Table 2)⁵⁷ (582.4 for D_{Ag^+}/T , diffusivity/temperature versus 726.8 for $1/\eta_V$, reciprocal of the bulk viscosity) is about 22 %. We are also able to mark the significant discrepancy between k_Y (Tables 7-10) as well as k_Y'' (Tables 12-15) terms for the conductance and fluidity study in the cases of molten salt systems investigated here. For example, the discrepancy between the k_Y terms (567.0 for conductance versus 670.0 for fluidity) is about 15 %. The discrepancy has almost identical magnitude in the case of k_Y'' term also. These discrepancies could probably be improved if one could dissect the shear and bulk viscosities into considerations from the appropriate relaxation times and moduli Litovitz and McDuffie and their coworkers^{24,58,59} have shown experimentally that better results are achieved when one takes into account the temperature and pressure dependences of shear and structural relaxation times rather than using the corresponding viscosities.

The linear dependence of T_0 on concentration is important in explaining the transport behaviour of particularly dilute aqueous melts with concentration. Therefore, much attention may be paid to study such a variation of T_0 with concentration. Qualitatively, there seems to be a number of factors which determine the value of T_0 for a substance. The most pronounced factors are

the molecular size and complexity. Since the constituent particles are quite small for molten salts, molecular complexity has only a secondary influence on the value of T_0 . On the other hand, for systems having small ionic or molecular aggregates the overall cohesive energy of the liquid seems to be responsible in determining the magnitude of T_0 . A low value of T_0 generally below 100°K is observed for the liquids in which cohesive energy arises from London and dipole-dipole forces. However, T_0 's in the range of 200 – 500°K are found in molten salts and highly concentrated solutions having strong coulomb forces. For net-work liquids such as silica glasses, B_2O_3 , etc., one may expect very strong coulomb and covalent bonding forces thereby T_0 's lie in the range 400 and 700°K . Hence, the important role of cohesive energy in setting the value of T_0 may be stressed.

The coulomb energy of a system is lower the lower the average charge/radius ratio of the anions or cations of the melt. The linear increase in T_0 with increase in concentration of $\text{Ca}(\text{NO}_3)_2$ in $\text{Ca}(\text{NO}_3)_2$ - KNO_3 melts was explained on the basis of cationic potential.²⁹ The cationic potential of a substance has already been defined in the previous Chapter. The increase in the value of T_0 in the above melt is due to a corresponding increase in the cationic potential with the addition of solute

having larger cationic charge/radius ratio. Assuming that there is no coulombic attraction in the structure, i.e., a condition of zero cationic strength one may obtain the value of T_0 nearly equal to 100°K . Such an extrapolated value of T_0 to zero cationic strength is comparable with the T_g values of $80\text{--}100^\circ\text{K}$ obtained for simple molecular liquids.⁶⁰ This concept of cationic potential may, therefore, be applied to any pure or mixed nitrate system to give T_0 value in a reasonable accord with the observed value. For the systems having halide anions and anions other than nitrate ions, linear plots with different slopes but similar T_0 values corresponding to zero cationic potential may be expected. Although, the above correlation between T_0 and the cationic potential seems to be feasible, preferably, for the systems having common anion, it fails to take into account the contribution of anionic species present in the system. Therefore, such^a relationship appears to be less reasonable. According to the above correlation between T_0 and the cationic potential larger differences in the relaxation behaviour should occur between Li^+ and Na^+ ions in their nitrate melts owing to the greater difference in cationic charge/radius ratios which contradicts the observed parallelism in relaxation behaviour of the two melts. Also the basis of the cationic potential to explain the observed T_0 values of $\text{Ca}(\text{NO}_3)_2 \cdot 4\text{H}_2\text{O}$ and $\text{Cd}(\text{NO}_3)_2$.

$4\text{H}_2\text{O}$ melts fails badly. On the basis of this correlation one might expect a higher T_0 value for $\text{Cd}(\text{NO}_3)_2 \cdot 4\text{H}_2\text{O}$ than for $\text{Ca}(\text{NO}_3)_2 \cdot 4\text{H}_2\text{O}$ due to higher cationic charge/radius ratio in the case of the former as compared to the latter. This, however, is contrary to the observed T_0 values in the two cases. Angell and Helphrey⁶¹ in their recent study of alkali metal nitrates have observed that the dependence of the glass transition temperatures on cation type are quite different from those reported previously for these melts on the basis of cationic radii⁴⁶ and anion-cation radius sums.⁶²

Qualitatively, the variation of T_0 with concentration may be visualized in terms of the configurational entropy of the system. As the concentration of the solute increases the system becomes successively more rigid. This, in turn, lowers the configurational entropy of the system and hence less cooling may be required to reach the glass transition region. This consideration supports the increase in the T_0 values. In the cases of $\text{Cd}(\text{NO}_3)_2 \cdot 4.03\text{H}_2\text{O}$ - $\text{MnCl}_2 \cdot 4.00\text{H}_2\text{O}$ and $\text{Ca}(\text{NO}_3)_2 \cdot 4.1\text{H}_2\text{O}$ - NaCNS melts T_0 values have been found to increase with increase in concentration of the solute reinforcing the above view. On the other hand, in the cases of $\text{Ca}(\text{NO}_3)_2 \cdot 4.23\text{H}_2\text{O}$ - NH_4CNS and $\text{Ca}(\text{NO}_3)_2 \cdot 3.96\text{H}_2\text{O}$ - $\text{Ni}(\text{NO}_3)_2 \cdot 6.03\text{H}_2\text{O}$ melts the decrease in the values of T_0 with solute concentration is contrary to that expected.

Such type of behaviour is also observed in other melts.^{25,36} The observed fact leads to conclusion that in almost ideal molten salts the values of T_0 depend on the T_0 's of the pure solvent and that of the solute. Consequently, a linear increase (or decrease) in the values of T_0 may be expected with successive increase in the concentration of solute having higher (or lower) T_0 than that of the solvent. Accordingly, a linear decrease in T_0 is observed with increase in concentration of $\text{Ni}(\text{NO}_3)_2 \cdot 6.03\text{H}_2\text{O}$ which has lower T_0 value.

Furthermore, the dependence of T_0 on the average molecular mass of the component particles of the melt through the correlation⁴⁴ as cited in the previous Chapter seems to be applicable in the cases of $\text{Cd}(\text{NO}_3)_2 \cdot 4.03\text{H}_2\text{O}$ - $\text{MnCl}_2 \cdot 4.00\text{H}_2\text{O}$, $\text{Ca}(\text{NO}_3)_2 \cdot 4.1\text{H}_2\text{O}$ - NaCNS , and $\text{Ca}(\text{NO}_3)_2 \cdot 3.96\text{H}_2\text{O}$ - $\text{Ni}(\text{NO}_3)_2 \cdot 6.03\text{H}_2\text{O}$ melts. Accordingly, an increase in the values of T_0 in the first two cases may presumably be due to the decrease in the average molecular mass of the system with the addition of solute having lower molecular weight than that of the solvent. The decrease in the values of T_0 in the latter case, on the other hand, is due to an increase in the average molecular mass of the system due to the addition of $\text{Ni}(\text{NO}_3)_2 \cdot 6.03\text{H}_2\text{O}$ which has higher molecular weight. However, the above $m^{-1/2}$ dependence relationship fails to explain the decreasing trend of T_0 on the

addition of NH_4CNS having lower molecular weight in molten $\text{Ca}(\text{NO}_3)_2 \cdot 4.23\text{H}_2\text{O}$. Such a reverse trend has also been noted in the case of $\text{Ca}(\text{NO}_3)_2 \cdot 4.1\text{H}_2\text{O}$ - $\text{Cu}(\text{NO}_3)_2 \cdot 2.92\text{H}_2\text{O}$ melts.³⁶

The variation of activation energies both for viscous and conductance flows with temperature and concentration (Tables 26-29) may be visualized in terms of configurational entropy model in a manner similar to that of VTF model discussed in Chapter III. The ratios, E_ϕ/E_Λ for $\text{Cd}(\text{NO}_3)_2 \cdot 4.03\text{H}_2\text{O}$ - $\text{MnCl}_2 \cdot 4.00\text{H}_2\text{O}$ (Table 30) and those of the other melts are found to be greater than unity. These values may be compared to those reported earlier.^{34,40,63}

TABLE 30 : The Ratio E_p/E_Λ as a Function of Temperature for $\text{Cd}(\text{NO}_3)_2 \cdot 4.03\text{H}_2\text{O} - \text{MnCl}_2 \cdot 4.00\text{H}_2\text{O}$ Melts

T, °K	Mol % Mn^{2+}				
	0.00	2.27	4.14	6.63	12.31
308.0	1.1485	1.1472	1.1292	1.1221	1.1107
313.0	1.1483	1.1478	1.1299	1.1236	1.1126
318.0	1.1483	1.1483	1.1306	1.1249	1.1144
323.0	1.1481	1.1487	1.1313	1.1259	1.1161
328.0	1.1479	1.1491	1.1320	1.1274	1.1176
333.0	1.1479	1.4965	1.1325	1.1285	1.1190

(continued)

C H A P T E R - V

Concentration Dependence of Transport Behaviour of
Molten Salt Systems

Introduction

In earlier Chapters III and IV only the temperature dependence of transport properties of the glass-forming molten mixtures of cadmium nitrate tetrahydrate with manganese(II)chloride tetrahydrate and those of calcium nitrate tetrahydrate with ammonium thiocyanate, sodium thiocyanate, and nickel(II)nitrate hexahydrate have been interpreted in the light of the parameters of equations (10) and (15).

Molten salt solutions are known to behave differently as compared to aqueous solutions. This is due to the fact that even in extremely dilute solutions of molten salts the solute is subject to strong inter-ionic effects because of close proximity of charged ions in such media. They may be regarded as very concentrated electrolytes and are of considerable theoretical interest. Attention has recently been directed to the fact that great majority of solutions which reach concentrations approaching their maximum solubility become very viscous on cooling to their melting temperatures and may readily supercool to vitreous state.^{30,32,45,64,65} This has led to the examination of relaxation processes in glass-forming melts in order to have a greater insight into the nature of transport processes in highly concentrated

solutions and to provide new empirical description of the concentration dependence of transport properties.

In order to achieve this aim Angell³² modified equation (10) to an isothermal expression for the variation of transport properties with concentration by assuming A_Y and k_Y as concentration independent and taking only T_0 as varying linearly with concentration. The resulting expression is of the form,

$$Y = A_Y T^{-\gamma/2} \exp \left[- k_Y / Q_{2Y} (N_0 - N) \right] \quad (22)$$

where Q_{2Y} is the slope of the linear plot of T_0 versus N ($=$ mol %) and N_0 , the characteristic concentration at which the isothermal temperature, T becomes the glass transition temperature, T_g of the system, i.e., the concentration at which the particle mobilities would fall to zero at the isothermal temperature. Recent studies on a large number of molten salt systems^{25,34} have revealed that the parameter A_Y also varies linearly with concentration. Accordingly, equation (22) was modified⁴¹ to the form

$$Y = (A_{0Y} + Q_{1Y} N) T^{-\gamma/2} \exp \left[- k_Y / Q_{2Y} (N_0 - N) \right] \quad (23)$$

in which Q_{1Y} represents the slope of the plot of A_Y versus

N and A_{OY} is the value of A_Y for the pure solvent. The above isothermal equation has been satisfactorily employed to describe the concentration dependence of transport properties of many molten salt mixtures.⁴¹ The limitations of this equation may, however, be pointed out. This equation has been found to be meaningfully applicable only within the T_0 values of the two components. If we try to go beyond this range of temperature the values of N_0 will be either less than zero or more than 100 mol % which are physically meaningless. For example, in the case of $\text{Ca}(\text{NO}_3)_2 \cdot 4.09\text{H}_2\text{O} - \text{Cd}(\text{NO}_3)_2 \cdot 4.07\text{H}_2\text{O}$ ²⁵ melts T_0 values of the solvent and that of the solute range between 205 and 193°K. Therefore, the concentration dependence of transport properties obtained above 205°K cannot be explained through this isothermal equation. For the mixtures of alkali metal nitrates in molten $\text{Cd}(\text{NO}_3)_2 \cdot 4\text{H}_2\text{O}$ and $\text{Ca}(\text{NO}_3)_2 \cdot 4\text{H}_2\text{O}$ similar difficulties arise in applying the above isothermal equation. Such difficulties are also encountered in the present molten salt systems. In order to get rid of such an inherent difficulty with the modified Angell's equation (23) another equation based on the configurational entropy model was looked into. According to this model⁵² at equal values of T/T_0 the entropies, according to the equation $S_c = \Delta C_p \ln(T/T_0)$ where ΔC_p is the difference

in heat capacities of liquid and glassy state, are taken as almost concentration independent provided that ΔC_p is also constant. Therefore, the feasibility of basically this expression in explaining the concentration dependence of transport properties of the systems under investigation have been examined. However, the assumption made here that ΔC_p is concentration independent has lack of support. Therefore, another modified expression based on the VTF equation (10) has been proposed to explain more satisfactorily the concentration dependence of transport properties of molten mixtures. Here at equal values of T/T_0 , the activation energies of the systems assume constant values. The resulting equation is thus an iso-energetic one. The temperature dependence of transport data of the systems under investigation has already been given in Chapters III and IV. The selected systems have been employed for examining the relative significance of the two expressions (30) and (31) in explaining the concentration dependence of viscosities and conductances.

Results and Discussion

In order to examine the concentration dependence of transport properties, variations in the values of A_Y and T_0 terms of VTF equation and that of A_Y'' term of configurational entropy model with concentration have been examined. Since the nature of their concentration dependence has already been emphasized in earlier Chapters, only a reference to this effect is made here. In the cases of the systems studied earlier, e.g., $\text{Ca}(\text{NO}_3)_2\text{-KNO}_3$ ²⁹, $\text{Ca}(\text{NO}_3)_2\text{-H}_2\text{O}$ ⁶⁷, $\text{TlNO}_3\text{-Ca}(\text{NO}_3)_2$ ⁶⁸, as well as in the systems studied here, e.g., $\text{Cd}(\text{NO}_3)_2\cdot 4.03\text{H}_2\text{O}\text{-MnCl}_2\cdot 4.00\text{H}_2\text{O}$, $\text{Ca}(\text{NO}_3)_2\cdot 4.23\text{H}_2\text{O}\text{-NH}_4\text{CNS}$, $\text{Ca}(\text{NO}_3)_2\cdot 4.1\text{H}_2\text{O}\text{-NaCNS}$, and $\text{Ca}(\text{NO}_3)_2\cdot 3.96\text{H}_2\text{O}\text{-Ni}(\text{NO}_3)_2\cdot 6.03\text{H}_2\text{O}$ the concentration dependence of transport properties has been found to be predominantly governed by the T_0 values. This sometimes leads one to assume that the preexponential terms A_Y and A_Y'' are concentration independent.³²

Concentration dependence of the preexponential terms

As cited in earlier Chapters the dependence of the parameter A_Y on the mean molecular mass of the component particles of the melt shows a qualitative approach in understanding the concentration dependence of A_Y . According to this qualitative reasoning²² the

term A_Y should increase with decrease in effective masses of the component particles on the addition of solute in molten solvent. The above correlation between the term A_Y and the mean molecular mass of the component particles holds good in the cases of $\text{Ca}(\text{NO}_3)_2 \cdot 4.23\text{H}_2\text{O} - \text{NH}_4\text{CNS}$, $\text{Ca}(\text{NO}_3)_2 \cdot 4.1\text{H}_2\text{O} - \text{NaCNS}$, and $\text{Ca}(\text{NO}_3)_2 \cdot 3.96\text{H}_2\text{O} - \text{Ni}(\text{NO}_3)_2 \cdot 6.03\text{H}_2\text{O}$ melts. In the former two cases the average molecular mass decreases on addition of solute and hence A_Y goes on increasing with concentration while in the latter melt A_Y has been found to decrease with concentration which fairly supports the $m^{-1/2}$ dependence relationship. On the other hand, the decrease in A_Y with increase in $[\text{Mn}^{2+}]$ having lower molecular weight in molten $\text{Cd}(\text{NO}_3)_2 \cdot 4.03\text{H}_2\text{O}$ shows a reverse of the effect expected from $m^{-1/2}$ dependence as was also reported by others.²⁵ However, the $m^{-1/2}$ dependence of the preexponential term, A_Y'' of configurational entropy equation (15) may not be explained on the basis of this correlation. An indirect explanation based on the rigidity of the system was proposed in Chapter IV. Accordingly, the term A_Y'' may be expressed as follows,

$$A_Y'' = T^{1/2} / \gamma_0 G \quad (24)$$

where the terms have their usual meaning. The above relation shows that as the concentration of the solute increases the system becomes increasingly more rigid and

consequently, G , the rigidity modulus of the system increases resulting in a decrease in the term A_Y'' . Furthermore, the larger values of the slopes of the linear plots of A_ϕ versus N than those of A_Λ versus N (Table 31) as well as those of A_ϕ'' versus N than A_Λ'' versus N (Table 32) imply that A_ϕ and A_ϕ'' decrease (or increase) with concentration more rapidly than those of A_Λ and A_Λ'' in the respective cases. Therefore, conductance appears to be less sensitive to the change in rigidity of the system than the fluidity. It may be anticipated on the basis of the differences in the slopes of the linear plots of A_ϕ and A_Λ versus N as well as those of A_ϕ'' and A_Λ'' versus N that the factors which determine the concentration dependence of these preexponential terms are not the same. This observation is contrary to the reported behaviour in the case of $\text{Ca}(\text{NO}_3)_2 \cdot 4.09\text{H}_2\text{O} - \text{Cd}(\text{NO}_3)_2 \cdot 4.09\text{H}_2\text{O}$ melts²⁵ where plots of $\ln A_\phi$ and $\ln A_\Lambda$ versus mol fraction of Cd^{2+} are linear and parallel, showing that the same factors determine the concentration dependence of the preexponential terms of both conductance and fluidity.

It may be noted from the optical spectra (Cf. optical spectra) of the thin films of $\text{Ni}(\text{NO}_3)_2 \cdot 6.03\text{H}_2\text{O}$ -rich solutions of $\text{Ca}(\text{NO}_3)_2 \cdot 3.96\text{H}_2\text{O}$ that the absorbing species have octahedral symmetry, i.e., $\text{Ni}(\text{H}_2\text{O})_6^{2+}$. Similarly, $\text{Mn}(\text{H}_2\text{O})_4\text{Cl}_2$ is expected to be present in the molten

TABLE 31 : Computed Parameters for Equation(30)for the Equivalent Conductance and Fluidity of Molten Mixtures*

Melt	c	A _{OY}	Q _{1Y}	K _Y	T _{O(o)}	Q _{2Y}	Std. dev. in ln Y
Cd(NO ₃) ₂ ·4.03H ₂ O	1.8	3610.0	3.493	585.0	192.5	0.560	0.030
+ MnCl ₂ ·4.00H ₂ O		(11163.0)	(94.40)	(664.1)	(192.2)	(0.470)	(0.031)
Ca(NO ₃) ₂ ·4.23H ₂ O	1.7	3620.0	7.720	567.0	201.3	0.104	0.019
+ NH ₄ CNS		(9140.0)	(12.29)	(672.0)	(201.7)	(0.125)	(0.006)
Ca(NO ₃) ₂ ·4.1H ₂ O	1.7	3300.0	16.12	580.0	203.6	0.210	0.035
+ NaCNS		(8357.0)	(19.48)	(670.0)	(203.9)	(0.205)	(0.004)
Ca(NO ₃) ₂ ·3.96H ₂ O	1.7	-	-	-	-	-	-
+ Ni(NO ₃) ₂ ·6.03H ₂ O		(8445.0)	(13.87)	(671.5)	(206.6)	(0.190)	(0.028)

* Fluidity data are within parentheses.

TABLE 32 : Computed Parameters for Equation(31) for the Equivalent Conductance and Fluidity of Molten Mixtures*

Melt	c	A _{oY} "	Q _{1Y} '	k _Y "	T _{o(o)}	Q _{2Y}	Std. dev. in ln Y
Ca(NO ₃) ₂ ·4.03H ₂ O	1.8	83.94	0.880	600.0	192.8	0.580	0.036
+ MnCl ₂ ·4.00H ₂ O		(239.0)	(4.280)	(686.5)	(193.0)	(0.330)	(0.027)
Ca(NO ₃) ₂ ·4.23H ₂ O	1.7	50.10	0.945	586.2	201.3	0.122	0.035
+ NH ₄ CNS		(160.0)	(0.946)	(693.5)	(201.5)	(0.141)	(0.019)
Ca(NO ₃) ₂ ·4.1H ₂ O	1.7	62.00	2.000	595.4	202.7	0.250	0.017
+ NaCNS		(180.0)	(0.530)	(694.7)	(204.0)	(0.190)	(0.017)
Ca(NO ₃) ₂ ·3.96H ₂ O	1.7	-	-	-	-	-	-
+ Ni(NO ₃) ₂ ·6.03H ₂ O		(179.5)	(0.400)	(695.5)	(206.0)	(0.150)	(0.025)

* Fluidity data are within parentheses.

mixtures of $\text{MnCl}_2 \cdot 4.00\text{H}_2\text{O}$ and $\text{Cd}(\text{NO}_3)_2 \cdot 4.03\text{H}_2\text{O}$. Such an association of water molecules with Ni^{2+} and Mn^{2+} ions to form $\text{Ni}(\text{H}_2\text{O})_6^{2+}$ and $\text{Mn}(\text{H}_2\text{O})_4\text{Cl}_2$ species is expected to contribute more to viscosities than to conductances. The linear variations of A_Y (Figs. 12-15) as well as of A_Y'' (Fig. 20) with concentration may be expressed as

$$A_Y = A_{OY} \pm Q_{1Y}N \quad (25)$$

$$\text{and } A_Y'' = A_{OY}'' \pm Q_{1Y}'N \quad (26)$$

respectively. A_{OY} and A_{OY}'' are the values of A_Y and A_Y'' , respectively, for the pure solvent and Q_{1Y} and Q_{1Y}' are the corresponding slopes of A_Y and A_Y'' versus N plots.

Concentration dependence of T_0

As mentioned in the earlier Chapters for the systems under investigation T_0 shows a linear relationship with mol % of solute (Figs. 12-15). Such a variation of T_0 with concentration of solute has also been reported earlier.^{29,34,41,66} The concentration dependence of T_0 has been viewed through the consideration of cohesive energy, molecular masses at several concentrations, and finally changes in molecular complexity. In the case of molten $\text{Cd}(\text{NO}_3)_2 \cdot 4.03\text{H}_2\text{O}$ - $\text{MnCl}_2 \cdot 4.00\text{H}_2\text{O}$, added solute cation

Mn^{2+} has higher charge/radius ratio than that of the solvent cation, Cd^{2+} . Hence, one finds an increase in the coulomb energy of the system with increase in $[\text{Mn}^{2+}]$. Consequently, this results in a linear increase in the values of T_0 with concentration. The coulomb energy in the case of $\text{Ca}(\text{NO}_3)_2 \cdot 4.23\text{H}_2\text{O} - \text{NH}_4\text{CNS}$ decreases with increase in the concentration of solute having cation of lower charge/radius ratio than that of Ca^{2+} which, in turn, causes a linear decrease in the values of T_0 with concentration. However, the above explanation may not be accorded to the cases of $\text{Ca}(\text{NO}_3)_2 \cdot 4.1\text{H}_2\text{O} - \text{NaCNS}$ and $\text{Ca}(\text{NO}_3)_2 \cdot 3.96\text{H}_2\text{O} - \text{Ni}(\text{NO}_3)_2 \cdot 6.03\text{H}_2\text{O}$ melts because in these systems a reverse trend of T_0 with solute concentration is observed. The correlation proposed by Angell⁴⁴ between T_0 and the effective masses of the component particles seems to be feasible in these melts. It may be noted that the value of m goes on decreasing as NaCNS is added to molten $\text{Ca}(\text{NO}_3)_2 \cdot 4.1\text{H}_2\text{O}$ and hence an increase in the values of T_0 with concentration is expected on the basis of the above correlation. In the case of $\text{Ca}(\text{NO}_3)_2 \cdot 3.96\text{H}_2\text{O} - \text{Ni}(\text{NO}_3)_2 \cdot 6.03\text{H}_2\text{O}$ the $m^{-1/2}$ dependence of T_0 also appears to be feasible where T_0 decreases with increase in the value of m on adding the solute of higher molecular weight in the molten solvent. Therefore, the concentration dependence of T_0 may be expressed by the linear relation,

$$T_o = T_{o(o)} \pm Q_{2Y}N \quad (27)$$

where Q_{2Y} is the slope of the plot of T_o versus N , and the intercept, i.e., $T_{o(o)}$ represents the value of T_o for the pure solvent. It may be noted that the values of T_o in the above equation are the average values of those obtained from the VTF and the Adam-Gibbs' equations.

It may be recalled from the derivative of the VTF equation (10) (Appendix C) that the corrected activation energies, E_{corr} for conductance and viscous flow were obtained as $E_{corr}/Rk_Y = [T/(T-T_o)]^2$ where R is the gas constant and k_Y is the exponential term which is an empirical constant in equation (10). Now, if we take T_o as a basis for the corresponding temperature, T in fused salts, then at constant values of T/T_o we have $E_{corr}/Rk_Y = [(T/T_o)/\{(T/T_o) - 1\}]^2$. Therefore, E_{corr}/Rk_Y may have a constant value at equal T/T_o values⁶⁹ which may be termed as an "isoenergetic" condition. According to the configurational entropy model, T_o is related to the macroscopic thermodynamic properties of the liquid by the equation $S_c = \Delta C_p \ln(T/T_o)$ where S_c is the configurational entropy and ΔC_p , the difference in heat capacities for the liquid and the glassy states which may be regarded as almost invariant with concentration, then T/T_o is directly proportional to the configurational entropy of the liquid at temperature T . Therefore, at equal values of T/T_o the

configurational entropies of the systems may apparently be treated as constant. Thus the conductances and fluidities of molten salt systems may be plotted against concentration at constant T/T_0 values and these graphs are termed as "pseudo-isentropes".⁵⁵ The significance of such plots is that a better quantitative illustration of the concentration dependence of transport properties may be made at equal T/T_0 values by accounting for the concentration dependences of individual parameters in equations (10) and (15). Substituting $T/T_0 = \text{constant}$, c , equations (10) and (15) may assume the following form,

$$Y = A_Y (cT_0)^{-\gamma/2} \exp \left[-k_Y/T_0 (c - 1) \right] \quad (28)$$

$$\text{and } Y = A_Y'' \exp \left[-k_Y''/T_0 c \ln c \right] \quad (29)$$

The concentration independent nature of k_Y and k_Y'' terms have been discussed in earlier Chapters. Now substituting for the linear concentration dependences of A_Y , A_Y'' , and T_0 terms the above equations (28) and (29) may be transformed into an isoenergetic as well as an apparently iso-entropic equations,

$$Y = (A_{0Y} \pm Q_{1Y}N) c^{-\gamma/2} (T_{0(o)} \pm Q_{2Y}N)^{-\gamma/2} \exp \left[-k_Y / (T_{0(o)} \pm Q_{2Y}N) (c - 1) \right] \quad (30)$$

$$\text{and } Y = (A_{OY}'' \pm Q_{1Y}'N) \exp \left[-k_Y'' / (T_{O(O)} \pm Q_{2Y}N) c \ln c \right] \quad (31)$$

The values of fluidities and equivalent conductances at constant T/T_0 ratios ranging from 1.2 to 1.9 in the case of $\text{Cd}(\text{NO}_3)_2 \cdot 4.03\text{H}_2\text{O} - \text{MnCl}_2 \cdot 4.00\text{H}_2\text{O}$, while from 1.3 to 1.9 in the cases of $\text{Ca}(\text{NO}_3)_2 \cdot 4.23\text{H}_2\text{O} - \text{NH}_4\text{CNS}$ and $\text{Ca}(\text{NO}_3)_2 \cdot 4.1\text{H}_2\text{O} - \text{NaCNS}$ melts were computed from equations (28) and (29). Fluidities were calculated for the system $\text{Ca}(\text{NO}_3)_2 \cdot 3.96\text{H}_2\text{O} - \text{Ni}(\text{NO}_3)_2 \cdot 6.03\text{H}_2\text{O}$ also at constant T/T_0 ratios in the range 1.3 to 1.2 from equations (28) and (29). These calculated values of the fluidities and equivalent conductances are least-squares fitted to the equations (30) and (31). The corresponding temperatures T lying in the experimental range and the value of c which gave reasonably good fits were selected. The values of the relevant parameters thus computed along with the standard deviations in $\ln \phi$ and $\ln \Lambda$ are listed in Tables 31-32. It is interesting to note that the computed parameters A_{OY} , Q_{1Y} , k_Y , Q_{2Y} , and $T_{O(O)}$ from equation (30) and A_{OY}'' , Q_{1Y}' , k_Y'' , Q_{2Y} , and $T_{O(O)}$ from that of the equation (31) were found to be very close to those obtained from the corresponding plots (Figs. 12-15 and 20). Furthermore, the values of $T_{O(O)}$ obtained from equation (30) and (31) are in good resemblance with those obtained by extrapolating the plots of T_0 versus N to zero mol % of solute in the respective molten salt systems. Finally, the

successful applicability of equations (30) and (31) in explaining the concentration dependence of the transport properties of the systems under investigation is also apparent from the linear plots of $1/\ln[Y(T_o(o) \pm Q_{2Y}N)c]^{1/2} / (A_{oY} \pm Q_{1Y}N)$ and $1/\ln[(A''_{oY} \pm Q'_{1Y}N)/Y]$ against N shown in Figs. (21 & 22) and (23 & 24), respectively.

It may be concluded that the isoenergetic as well as apparently isentropic conditions used in the present systems satisfactorily represent the concentration dependence of viscosities and conductances in the glass forming melts irrespective of the geometry of the species present. However, the isoenergetic condition appears to have a direct experimental relevance as compared to that involving apparently constant entropy (the latter, however, is far from constant). Such an analysis emphasizes further the importance of choosing T/T_o as a better corresponding state for the comparison of liquid properties.

Furthermore, an interesting relationship for the dependence of A_Y on T_o may be derived from the linear variations of A_Y and T_o with concentration. The linear variations of A_Y and T_o with concentration have already been expressed by equations (25) and (27), respectively. Combining these two equations we arrive at the following,

$$A_Y = [A_{oY} - (Q_{1Y}/Q_{2Y})T_o(o)] + (Q_{1Y}/Q_{2Y})T_o \quad (32)$$

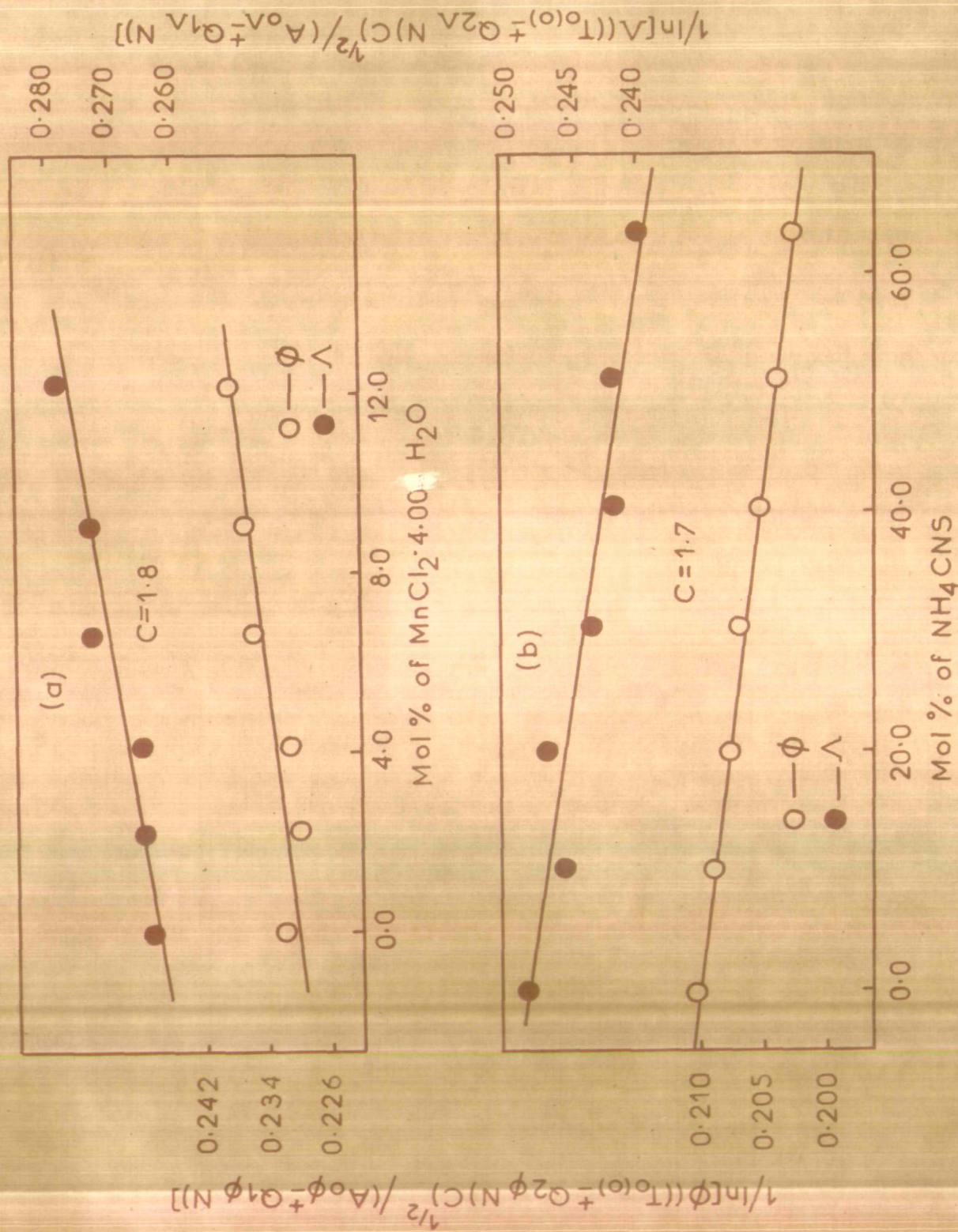


Fig. 21. Plots of $1/\ln[\phi((T_{0(o)} \pm Q_{2\phi} N)C)^{1/2} / (A_{0\phi} \pm Q_{1\phi} N)]$ vs. $N(= \text{mol } \%)$ for (a) $\text{Cd}(\text{NO}_3)_2 \cdot 4.03\text{H}_2\text{O}$ and (b) $\text{Ca}(\text{NO}_3)_2 \cdot 4.23\text{H}_2\text{O}$ - NH_4CNS melts.

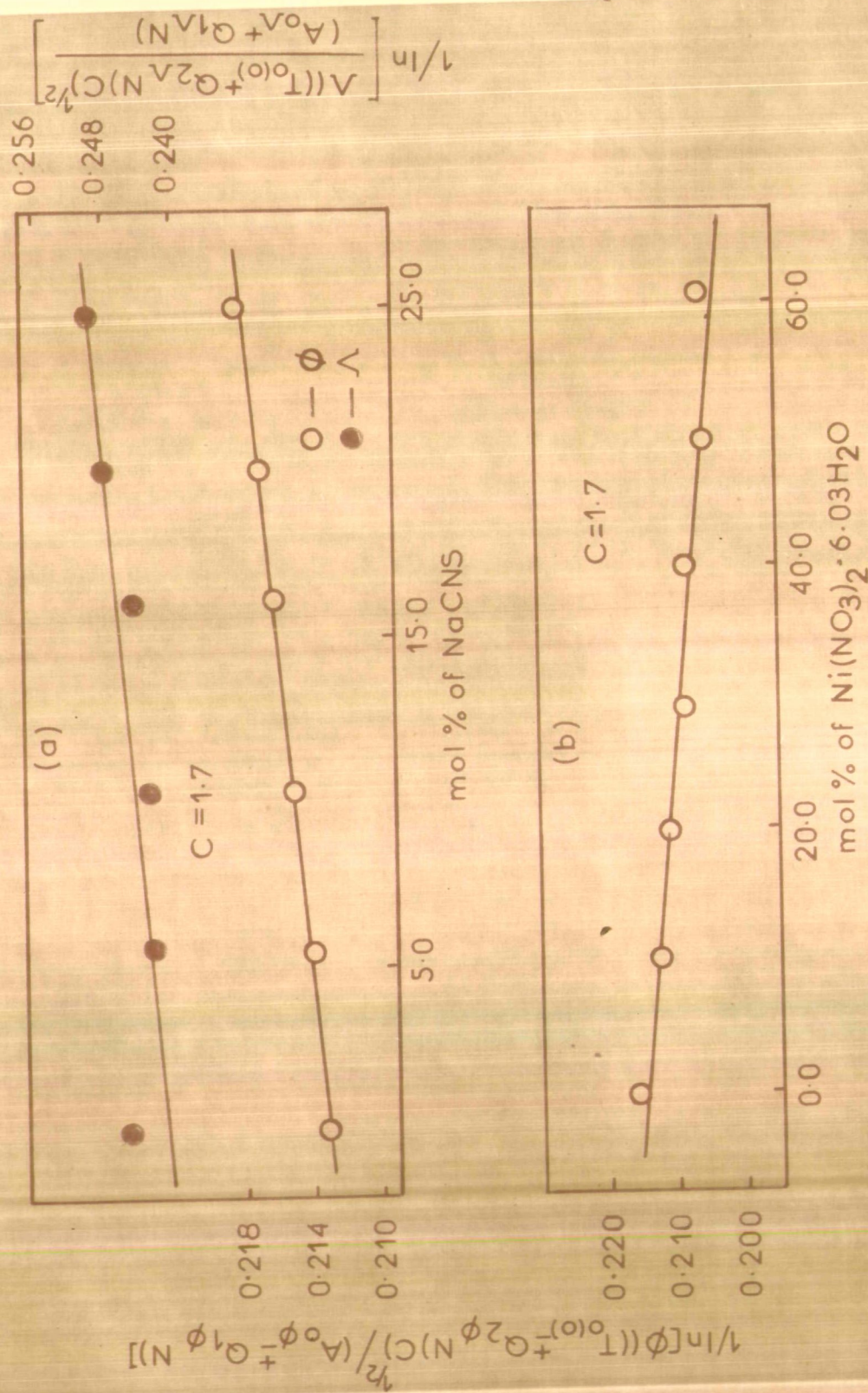


Fig. 22. Plots of $1/\ln \left[\frac{Y((T_{o(o)} + Q_2\gamma N)C)^{1/2}}{(A_o\phi + Q_1\phi N)} \right]$ vs. $N(= \text{mol} \%)$ for
 (a) $\text{Ca}(\text{NO}_3)_2 \cdot 4.1\text{H}_2\text{O} - \text{NaCNS}$ and (b) $\text{Ca}(\text{NO}_3)_2 \cdot 3.96\text{H}_2\text{O} - \text{Ni}(\text{NO}_3)_2 \cdot 6.03\text{H}_2\text{O}$ melts.

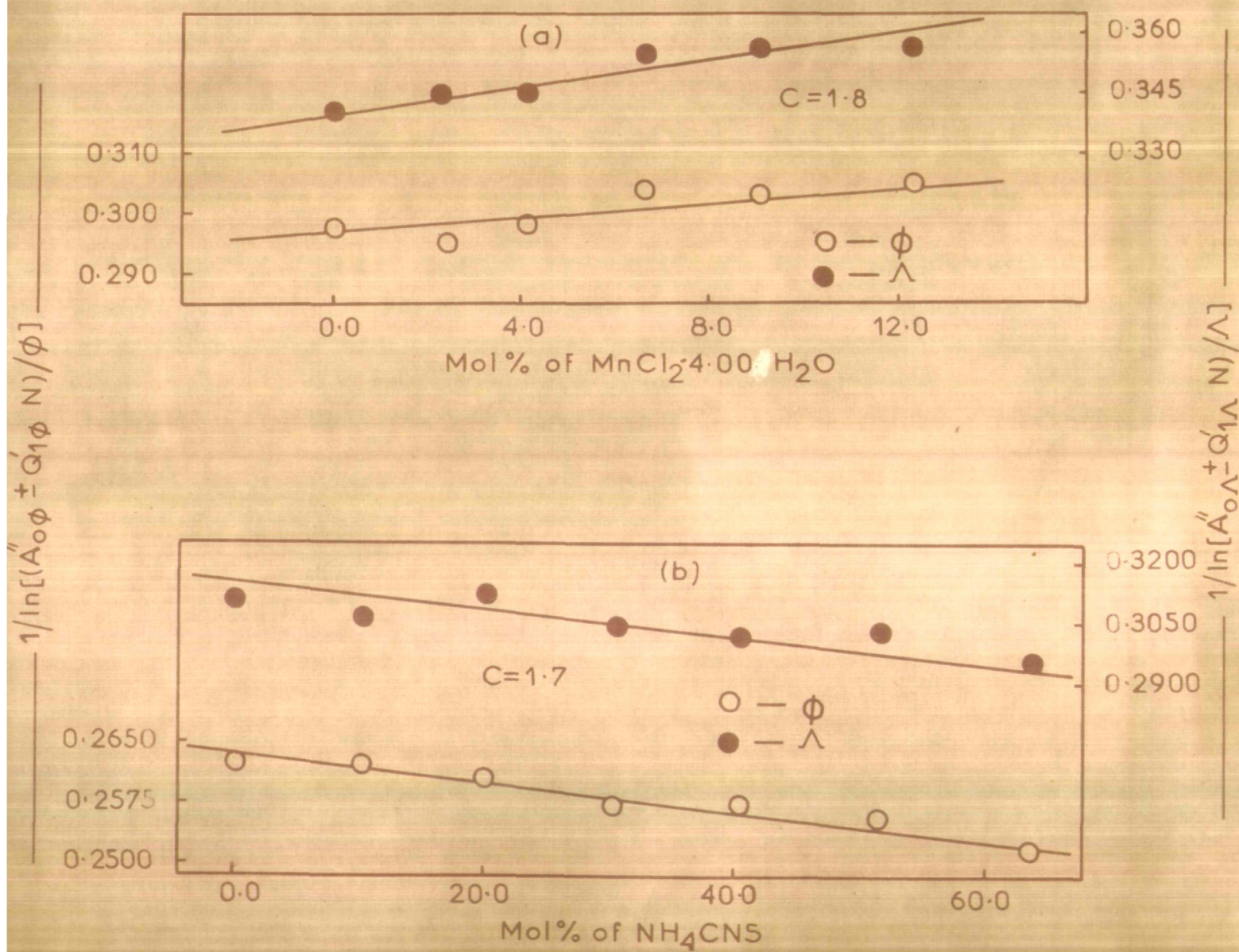


Fig. 23. Plots of $1/\ln[(\ddot{A}_{0Y} \pm Q'_1Y N)/Y]$ vs. N (= mol %) for
 (a) $\text{Cd}(\text{NO}_3)_2 \cdot 4.03\text{H}_2\text{O} - \text{MnCl}_2 \cdot 4.00\text{H}_2\text{O}$ and
 (b) $\text{Ca}(\text{NO}_3)_2 \cdot 4.23\text{H}_2\text{O} - \text{NH}_4\text{CNS}$ melts.

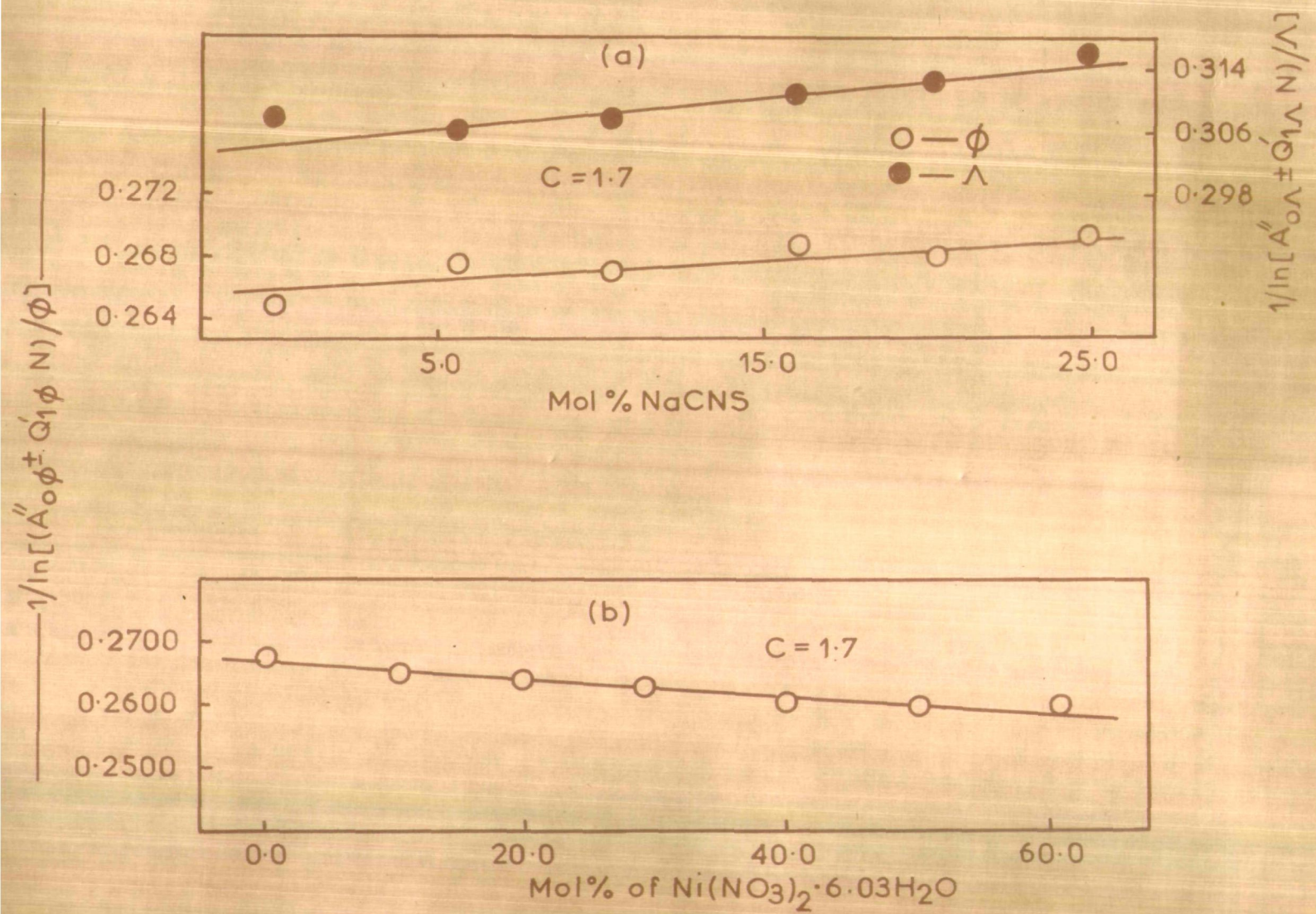


Fig.24 Plots of $1/\ln[(A''_{0Y} \pm Q'_{1Y} N)/Y]$ vs. N (=mol %) for (a) $\text{Ca}(\text{NO}_3)_2 \cdot 4.1\text{H}_2\text{O}$ -NaCNS and (b) $\text{Ca}(\text{NO}_3)_2 \cdot 3.96\text{H}_2\text{O}$ - $\text{Ni}(\text{NO}_3)_2 \cdot 6.03\text{H}_2\text{O}$ melts.

which may be applied to any system in which A_Y and T_o both vary linearly with concentration. The preexponential term A_Y' of equation (4) like those of A_Y and A_Y'' terms shows a linear dependence on concentration and is, therefore, expressed as

$$A_Y' = A_{oY}' \pm Q_{3Y}N \quad (33)$$

where A_{oY}' is the value of A_Y' for pure solvent and Q_{3Y} is the slope of the plot of A_Y' versus N . It is also apparent from the plots of V_o versus N (Figs. 12-15) that V_o varies linearly with concentration and may similarly be represented as

$$V_o = V_{o(o)} \pm Q_{4Y}N \quad (34)$$

where $V_{o(o)}$ is the value of V_o for the pure solvent and Q_{4Y} is the slope of the plot of V_o versus N . Equations (33) and (34) may be combined to yield

$$A_Y' = [A_{oY}' - (Q_{3Y}/Q_{4Y})V_{o(o)}] + (Q_{3Y}/Q_{4Y})V_o \quad (35)$$

Finally, a meaningful correlation between the two thermodynamic variables T_o and V_o may be obtained by combining equations (27) and (34), and we have,

$$T_o = [T_{o(o)} - (Q_{2Y}/Q_{4Y})V_{o(o)}] + (Q_{2Y}/Q_{4Y})V_o \quad (36)$$

The equations (32), (35) and (36) represent linear dependences of A_Y on T_0 , A_Y' on V_0 , and T_0 on V_0 , respectively, as shown in Figs. 25-30. The data for these parameters were least-squares fitted to the above derived equations. The computed values of the slopes and the intercepts may be compared with those obtained from the plots of A_Y , A_Y' , and T_0 against T_0 , V_0 , and V_0 , respectively and are found to be in good agreement.

The fluidities and conductances of the systems under investigation are found to change quite markedly with concentration above their melting points and the corresponding isotherms are plotted in Figs. 31 and 32. The viscosity of a system is determined mainly by the bulky or less mobile entities while ions of higher mobilities appear to be mainly responsible for the conductance behaviour. Therefore, both are expected to show opposite trends with concentration for a given system. On examining the isotherms (Figs. 31 & 32) it is apparent that in the case of the molten $\text{Cd}(\text{NO}_3)_2 \cdot 4.03\text{H}_2\text{O}$ - $\text{MnCl}_2 \cdot 4.00\text{H}_2\text{O}$ system viscosity increases almost linearly from 0.00 to ~ 4 mol % until a maximum is attained at ~ 4.14 mol %. It then passes through a minimum at ~ 6.63 mol %. Finally, it shows a sort of monotonous increase in viscosity from ~ 6.63 to ~ 12.31 mol %. In the case of the conductance an exactly opposite trend to that of the viscosity has been recorded

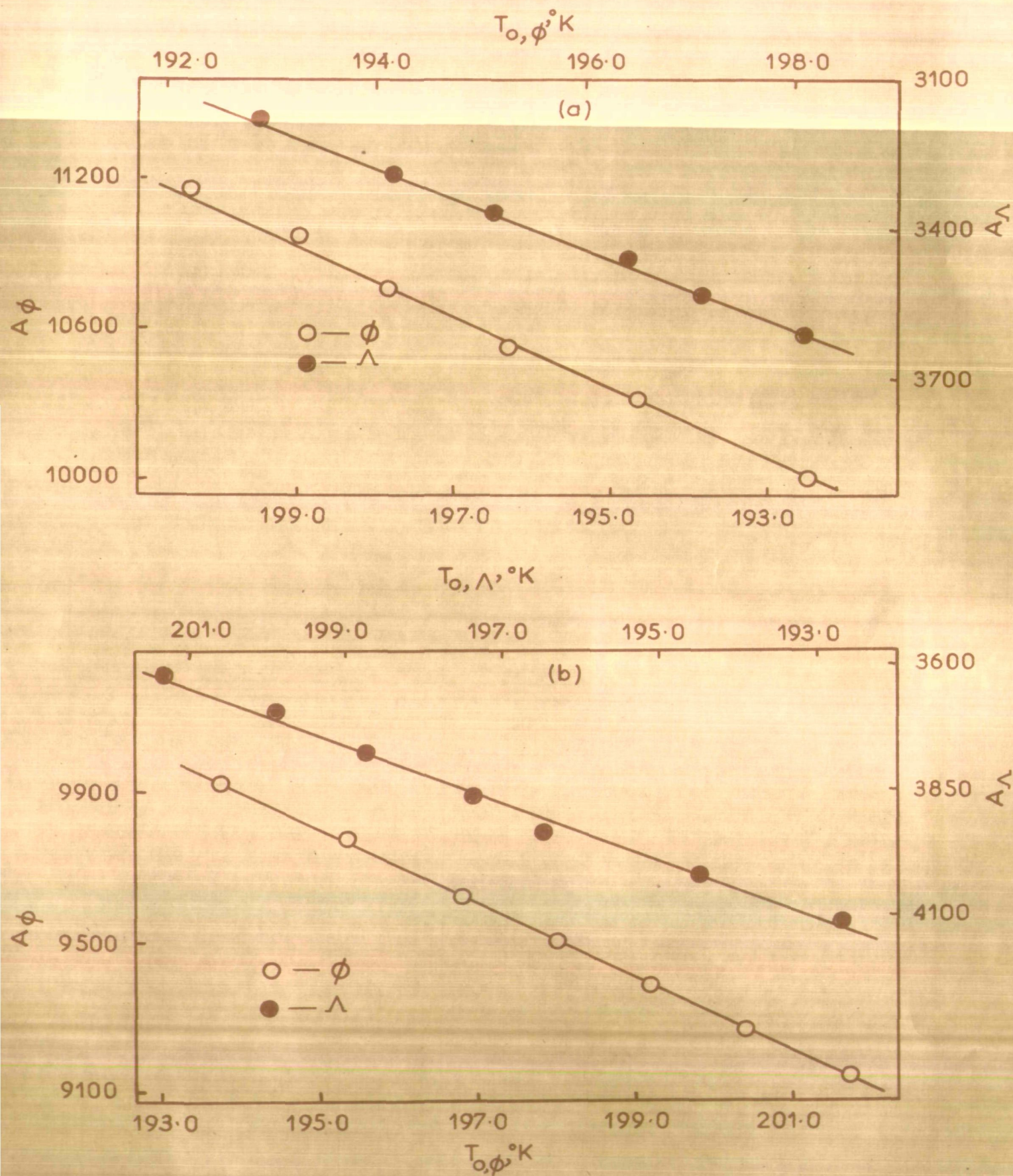


Fig.25. Variation of A_Y with $T_{O,Y}$ for (a) $\text{Cd}(\text{NO}_3)_2 \cdot 4.03\text{H}_2\text{O} - \text{MnCl}_2 \cdot 4.00\text{H}_2\text{O}$ and (b) $\text{Ca}(\text{NO}_3)_2 \cdot 4.23\text{H}_2\text{O} - \text{NH}_4\text{CNS}$ melts.

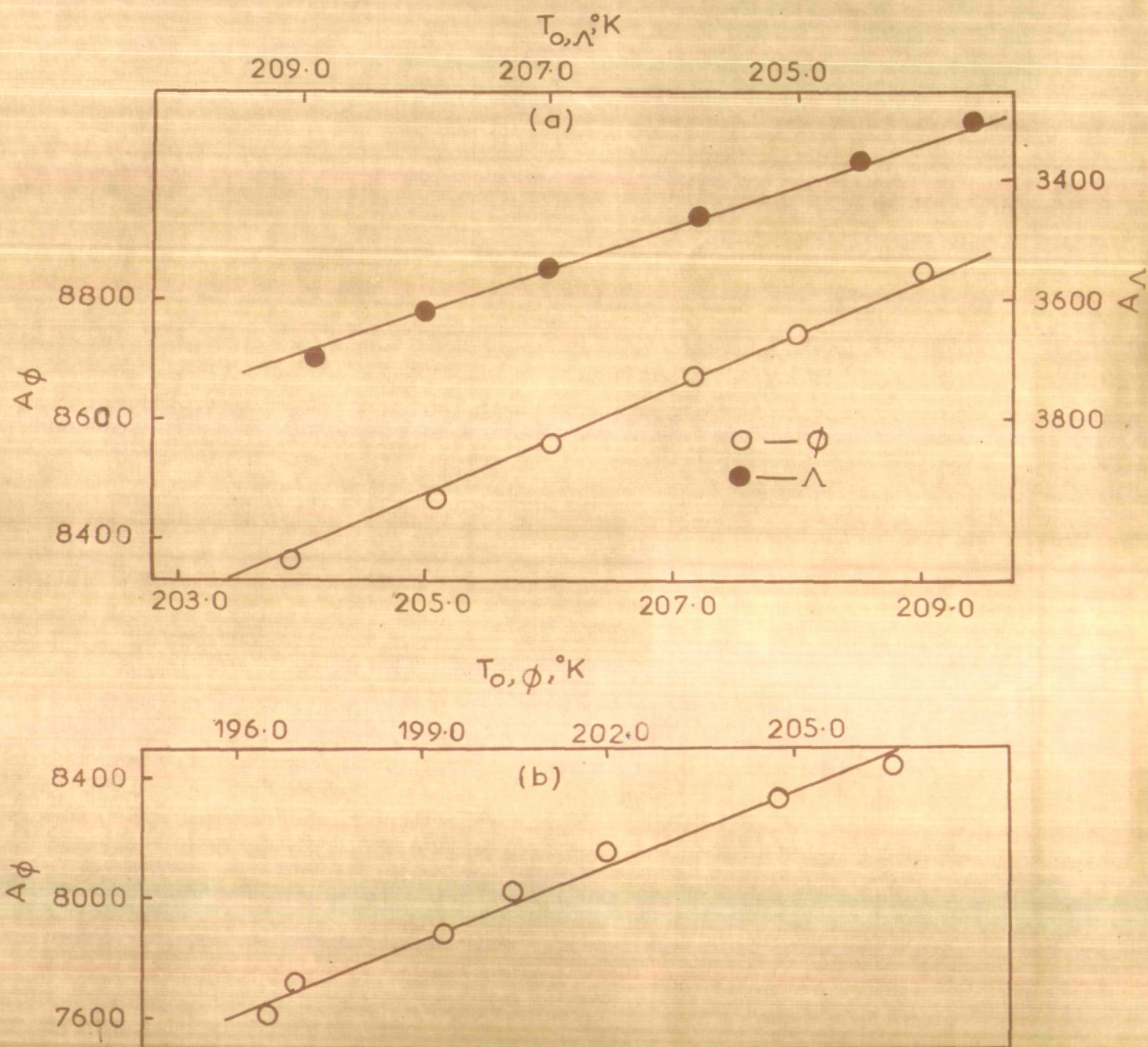


Fig.26. Variation of (a) A_Y with $T_{0,Y}$ for $\text{Ca}(\text{NO}_3)_2 \cdot 4.1\text{H}_2\text{O} - \text{NaCNS}$ and (b) A_ϕ with $T_{0,\phi}$ for $\text{Ca}(\text{NO}_3)_2 \cdot 3.96\text{H}_2\text{O} - \text{Ni}(\text{NO}_3)_2 \cdot 6.03\text{H}_2\text{O}$ melts.

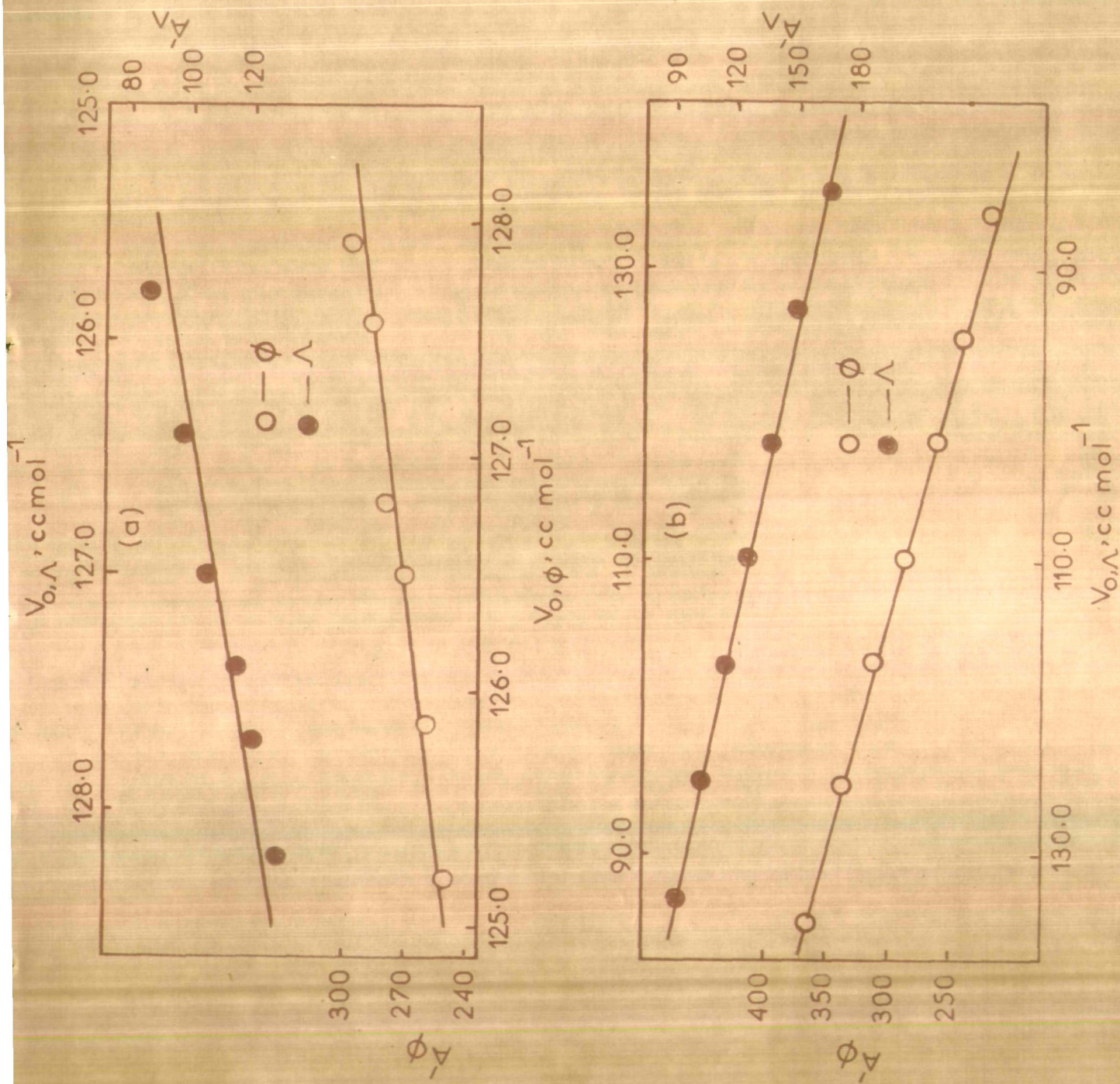


Fig. 27. Variation of $\Delta\phi$ with $V_{0,\gamma}$ for

(a) $\text{Cd}(\text{NO}_3)_2 \cdot 4.03\text{H}_2\text{O} - \text{MnCl}_2 \cdot 4.00 \text{H}_2\text{O}$ and (b) $\text{Ca}(\text{NO}_3)_2 \cdot 4.23\text{H}_2\text{O} - \text{NH}_4\text{CNS}$ melts.

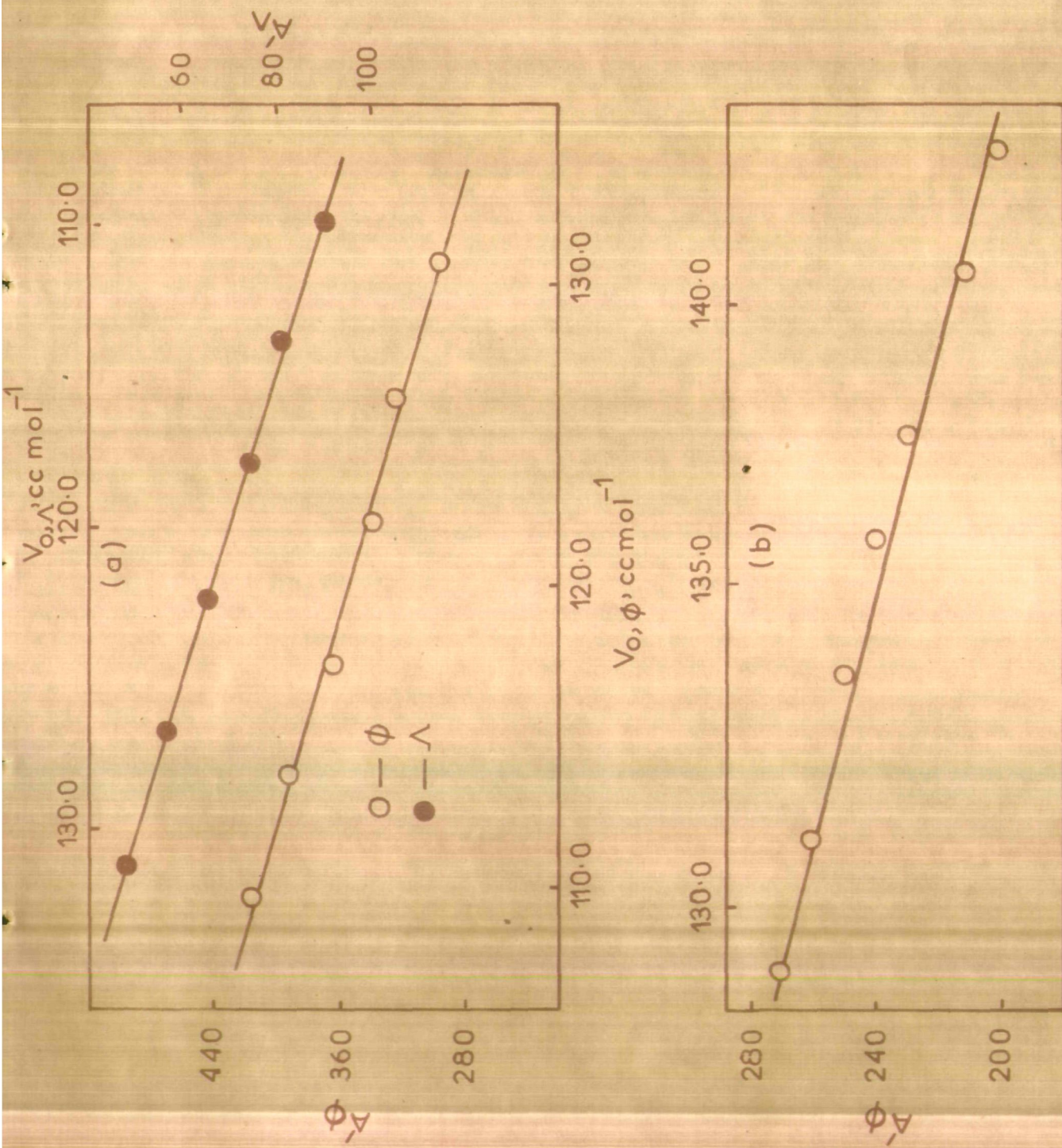


Fig.28. Variation of (a) A'_γ with $V_{0,\gamma}$ for $\text{Ca}(\text{NO}_3)_2 \cdot 4.1\text{H}_2\text{O} - \text{NaCNS}$ and (b) A'_ϕ with $V_{0,\phi}$ for $\text{Ca}(\text{NO}_3)_2 \cdot 3.96\text{H}_2\text{O} - \text{Ni}(\text{NO}_3)_2 \cdot 6.03\text{H}_2\text{O}$ melts.

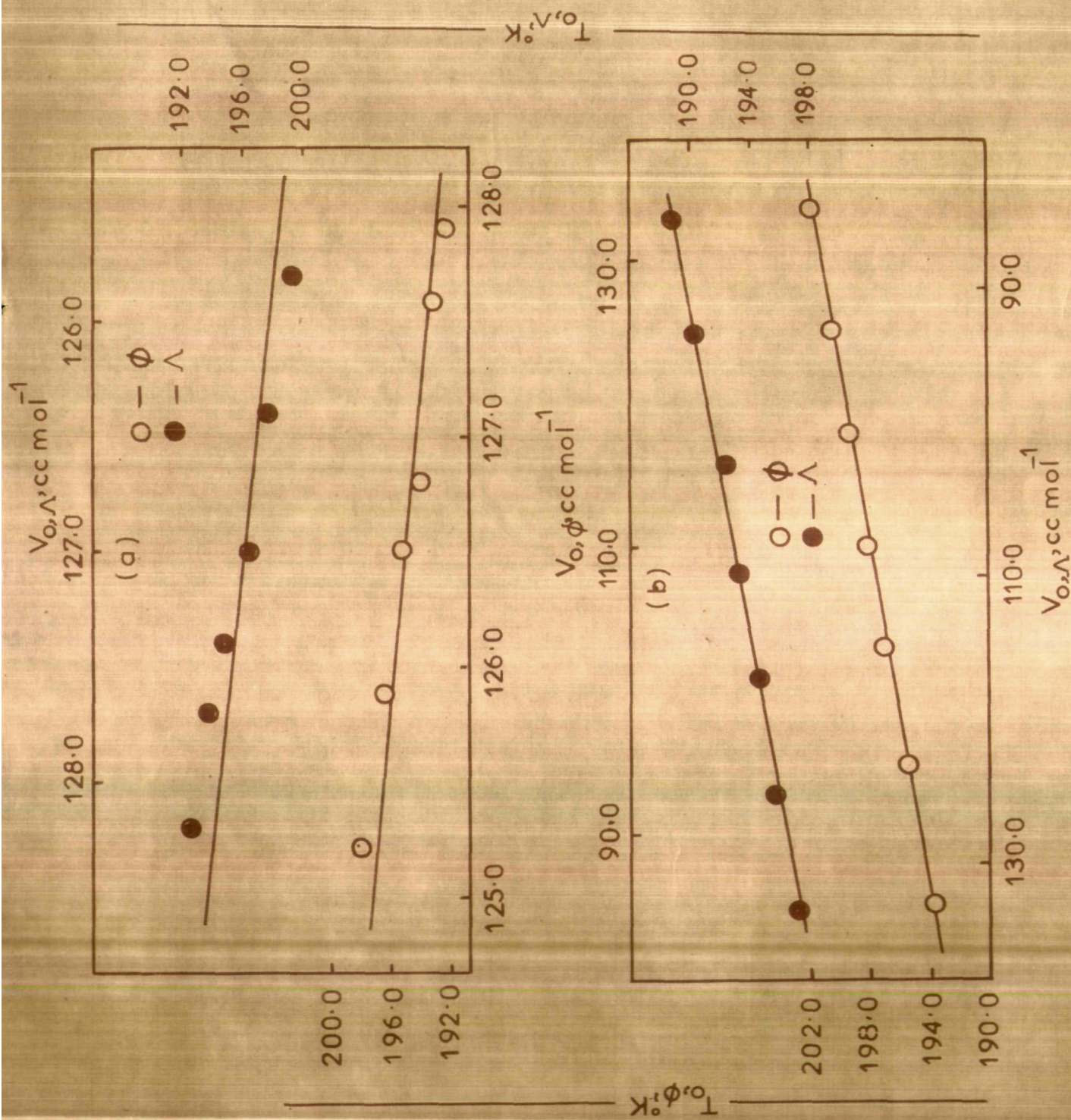


Fig. 29. Variation of $T_{0,\gamma}$ with $V_{0,\gamma}$ for (a) $\text{Cd}(\text{NO}_3)_2 \cdot 4.03\text{H}_2\text{O} - \text{MnCl}_2 \cdot 4.00\text{H}_2\text{O}$ and (b) $\text{Ca}(\text{NO}_3)_2 \cdot 4.23\text{H}_2\text{O} - \text{NH}_4\text{CNS}$ melts.

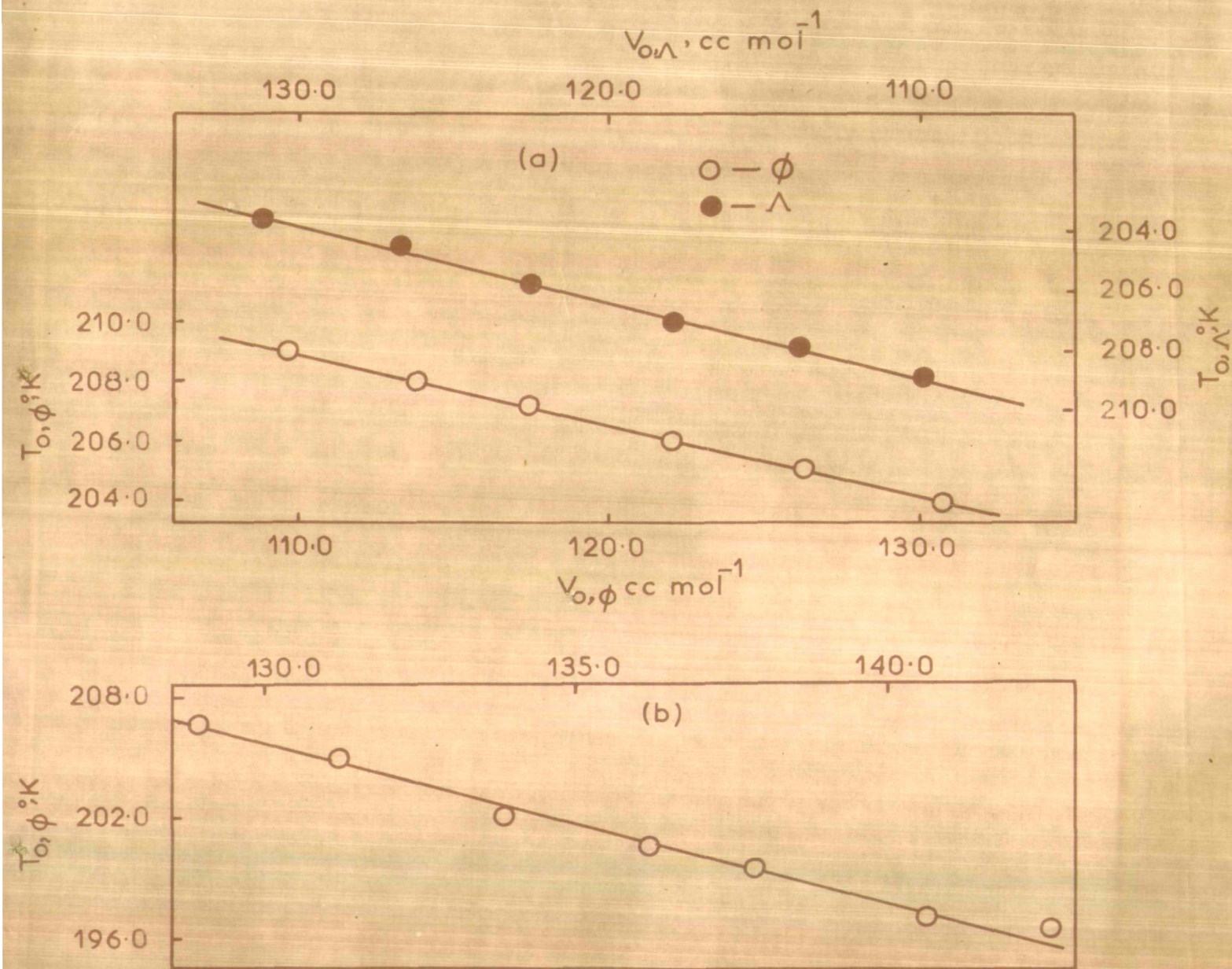


Fig.30. Variation of (a) $T_{o,\gamma}$ with $V_{o,\gamma}$ for $\text{Ca}(\text{NO}_3)_2 \cdot 4.1\text{H}_2\text{O} - \text{NaCNS}$ and (b) $T_{o,\phi}$ with $V_{o,\phi}$ for $\text{Ca}(\text{NO}_3)_2 \cdot 3.96\text{H}_2\text{O} - \text{Ni}(\text{NO}_3)_2 \cdot 6.03\text{H}_2\text{O}$ melts.

At 348°K

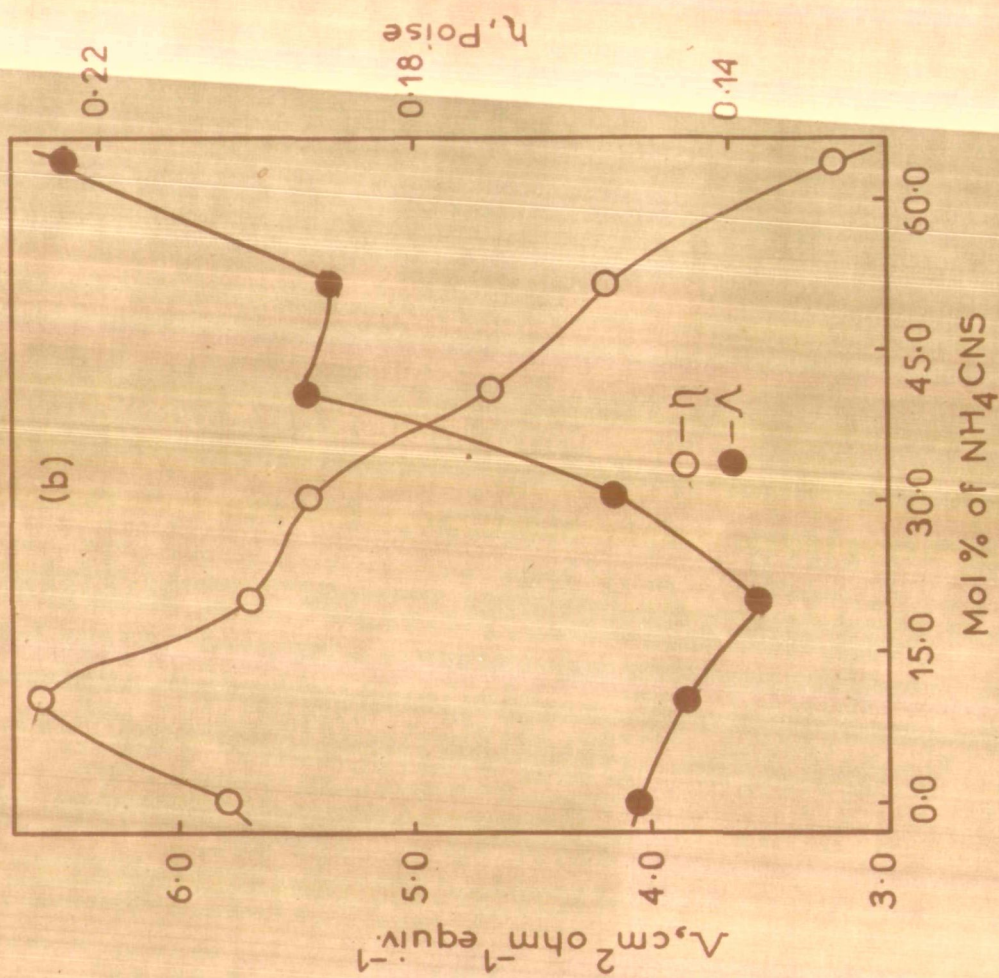
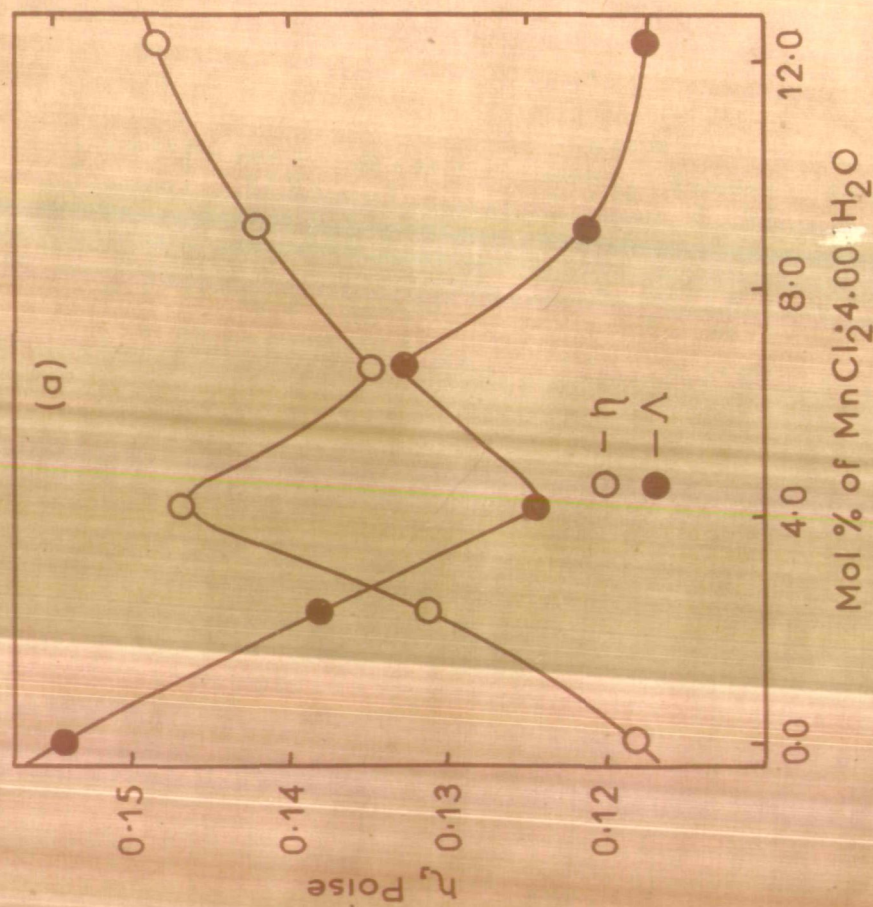


Fig.31. Viscosity and conductance isotherms for molten (a) $\text{Cd}(\text{NO}_3)_2 \cdot 4.03\text{H}_2\text{O} - \text{MnCl}_2 \cdot 4.00 \cdot \text{H}_2\text{O}$ and (b) $\text{Ca}(\text{NO}_3)_2 \cdot 4.23\text{H}_2\text{O} - \text{NH}_4\text{CNS}$ systems.

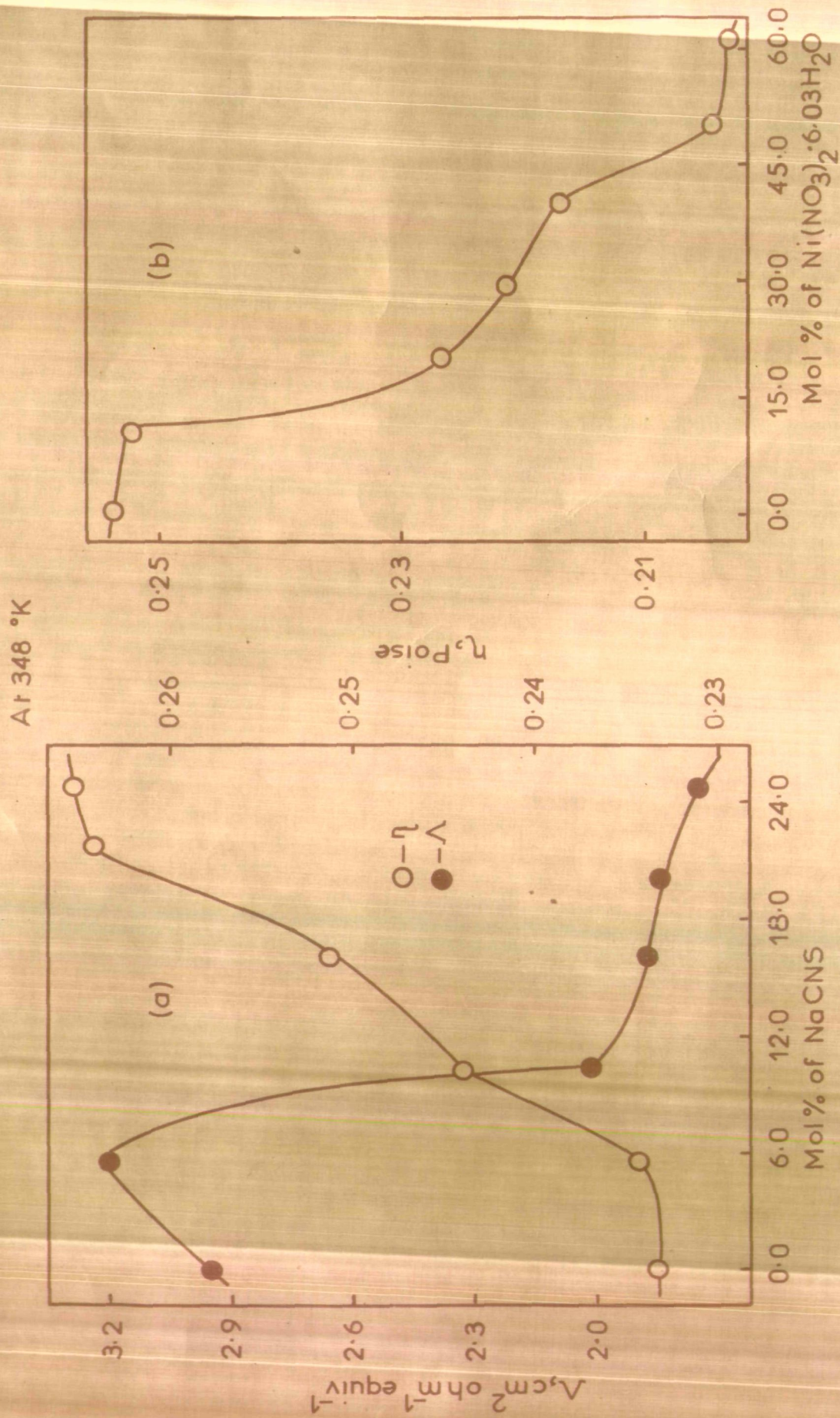


Fig.32 (a) Viscosity and conductance isotherms for molten $\text{Ca}(\text{NO}_3)_2 \cdot 4.1\text{H}_2\text{O} - \text{NaCNS}$ and (b) Viscosity isotherm for molten $\text{Ca}(\text{NO}_3)_2 \cdot 3.96\text{H}_2\text{O} - \text{Ni}(\text{NO}_3)_2 \cdot 6.03\text{H}_2\text{O}$ systems.

with minimum and maximum at ~ 4.14 and ~ 6.63 mol %, respectively. In the case of $\text{Ca}(\text{NO}_3)_2 \cdot 4.23\text{H}_2\text{O} - \text{NH}_4\text{CNS}$ melts viscosity has been found to increase from 0.00 to ~ 10.11 mol % where it has a maximum and then decreases almost monotonously from ~ 10.11 to ~ 63.42 mol %. Similarly, the behaviour of conductance with successive variations in concentration follows an almost opposite pattern to that found in the case of viscosity except that the expected minimum at ~ 10.11 mol % has shifted to ~ 20.02 mol %. The minimum is then followed by an apparently monotonous increase in conductance from ~ 20.02 to ~ 63.42 mol %. In the case of $\text{Ca}(\text{NO}_3)_2 \cdot 4.1\text{H}_2\text{O} - \text{NaCNS}$ melts viscosity has nearly constant value from 0.00 to ~ 5.58 mol % and then increases monotonously from ~ 5.58 to 20.13 mol % approaching a limiting value at ~ 24.84 mol %. On the other hand, conductance shows a maximum at ~ 5.58 mol % and then falls off rapidly until ~ 10.28 mol %. Further variations in Λ values are almost insignificant reaching apparently limiting value at ~ 24.84 mol %. Finally, in the case of molten $\text{Ca}(\text{NO}_3)_2 \cdot 3.96\text{H}_2\text{O} - \text{Ni}(\text{NO}_3)_2 \cdot 6.03\text{H}_2\text{O}$ system viscosity shows an almost constant value from 0.00 to ~ 10.19 mol % and then it is followed by an apparently monotonous decrease from ~ 10.19 to 49.65 mol % reaching again a limiting value at ~ 60.83 mol %. The irregular trends in fluidity and conductance isotherms at intermediate

concentrations have been found to be similar to those reported earlier.^{55,66,70,71} In the case of $\text{Cd}(\text{NO}_3)_2 \cdot 4.03\text{H}_2\text{O}$ - $\text{MnCl}_2 \cdot 4.00\text{H}_2\text{O}$ system the overall decrease in conductance and fluidity with increase in concentration may be due to decrease in the free volume resulting, consequently, in an increase in compactness of the system. According to the configurational entropy model also the configurational entropy of the system will decrease with increase in concentration of the solute due to increase in compactness of the system and hence a decrease in conductance and fluidity may be expected. Conductivity is presumed to occur mainly by the migration of the more mobile ion while the viscosity is mainly guided by the less mobile or rather bulky entity. A decrease in conductance with increase in $[\text{Mn}^{2+}]$ may be attributed to decrease in the number of free Cl^- ions due to the formation of associated species of the type, $\text{Mn}(\text{H}_2\text{O})_4\text{Cl}_2$. This may also account for the increase in viscosity of the system with increase in $[\text{Mn}^{2+}]$. However, in the case of $\text{Zn}(\text{NO}_3)_2 \cdot 6.18\text{H}_2\text{O}$ - $\text{MnCl}_2 \cdot 4.43\text{H}_2\text{O}$ melts³⁷ viscosity decreases with increase in concentration of solute which is a reverse effect to the observed increase in viscosity in the case of $\text{Cd}(\text{NO}_3)_2 \cdot 4.03\text{H}_2\text{O}$ - $\text{MnCl}_2 \cdot 4.00\text{H}_2\text{O}$ melts studied here. In the case of $\text{Ca}(\text{NO}_3)_2 \cdot 4.1\text{H}_2\text{O}$ - NaCNS system both fluidity and conductance decrease with increase in $[\text{Na}^+]$. Here

the substitution of less mobile Na^+ for $\frac{1}{2}\text{Ca}^{2+}$ (absolute mobilities at 25°C of Na^+ and Ca^{2+} ions are 0.000520 and 0.000616 $\text{cm}^2 \text{ volt}^{-1} \text{ sec}^{-1}$, respectively) appears to be responsible for the decrease in conductance with increase in the concentration of NaCNS . Decrease in the viscosity with concentration may presumably be due to increase in the compactness or rigidity of the system. In the case of the system $\text{Ca}(\text{NO}_3)_2 \cdot 4.23\text{H}_2\text{O} - \text{NH}_4\text{CNS}$ fluidity and conductance both increase with increase in concentration of NH_4CNS . In this melt the hydrated solvent cation $\text{Ca}(\text{H}_2\text{O})_4^{2+}$ seems to be less mobile than the added solute cation NH_4^+ . Therefore, on adding NH_4CNS we are increasing the concentration of the highly conducting NH_4^+ ions which lead to an increase in conductance with $[\text{NH}_4^+]$. It may, however, be pointed out that the resultant viscosities of the mixtures of molten salts may also depend on the respective values of the two components. The above fact may be visualized from decrease in the activation energies with increase in $[\text{NH}_4^+]$. Similarly, an increase in fluidity on the addition of $\text{Ni}(\text{NO}_3)_2 \cdot 6.03\text{H}_2\text{O}$ in molten $\text{Ca}(\text{NO}_3)_2 \cdot 3.96\text{H}_2\text{O}$ may be understood on the basis of the relative viscosities of the solvent and that of the solute.

A P P E N D I X

A. Calculation of Viscosity

Let us consider a cylindrical liquid layer of area A sq. cm. moving over another similar layer at a distance d cm. with a velocity difference v cm./sec. Then, the tangential frictional force, f required to maintain constant difference of velocity is given as

$$f \propto \frac{Av}{d}$$

or
$$f = \eta \frac{Av}{d}$$

where η is a constant at a given temperature, depending upon the nature of the liquid is known as the coefficient of viscosity. Hence

$$\eta = \frac{f}{A} \left(\frac{d}{v} \right)$$

in which f/A or force/unit area is called as shear stress. From the above expression it is clear that the unit of viscosity is g/cm/sec and is denoted by 'poise'.

The reciprocal of viscosity is called fluidity,

$$\phi = 1/\eta$$

For the flow of homogeneous liquid through a

capillary Poiseuill's law states that the rate of flow of the liquid is given by the equation

$$\eta = \pi r^4 t P / 8 V l$$

where V is the volume in c.c. of the liquid flowing in t seconds through a narrow tube of radius r cm. and length l cm. under a hydrostatic pressure of P dynes/sq. cm. Since the hydrostatic pressure of a liquid column is given by

$$P = h \rho g$$

where h is the height of the column and ρ the density of the liquid, the Poiseuille's equation may be written as

$$\eta = \pi r^4 t h \rho g / 8 V l$$

In actual practice we measure the relative viscosity of the test liquid with respect to a reference liquid. Let us take quinoline as the reference one. Suppose that t_1 and t_2 are the times of flow of the same volume of quinoline and test liquid through the same capillary tube, respectively, and η_1 and η_2 are their respective coefficients of viscosities, then

$$\eta_1/\eta_2 = \pi r^4 t_1 h \rho_1 g \times 8V_1/8V_1 \times \pi r^4 t_2 h \rho_2 g$$

$$\text{or } \eta_1/\eta_2 = \rho_1 t_1 / \rho_2 t_2 \quad (1)$$

where ρ_1 and ρ_2 are the densities of the reference and the test liquids, respectively.

Now by knowing the viscosity of quinoline at the required temperature as well as densities and times of fall of the two liquids, one can easily calculate the viscosity of the test liquid.

B. Calculation of equivalent conductance

From the specific conductance data K , equivalent weight, e , and the density, ρ , the equivalent conductance, that is, the conductance of one equivalent of electrolyte between parallel electrodes 1 cm. apart, was calculated using the equation established by Harry Bloom⁷²

$$\Lambda = K e / \rho = K V_e \quad (2)$$

where V_e is the equivalent volume of the molten salt in ml.

For mixtures of molten salts

$$\Lambda = K \bar{e} / \rho \quad (3)$$

where \bar{e} is the mean equivalent weight calculated from the equation

$$\bar{e} = f_1 e_1 + f_2 e_2 \quad (4)$$

where f_1 and f_2 are the equivalent fractions and e_1 , and e_2 are the equivalent weights of component 1 and 2, respectively.

C. Calculation of activation energy

(i) From the VTF equation

The Arrhenius equation can be written as

$$Y = A_Y \exp \left[-E_Y/RT \right]$$

$$\text{or } \ln Y = \ln A_Y - E_Y/RT \quad (5)$$

Now, differentiating with respect to inverse of temperature gives

$$\frac{d \ln Y}{d(1/T)} = -E_Y/RT \quad (6)$$

The VTF equations for the fluidity, ϕ , and equivalent conductance, Λ are given as

$$Y (= \phi \text{ or } \Lambda) = A_Y T^{-1/2} \exp \left[-k_Y/(T - T_0) \right]$$

$$\text{or } \ln Y = \ln A_Y - \frac{1}{2} \ln T - k_Y/(T - T_0) \quad (7)$$

$$\therefore \frac{d \ln Y}{d(1/T)} = \left[\frac{1}{2T} - k_Y/(T - T_0)^2 \right] T^2 \quad (8)$$

Comparing equations (6) and (8), we get,

$$E_Y = R \left[k_Y / (T - T_0)^2 - \frac{1}{2} T \right] T^2 \quad (9)$$

The corrected activation energy may be written as

$$E_{\text{corr}} = E_Y + \frac{1}{2} RT = Rk_Y \left[T / (T - T_0) \right]^2 \quad (10)$$

(ii) From the configurational entropy model

The equations for fluidity, ϕ and equivalent conductance, Λ are given as follows:

$$Y (= \phi \text{ or } \Lambda) = A_Y'' \exp \left[-k_Y'' / T \ln (T/T_0) \right] \quad (11)$$

Taking natural logarithm and differentiating with respect to T^{-1} the above equation is written as

$$\frac{d \ln Y}{d(1/T)} = -k_Y'' \left[(1 + \ln (T/T_0) / (\ln (T/T_0))^2) \right] \quad (12)$$

Comparing equations (6) and (11), we obtain

$$E_Y = Rk_Y'' \left[(1 + \ln (T/T_0) / (\ln (T/T_0))^2) \right] \quad (13)$$

At $T/T_0 = c$, constant, equation (11) on differentiation with respect to T^{-1} becomes

$$\frac{d \ln Y}{d(1/T)} = -k_Y'' / \ln c \quad (14)$$

Therefore, E_Y at constant $T/T_0 = c$ may be written as

$$E_Y = Rk_Y''/\ln (T/T_0) \quad (15)$$

B I B L I O G R A P H Y

1. D. Turnbull and M.H. Cohen, J. Chem. Phys., 29, 1049 (1958).
2. W.W. Eving and C.H. Herty, J. Phys. Chem., 57, 245 (1953).
3. W.W. Eving and R.J. Mikovsky, J. Am. Chem. Soc., 72, 1390 (1950).
4. C.N. Reilly, R.W. Schmid, and Fawzy S. Sadek, J. Chem. Edu., 36, 555 (1959); *ibid.*, 36, 619 (1959).
5. C. Tanford, "Physical Chemistry of Macromolecules", John Wiley and Sons, Inc., New York, N.Y., 1961, p 329.
6. H.C. Cowen and H.J. Axon, Trans. Faraday Soc., 52, 242 (1956).
7. E.R. Van Artsdalen and I.S. Yaffe, J. Phys. Chem., 59, 118 (1955).
8. G.P. Smith in "Molten Salt Chemistry", M. Blander, Ed. Interscience Publishers, Inc., New York, N.Y., 1964, pp 427-505.
9. C.A. Angell and D.M. Gruen, J. Am. Chem. Soc., 88, 5192 (1966).
10. A.D. Liehr and C.J. Ballhausen, Ann. Phys., 6, 134 (1959).
11. L.L. Sperry and J.D. Mackenzie, Phys. Chem. Glasses, 9, 91 (1968).

12. A.J. Batchinski, Z. Physik, Chim., 84, 643 (1913).
13. P.W. Bridgman, "The Physics of High Pressure", G. Bell and Sons, London, 1949, pp 330-357.
14. J. Frenkel, "Kinetic Theory of Liquids", Dover Publications, Inc., New York, 1955, pp 174-182.
15. H. Eyring, J. Chem. Phys., 4, 283 (1936); Hirschfelder, Stevenson, and Eyring, *ibid.*, 5, 896 (1937).
16. T.G. Fox and P.J. Flory, J. Appl. Phys., 21, 581 (1950); J. Phys. Chem., 55, 221 (1951); J. Polymer Sci., 14, 315 (1954).
17. J.H. Hildebrand and R.H. Lamoreaux, J. Phys. Chem., 77, 1471 (1973); J.H. Hildebrand, Science, 174, 490 (1971).
18. A.K. Doolittle, J. Appl. Phys., 22, 147 (1951).
19. M.L. Williams, R.F. Landel, and J.D. Ferry, J. Am. Chem. Soc., 77, 3701 (1955).
20. T.A. Litovitz, J. Chem. Phys., 20, 1088 (1952).
21. A.J. Barlow and J. Lamb, Proc. Roy. Soc., A253, 52 (1959).
22. M.H. Cohen and D. Turnbull, J. Chem. Phys., 31, 1164 (1959).
23. H. Bloom, "The Chemistry of Molten Salts", W.A. Benjamin, Inc., New York, N.Y., 1967, p 100.

24. T.A. Litovitz and C.M. Davis, "Physical Acoustics", Vol. 2, Part A, W.P. Mason, Ed., Academic Press, New York, N.Y., 1965, p 281.
25. C.T. Moynihan, C.R. Smalley, C.A. Angell, and E.J. Sare, J. Phys. Chem., 73, 2287 (1969).
26. C.T. Moynihan, J. Phys. Chem., 70, 3399 (1966).
27. C.A. Angell and R.D. Brassel, J. Phys. Chem., 76, 3244 (1972).
28. C.A. Angell and C.T. Moynihan, "Transport Processes in Low-Melting Molten Salt Systems" in "Molten Salts", G. Mamantov, Ed., Marcel Dekker, New York, N.Y., 1969, pp 351-353.
29. C.A. Angell, J. Phys. Chem., 68, 1917 (1964).
30. C.A. Angell, J. Chem. Phys., 46, 4673 (1967).
31. C.A. Angell, J. Electrochem. Soc., 112, 1224 (1965).
32. C.A. Angell, J. Phys. Chem., 70, 3988 (1966).
33. C.A. Angell, J. Phys. Chem., 70, 2793 (1966).
34. N. Islam and Ismail K., J. Phys. Chem., 79, 2180 (1975).
35. Ismail K., Doctoral Dissertation, "Physico-Chemical Studies of Molten Salt Systems", A.M.U., Aligarh (1976).

36. K.P. Singh, Doctoral Dissertation, "Physico-Chemical Studies of Molten Salt Systems", A.M.U., Aligarh, (1977).
37. S. Kumar, Doctoral Dissertation, "Physico-Chemical Studies of Molten Salt Systems", A.M.U., Aligarh (1977).
38. N. Islam, S. Kumar, and K.P. Singh, ~~Can. J. Chem.~~, 56, 1231 (1978).
39. Frame, Rhodes, A.R. Ubbelohde, Trans. Faraday Soc., 55, 2039 (1959).
40. N. Islam, M.R. Islam, S. Ahmad, and B. Waris, J. Am. Chem. Soc., 97, 3026 (1975).
41. N. Islam and Ismail K., J. Phys. Chem., 80, 1929 (1976).
42. D.J. Denney, J. Chem. Phys., 30, 159 (1959).
43. D.W. Davidson and R.H. Cole, J. Chem. Phys., 19, 1484 (1951).
44. C.A. Angell, J. Am. Ceram. Soc., 51, 117 (1968).
45. C.A. Angell, J. Phys. Chem., 69, 2137 (1965).
46. C.A. Angell, J. Phys. Chem., 69, 399 (1965).
47. Reference 19, p 61.
48. B.J. Alder and T. Einwohner, J. Chem. Phys., 43, 3399 (1965).

49. J.M. O'Reilly, J. Polym. Sci., 57, 429 (1962).
50. M. Goldstein, J. Chem. Phys., 39, 3369 (1963).
51. B. Cleaver, S.I. Smedley, and P.N. Spencer, J. Chem. Soc., Faraday Trans., 1, 68, 1720 (1972).
52. G. Adam and J.H. Gibbs, J. Chem. Phys., 43, 139 (1965).
53. W. Kauzmann, Chem. Rev., 43, 219 (1948).
54. J.H. Gibbs and E.A. DiMarzio, J. Chem. Phys., 28, 373 (1958); 28, 807 (1958); J. Polym. Sci., 40, 121 (1959).
55. A.J. Easteal and I.M. Hodge, J. Phys. Chem., 74, 730 (1970).
56. C.A. Angell, J. Chem. Phys., 43, 2899 (1965).
57. C.T. Moynihan and C.A. Angell, J. Phys. Chem., 74, 736 (1970).
58. F.J. Bartoli, J.N. Birch, N.H. Toan, and G.E. McDuffie, J. Chem. Phys., 49, 1916 (1968).
59. T.A. Litovitz and G.E. McDuffie, J. Chem. Phys., 39, 729 (1963).
60. D. Turnbull and M.H. Cohen, "Modern Aspects of the Vitreous State", J.D. Mackenzie, Ed. Butterworth's Scientific Publications, Ltd. London, 1960.

61. C.A. Angell and D.B. Helphrey, J. Phys. Chem., 75, 2306 (1971).
62. H. Reiss, S.W. Mayer, and J.L. Katz, J. Chem. Phys., 35, 820 (1961).
63. M.V. Susic and S.V. Mentus, J. Chem. Phys., 62, 744 (1975).
64. C.A. Angell and E.J. Sare, J. Chem. Phys., 52, 1058 (1970).
65. G. Vuillard, Ann. Chem. (Paris), 2, 233 (1957).
66. N. Islam, M.R. Islam, B. Waris, and Ismail K., J. Phys. Chem., 80, 291 (1976).
67. C.A. Angell, E.J. Sare, and R.D. Brassel, J. Phys., Chem., 71, 2759 (1967).
68. Reference 24, p 346.
69. C.A. Angell, Aust. J. Chem., 23, 929 (1970).
70. Reference 24, pp 87-104.
71. H. Bloom and E. Heymann, Proc. Roy. Soc. (London), 188, 392 (1947).
72. Reference 19, p 80.